

Effects of **tropical cyclone** interaction with **monsoon**



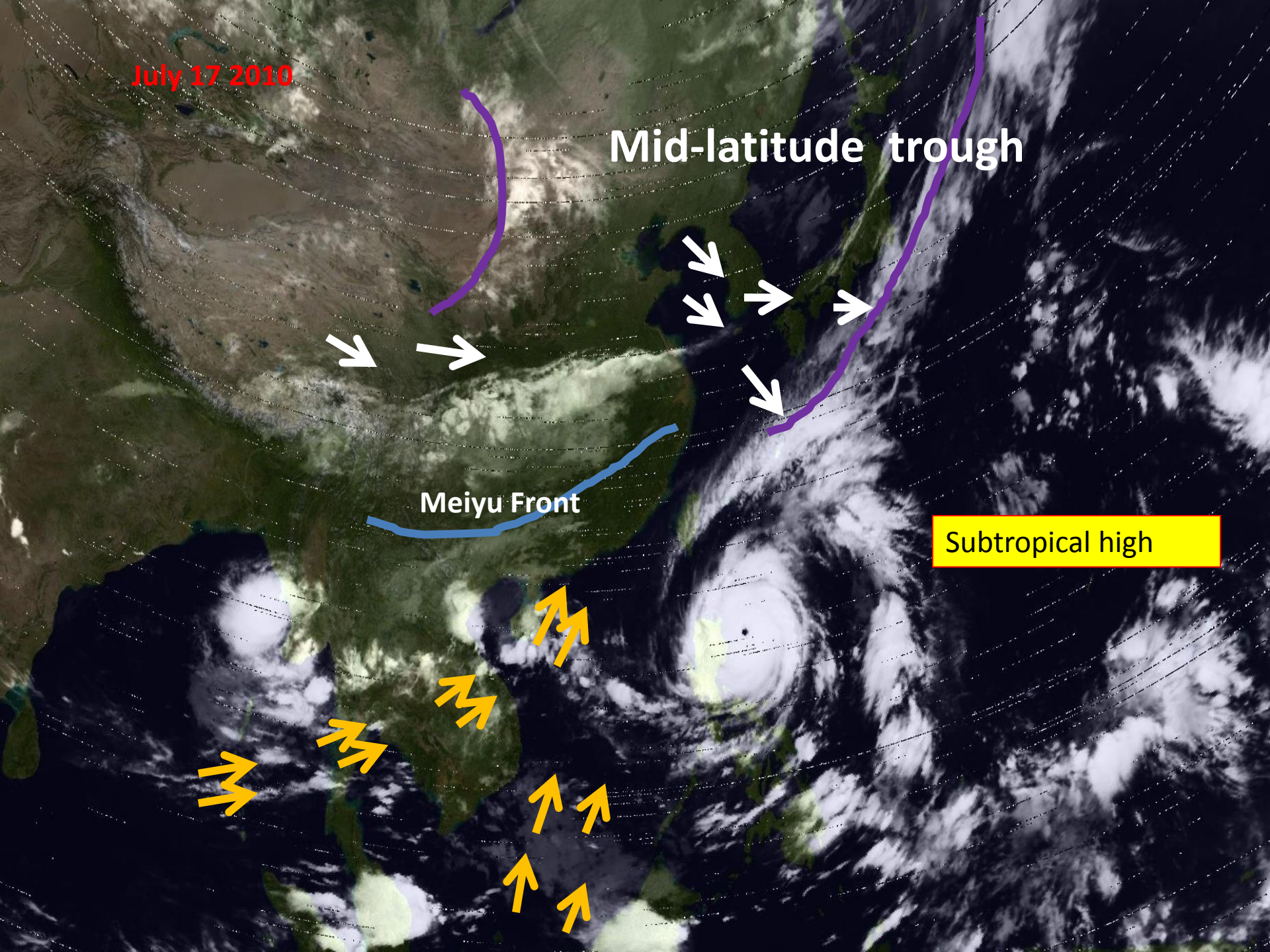
Qinghong Zhang
Department of atmospheric and oceanic
science, Peking University
qzhang@pku.edu.cn

July 17 2010

Mid-latitude trough

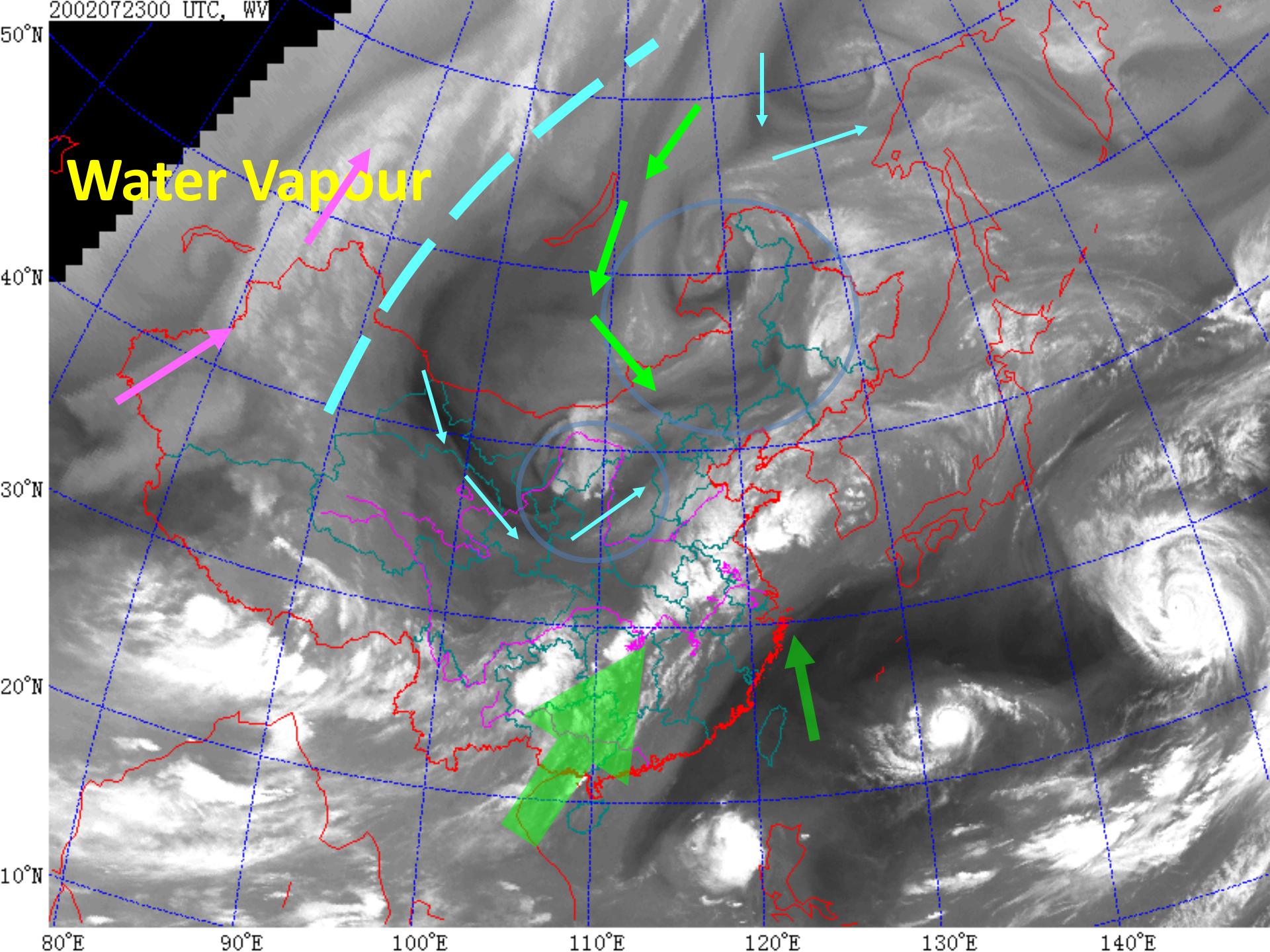
Meiyu Front

Subtropical high



2002072300 UTC, WV

Water Vapour



Effects of **tropical cyclone** interaction with **monsoon** with emphasis on rainfall



Qinghong Zhang

Department of atmospheric and oceanic science, Peking University

qzhang@pku.edu.cn

Index

- **Overview of TC rainfall over Monsoon region in Western North Pacific**
 - Early development
 - TC rainfall climatology
 - TC rainfall structure
- **Monsoon influence on TC precipitation**
 - SST
 - Meiyu front
 - subtropical high
 - Southwesterly monsoon
 - Northwesterly monsoon
- **Interaction between tropical cyclone and southwesterly monsoon**
 - Case study on Bilis 2006
 - Climatology
- **Study on the potential impact of landfalling TC in Mainland China (How to estimate economic loss by TC before their landfall in Mainland China)**
- *How to predict the development of tropical disturbance over SCS.*

Home work

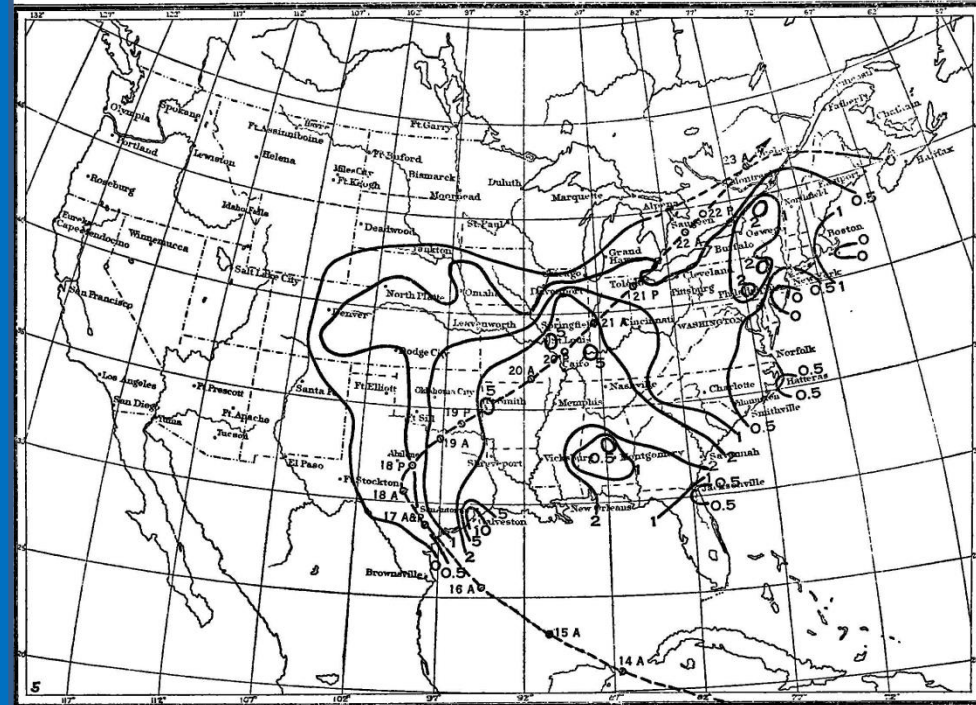
- How to improve our forecast skill for TC rainfall?

“First” study on rainfall of tropical cyclone in 1916

CO-CHINQ CEU, A. M. 1916

five tropical storms in 1911 are concerned

- (1) That the distribution of rainfall in tropical storms is uniform
- (2) the heaviest rainfall usually occurs on that portion of the coast where the storm passed from sea to land
- (3) that the heaviest precipitation usually occurs along the trajectory.



Early development

- **Allison et al. 1974** : from the unique combination of infrared visible, and microwave data from the nimbus 5 Electronically Scanning Microwave Radiometer(ESMR), the Temperature-Humidity Infrared Radiometer(THIP) NOAA-2 and USAF DMSP imageries, to estimate **semi-quantitatively area of light, moderate and heavy rainfall rates.**

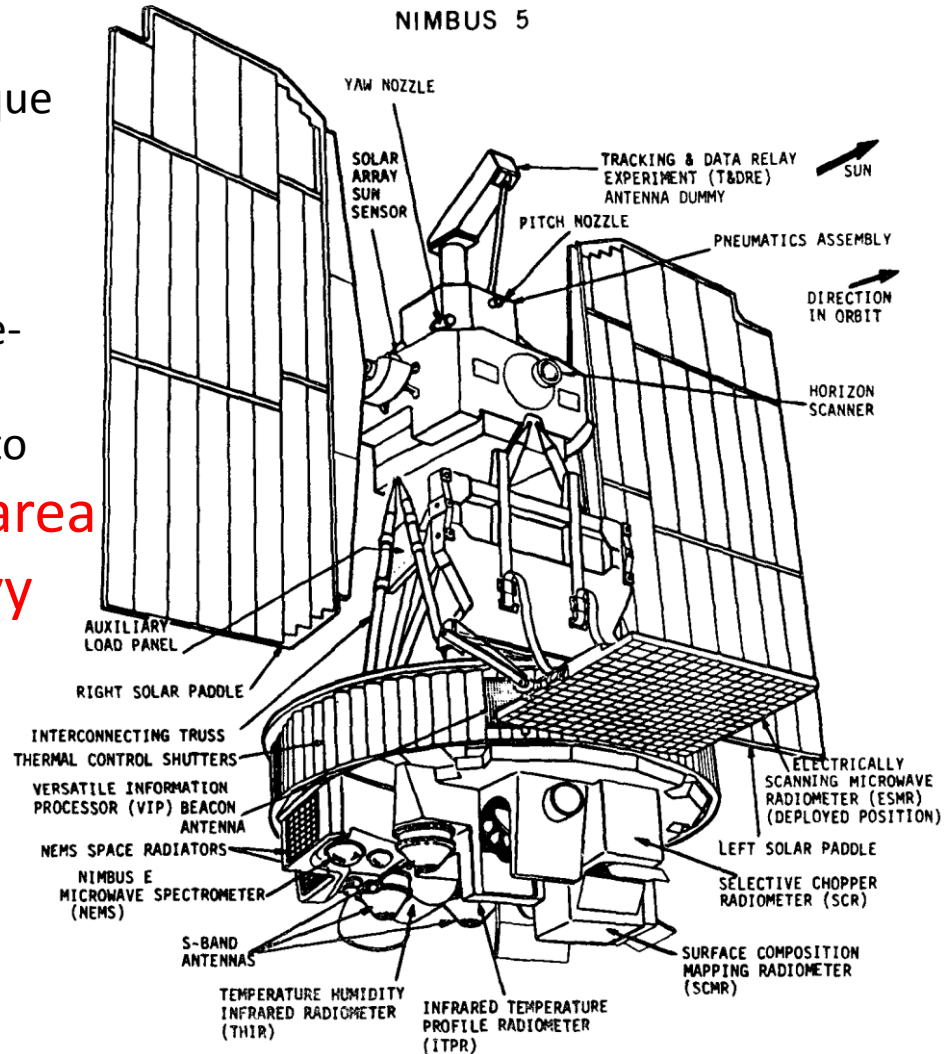


FIG. 1. The Nimbus 5 spacecraft with associated experiments.

Early development

• **Rodgers and Adler 1980:** used ESMR to derive Latent heat release (LHR)

• 1) TC intensification is indicated by the increase in the RSMR-5 derived LHR, increase in the relative contribution of the heavier rain rate ($> 5\text{mm/h}$) to the total storm rainfall, and the decrease in the radius of the maximum rain rate from the cyclone center.

2) Increasing LHR is the first indication of TC intensification 1-2 days prior to the TC reaching storm stage

3) As the mean tropical cyclone intensify from disturbance to Typhoon stage the average LHR increases steadily. The mean relative contribution of the heavier rate to the total storm rainfall increases from 0.24 at depression stage to 0.33 at storm at storm stage and finally to 0.39 at typhoon stage.

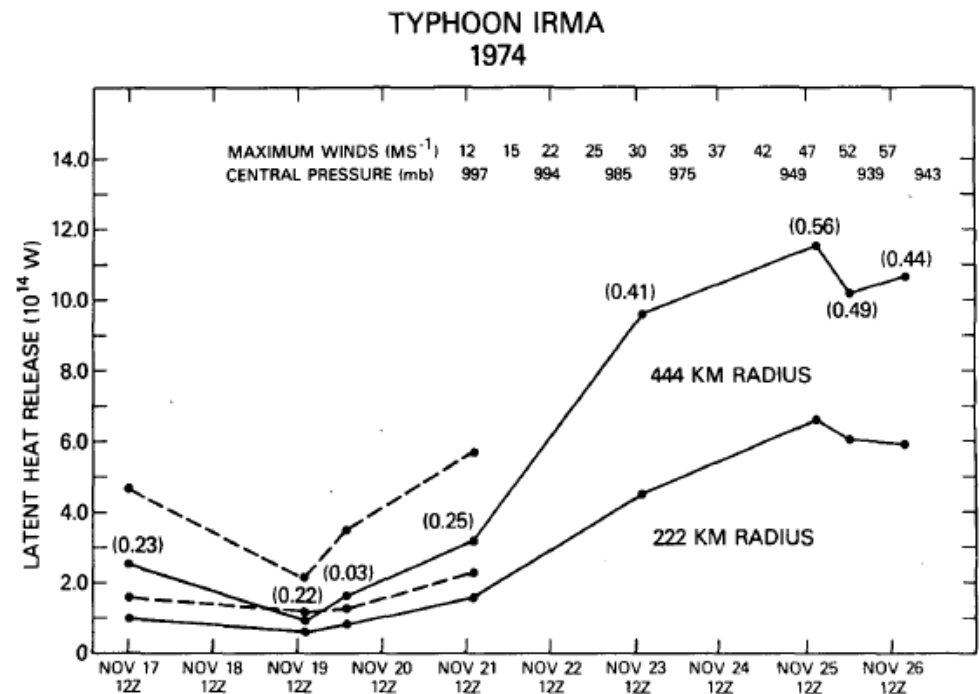


FIG. 3. Latent heat release (LHR) as a function of time for tropical cyclone Irma. Calculations are shown for circular areas of 222 and 444 km radius for freezing levels 4.5 km (dashed) and 5 km (solid). Numbers in parentheses are fractions of rainfall contributed by rainfall rates $> 5\text{mm h}^{-1}$.

TC rainfall study are based on satellite observation

ESMR , SSM/I , TRMM

Based on surface observation (landfalling TC)

◆ Overview of TC rainfall over Monsoon region in Western North Pacific

➤ Early development

➤ **TC rainfall climatology**

➤ TC rainfall structure

What is TC rainfall?

How to separate TC rainfall from total rainfall ?

How to deal with the issue ?

Subjective methods

accurate but slow

what weather forecasters do

the **expert subjective method (ESM)** using in Shanghai Typhoon Institute for more than 50 years

accurate

Objective ESM

Objective methods

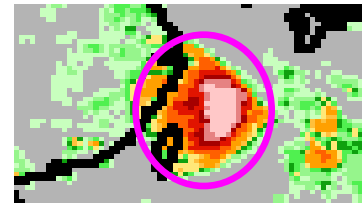
quick but not easy to be accurate
Homogeneity

a **certain circle** around the TC center (Phil et al., 2001; Akira, 2005).

an adaptive circle ?

not ok

relationship between the TC's size and its intensity is not good enough (Merrill, 1984, Weatherford and Gray, 1988a ,b, Liu and Chan, 1999)

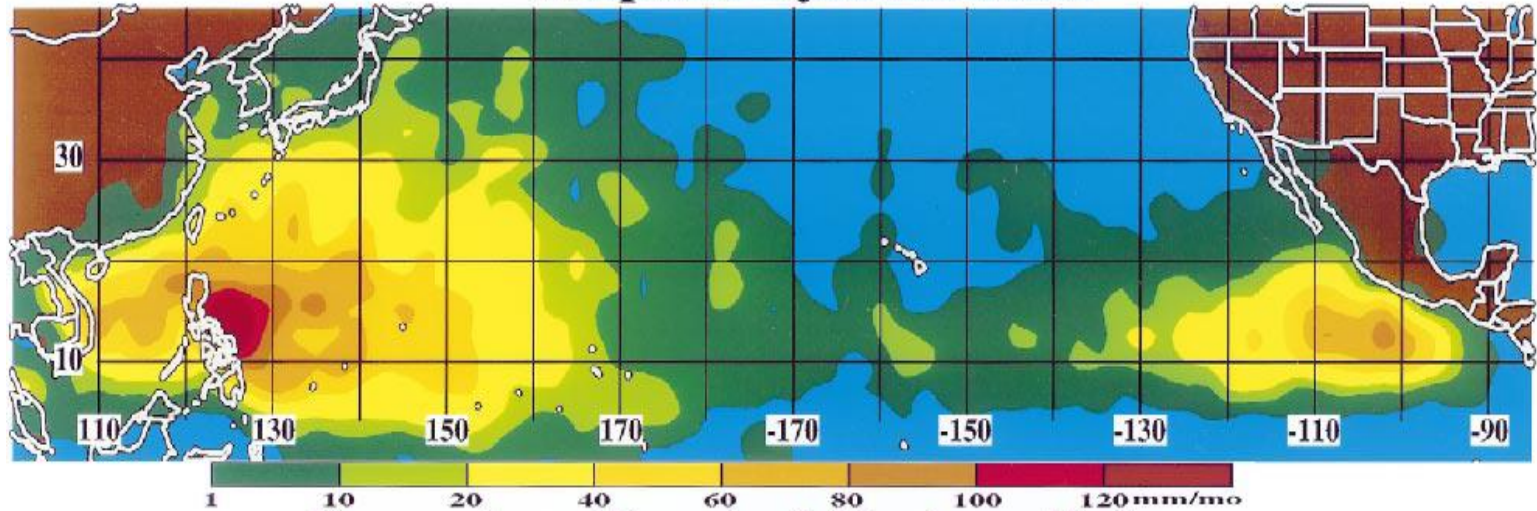


and quick

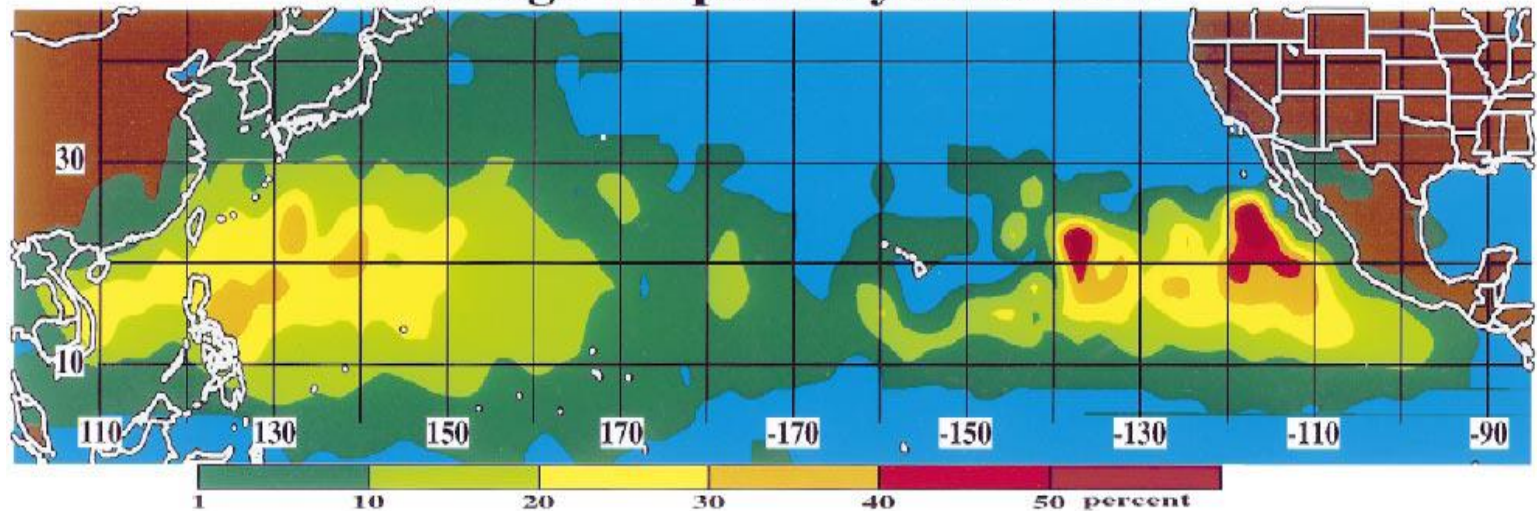
a new method is needed

Contribution of Tropical Cyclones to the North Pacific Climatological Rainfall as Observed from Satellite (June-November) (a certain radius)

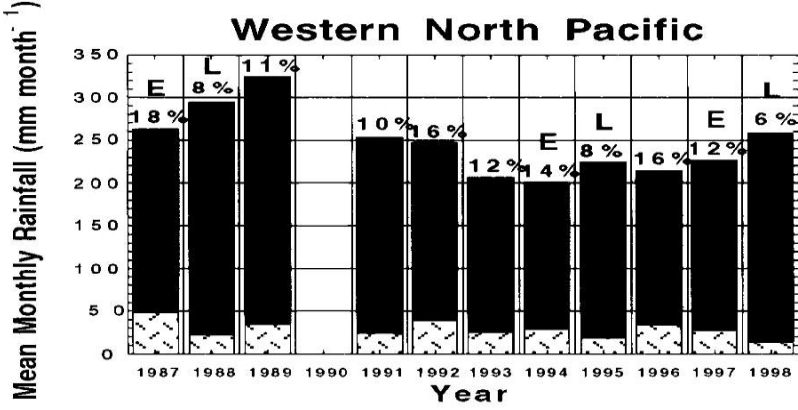
Tropical Cyclone Rain



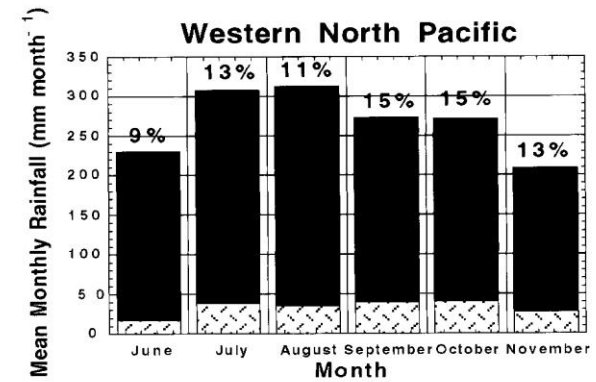
Percentage Tropical Cyclone Rain



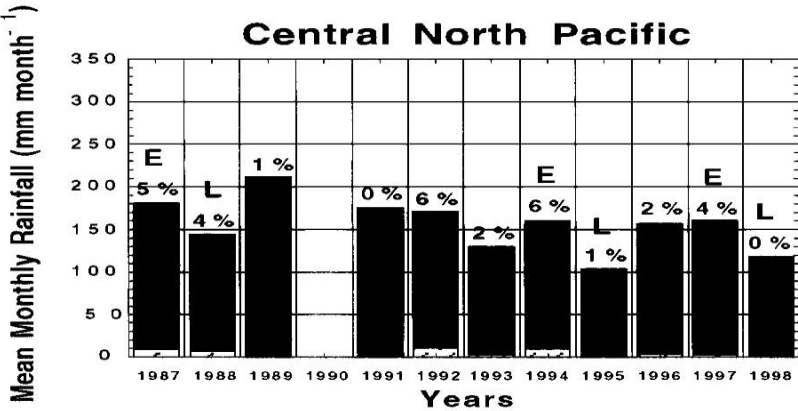
Rodgers 2000



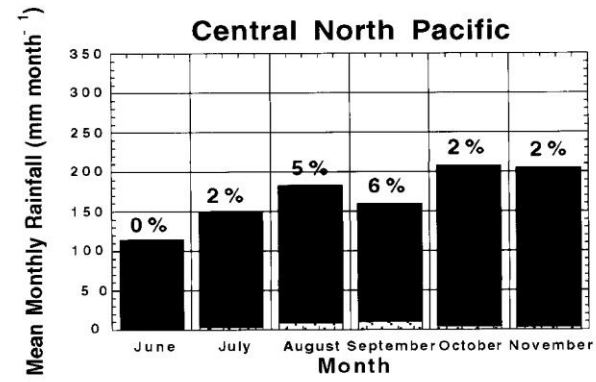
a



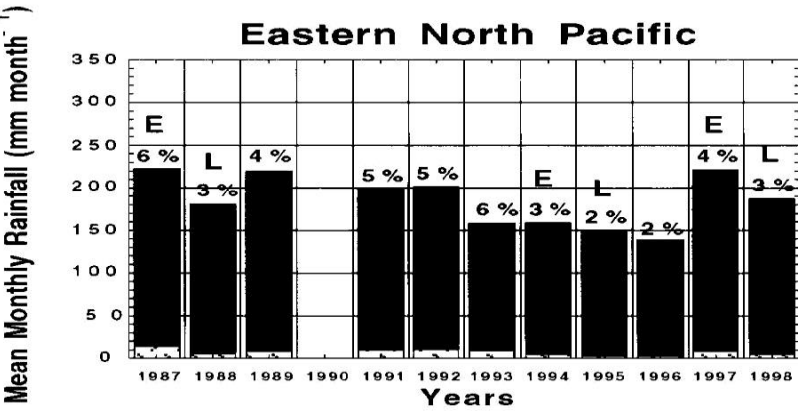
a



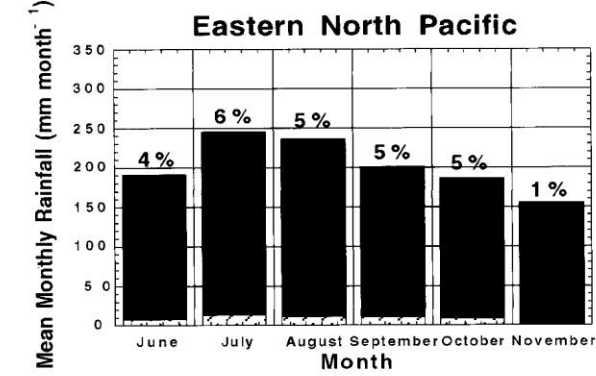
b



b

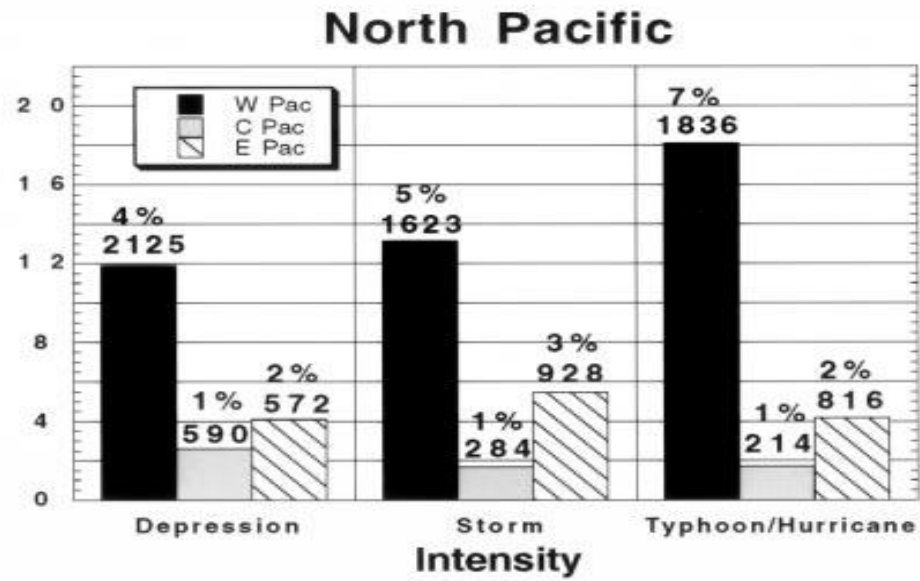


c



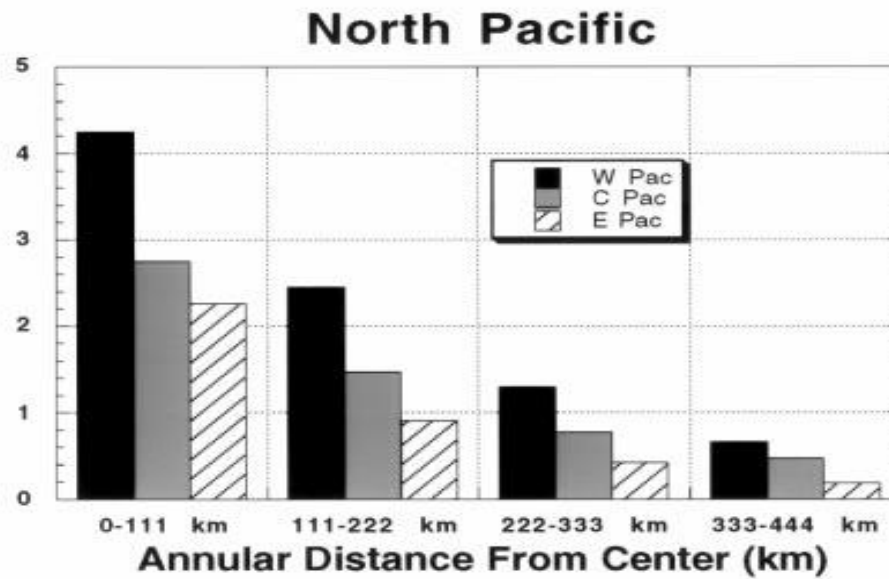
c

Mean Monthly Rainfall (mm month^{-1})



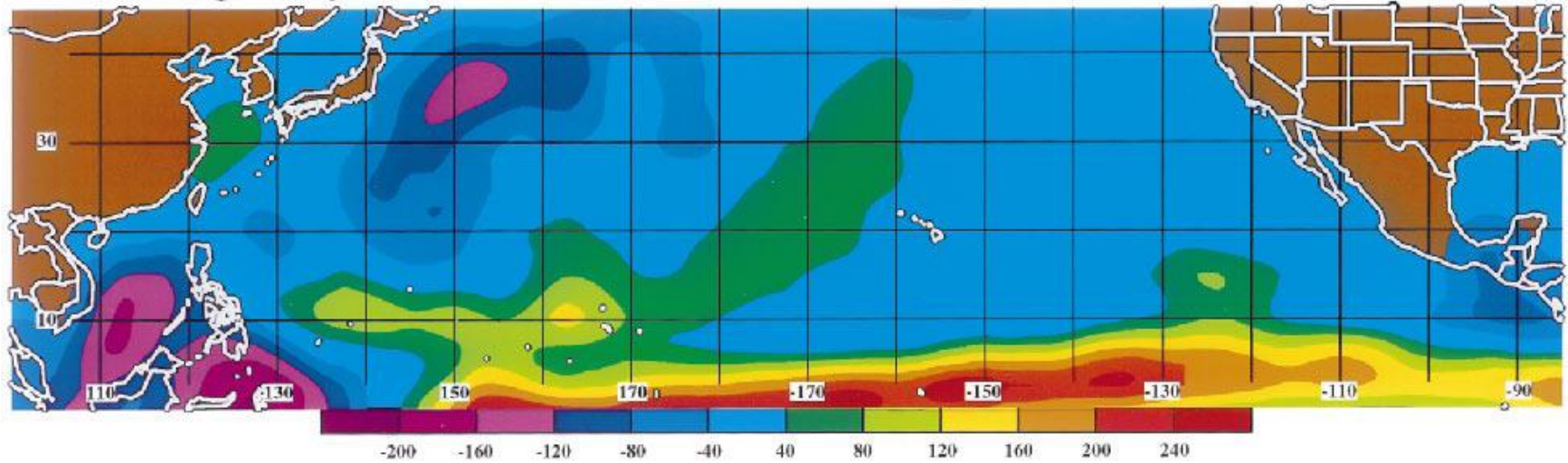
a

Mean Rain Rate (mm h^{-1})

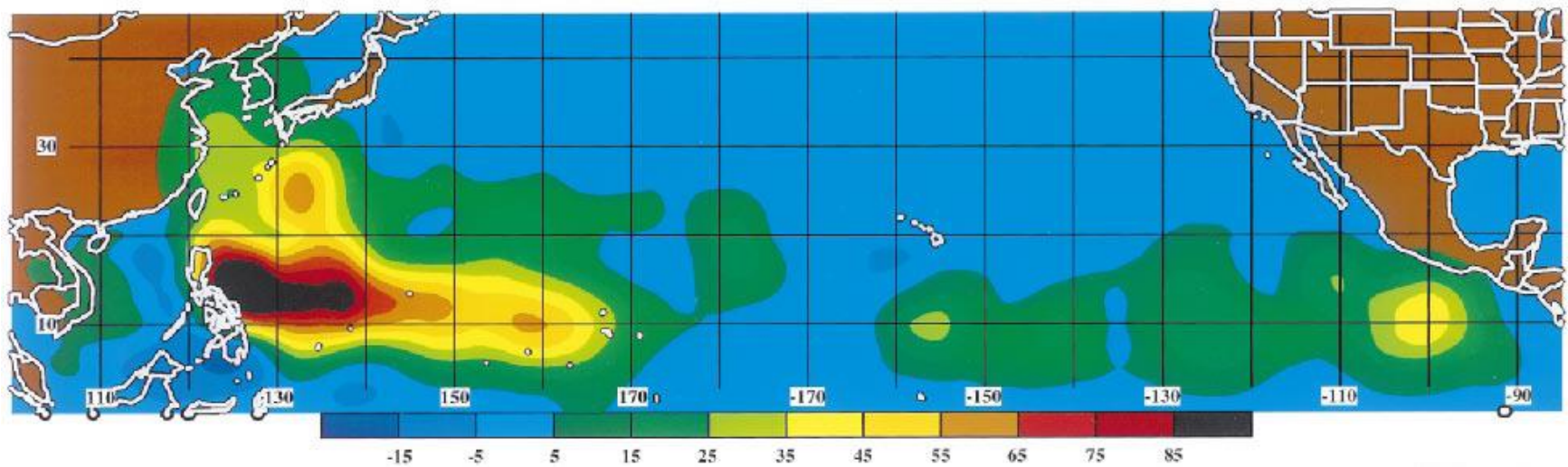


b

Non-Tropical Cyclone Rain Difference (mm/mo) Between El Nino and La Nina Years



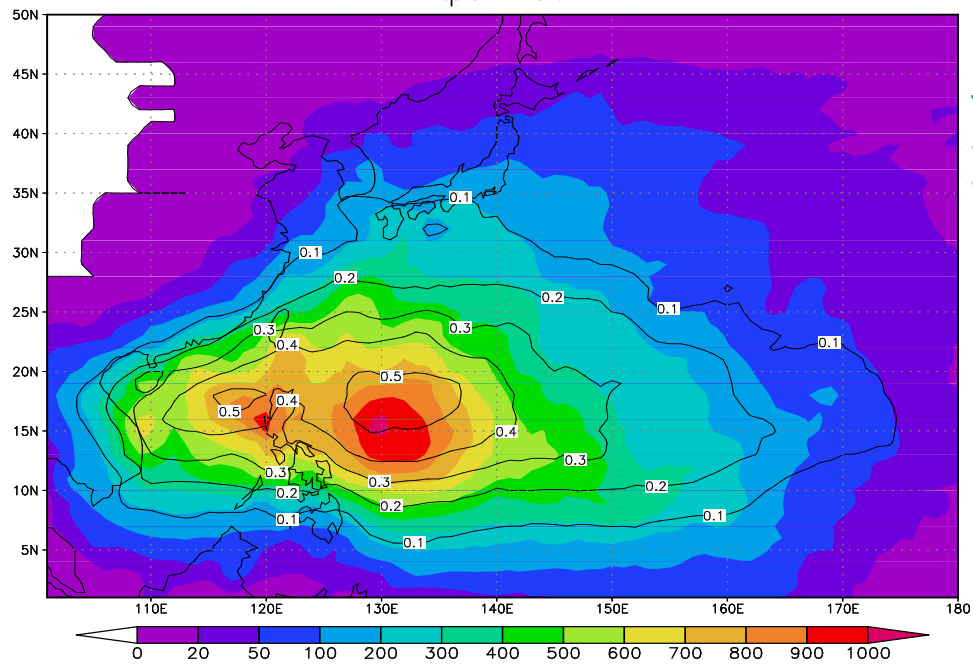
Tropical Cyclone Rain Difference (mm/mo) Between El Nino and La Nina Years



Roger

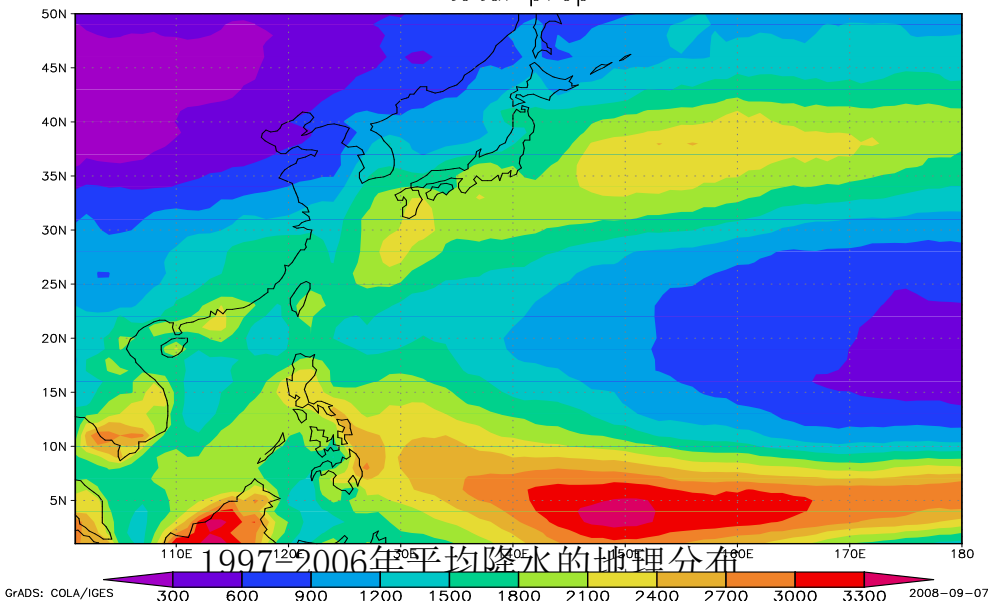
- 1) tropical cyclones contribute 12% of the rainfall to the Western North Pacific during the tropical cyclone
- 2) tropical cyclones contribute a maximum of 30% northeast of the Philippine Islands
- 3) in general, tropical cyclone rainfall is enhanced during the El Niño years by warm SSTs in the eastern North Pacific and by the monsoon trough in the western and central North Pacific.

tp97-06



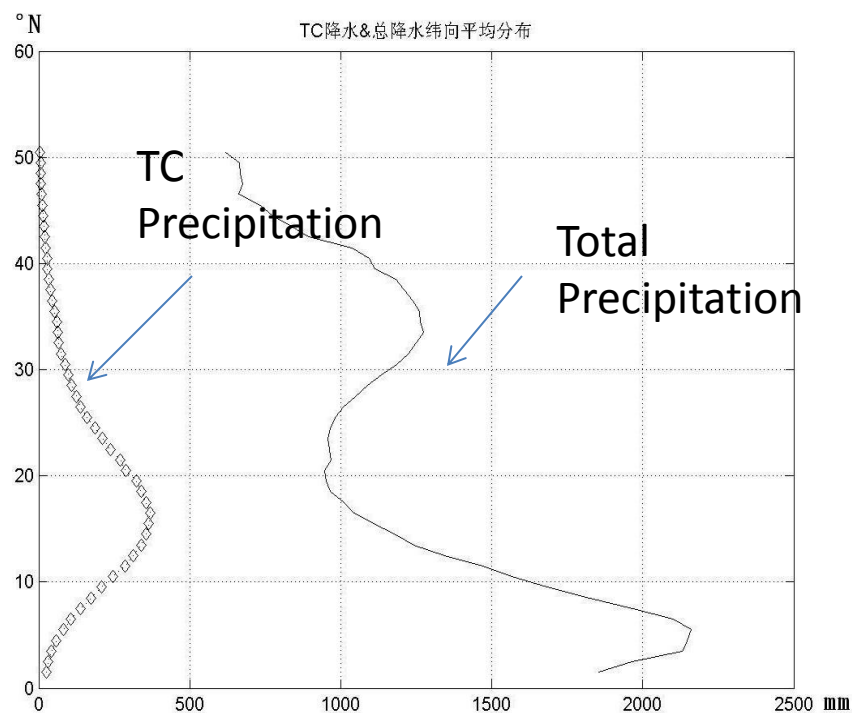
Annual TC rain and its percentage in total rain from 1997 to 2006 (after Wei 2010 using CMORPH data objective method)

total prcp



1997-2006年平均降水的地理分布

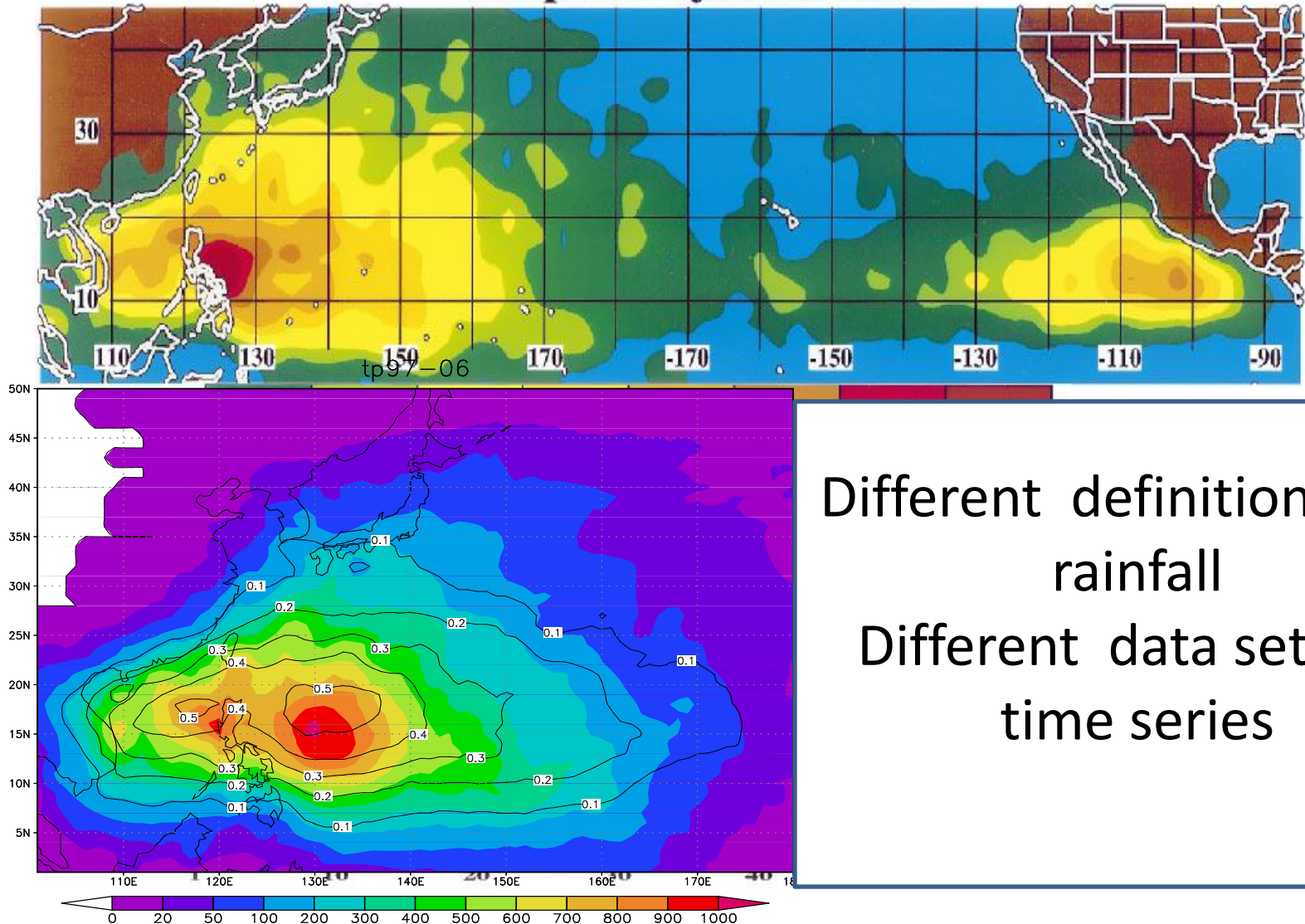
TC降水&总降水纬向平均分布



Average TC precipitation and Total precipitation with Latitude over northwestern Pacific

Comparison between Roger and Wei

Tropical Cyclone Rain



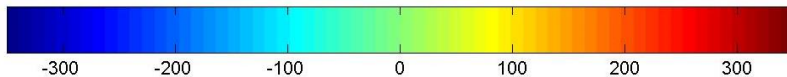
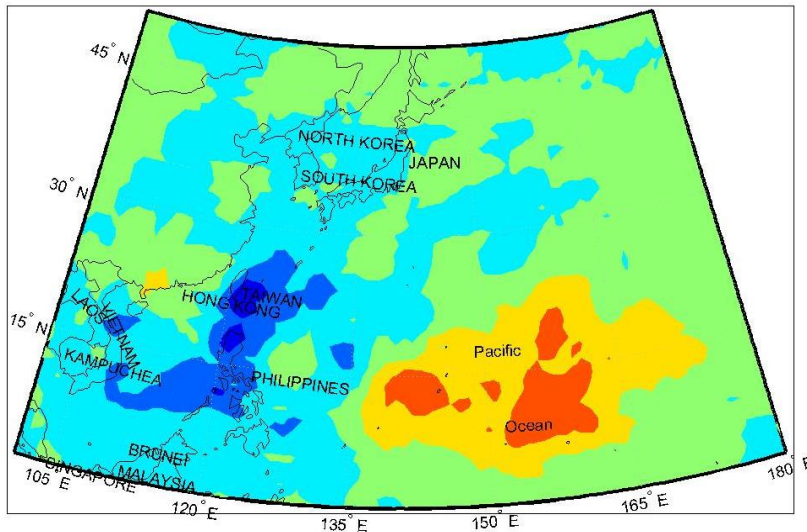
Anomalies of TC precipitation in El Nino and La Nina year from 1997-2006

El Nino年: 1997 2002 2006

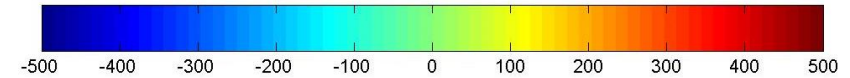
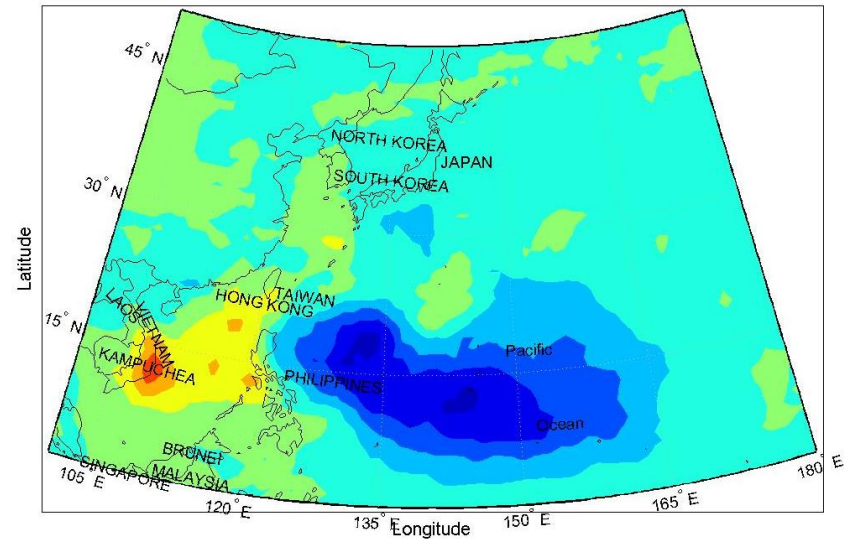
La Nina年: 1998 1999 2000

El Nino

el-a



La Nina



TC frequency, influence day duration and average rainfall of TC

El Nino **La Nina**

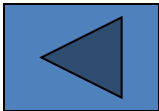
| year | 1997 | 1998 | 1999 | 2000 | 2001 | 2002 | 2003 | 2004 | 2005 | 2006 |
|---|------|------|------|------|------|------|------|------|------|------|
| TC Frequency | 29 | 21 | 28 | 28 | 29 | 29 | 25 | 34 | 24 | 28 |
| Influence day | 167 | 89 | 109 | 141 | 157 | 154 | 169 | 202 | 118 | 172 |
| Duration (day) | 5.8 | 4.2 | 3.9 | 5.0 | 5.4 | 5.3 | 6.8 | 5.9 | 4.9 | 6.1 |
| Volume of TC rainfall 10^4km^3 | 0.29 | 0.22 | 0.18 | 0.24 | 0.29 | 0.29 | 0.32 | 0.3 | 0.25 | 0.25 |

Climate Features of TCP over China 1957-2005

Annual climatic characteristics

Seasonal variations

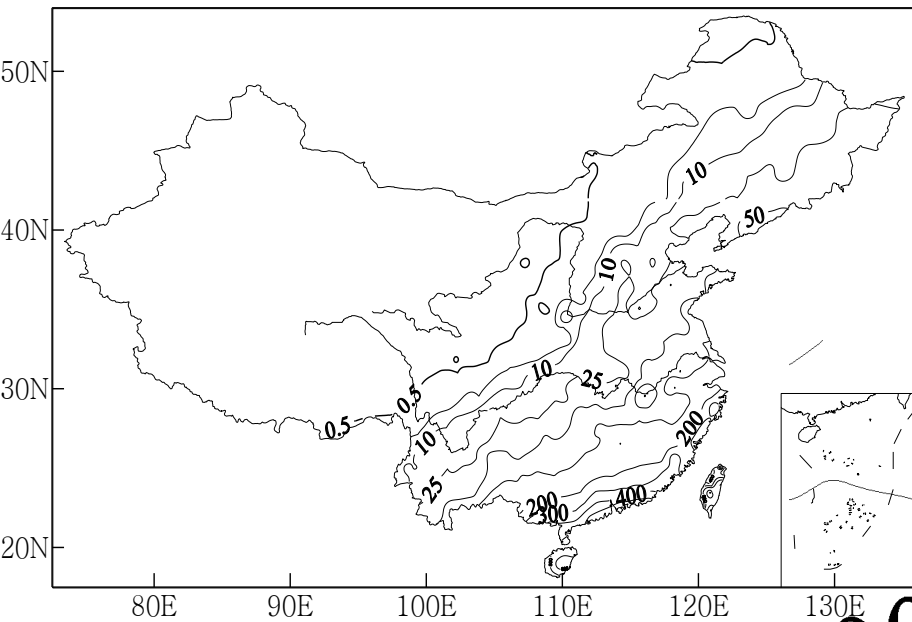
**Climate changes
(Fu et. al 2008)**



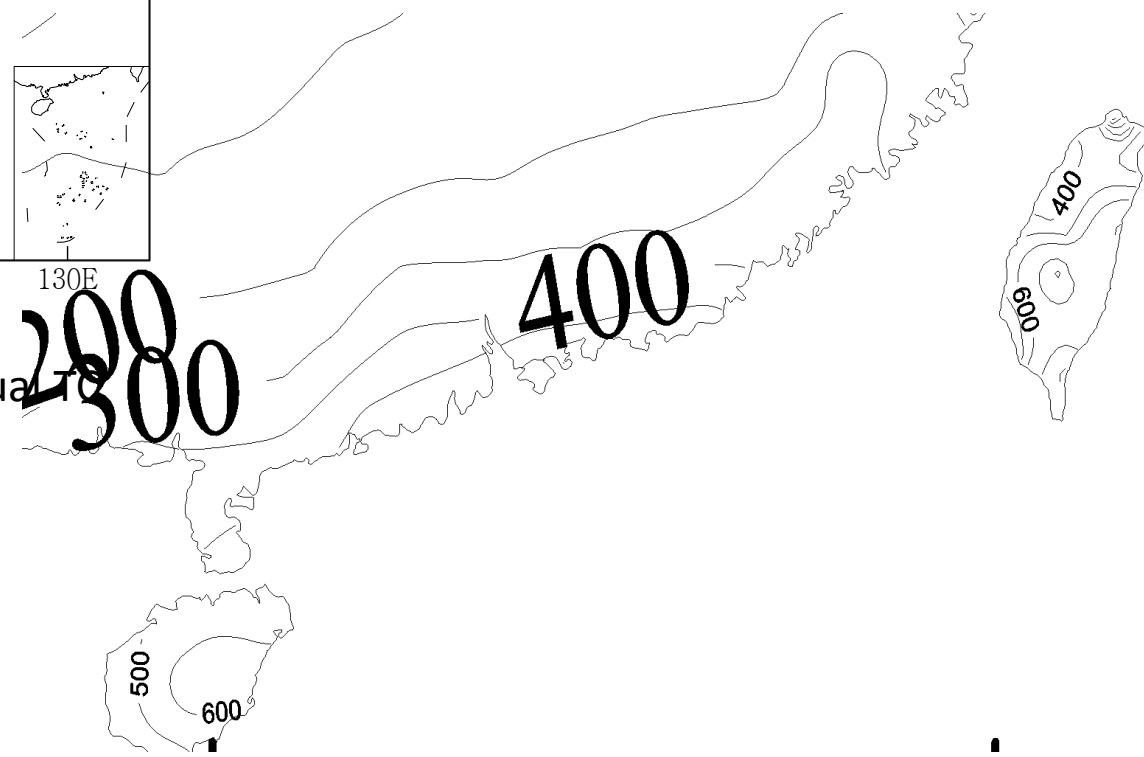
Climate Features of TCP over China

Climate Features of TCP over China

Annual climatic characteristics(1)



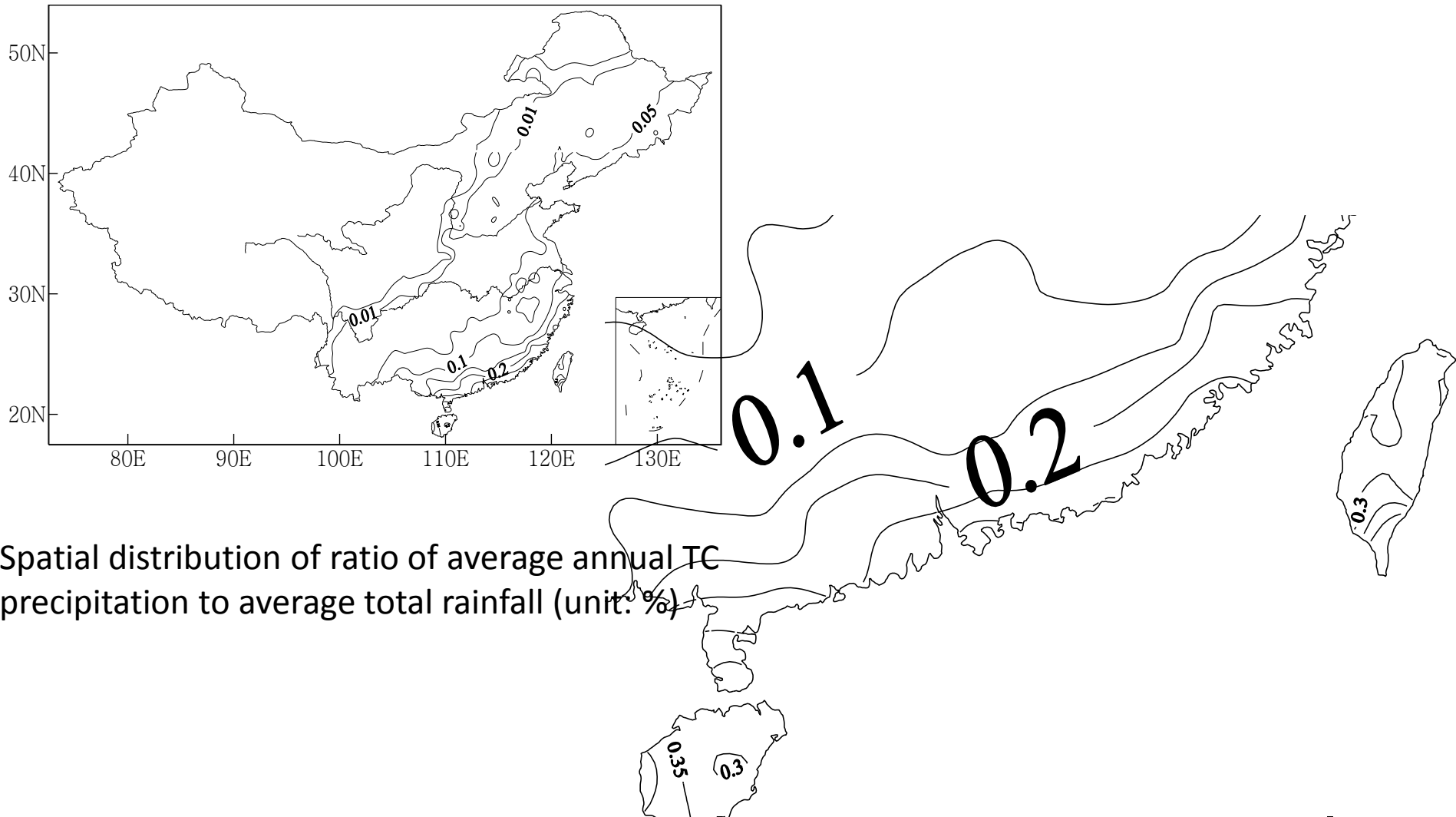
Spatial distribution of average annual TCP precipitation (unit: mm)



Climate Features of TCP over China

Climate Features of TCP over China

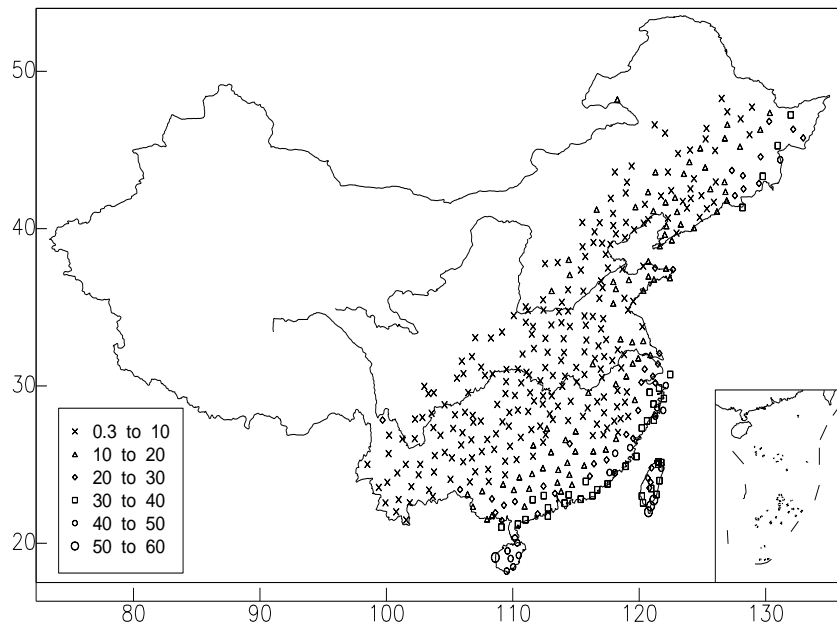
Annual climatic characteristics(2)



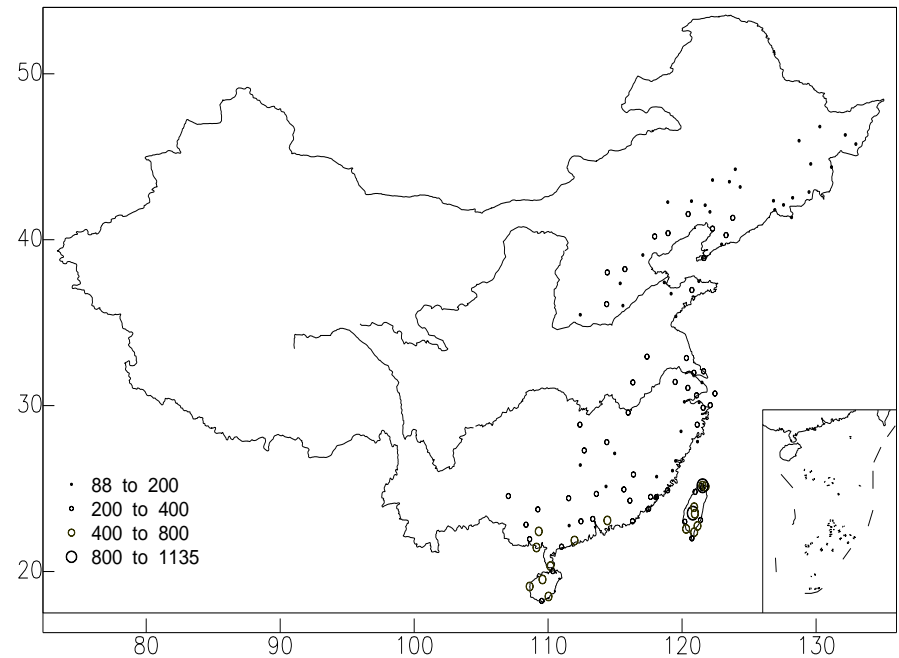
Climate Features of TCP over China

Annual climatic characteristics(3)

statistics of station TC torrential precipitation($\geq 50\text{mm}/\text{day}$)



Spatial distribution of ratio of number of days with TC torrential precipitation to number of days with precipitation (unit: %)



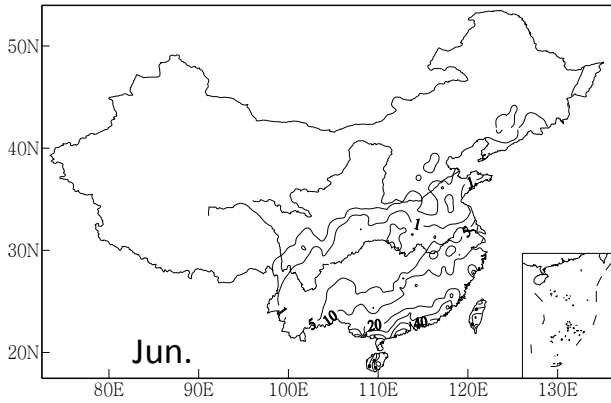
Spatial distribution of record torrential precipitation which is from TC (unit: mm)

Climate Features of TCP over China

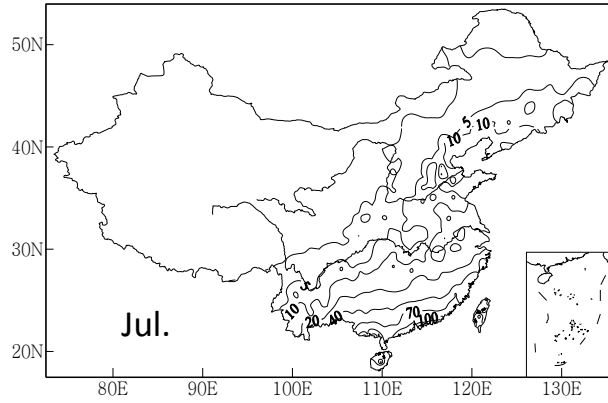
Seasonal variations(1)

Spatial distribution of average monthly typhoon precipitation (unit: mm)

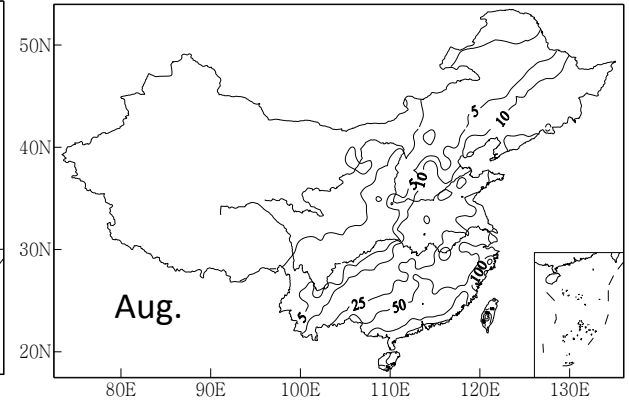
monthly mean TCP for Jun.



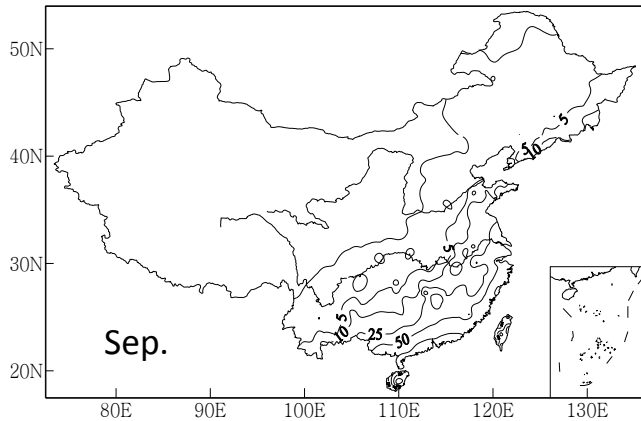
monthly mean TCP for Jul.



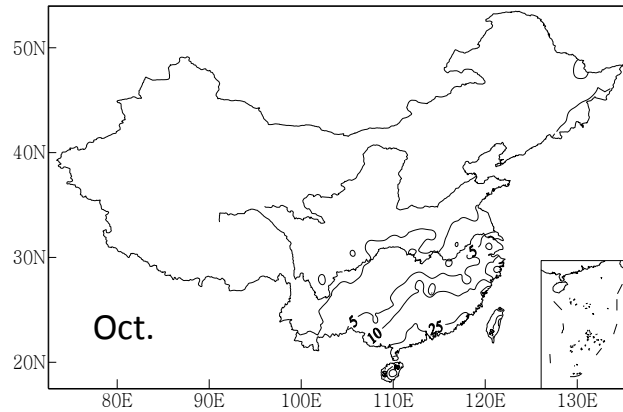
monthly mean TCP for Aug.

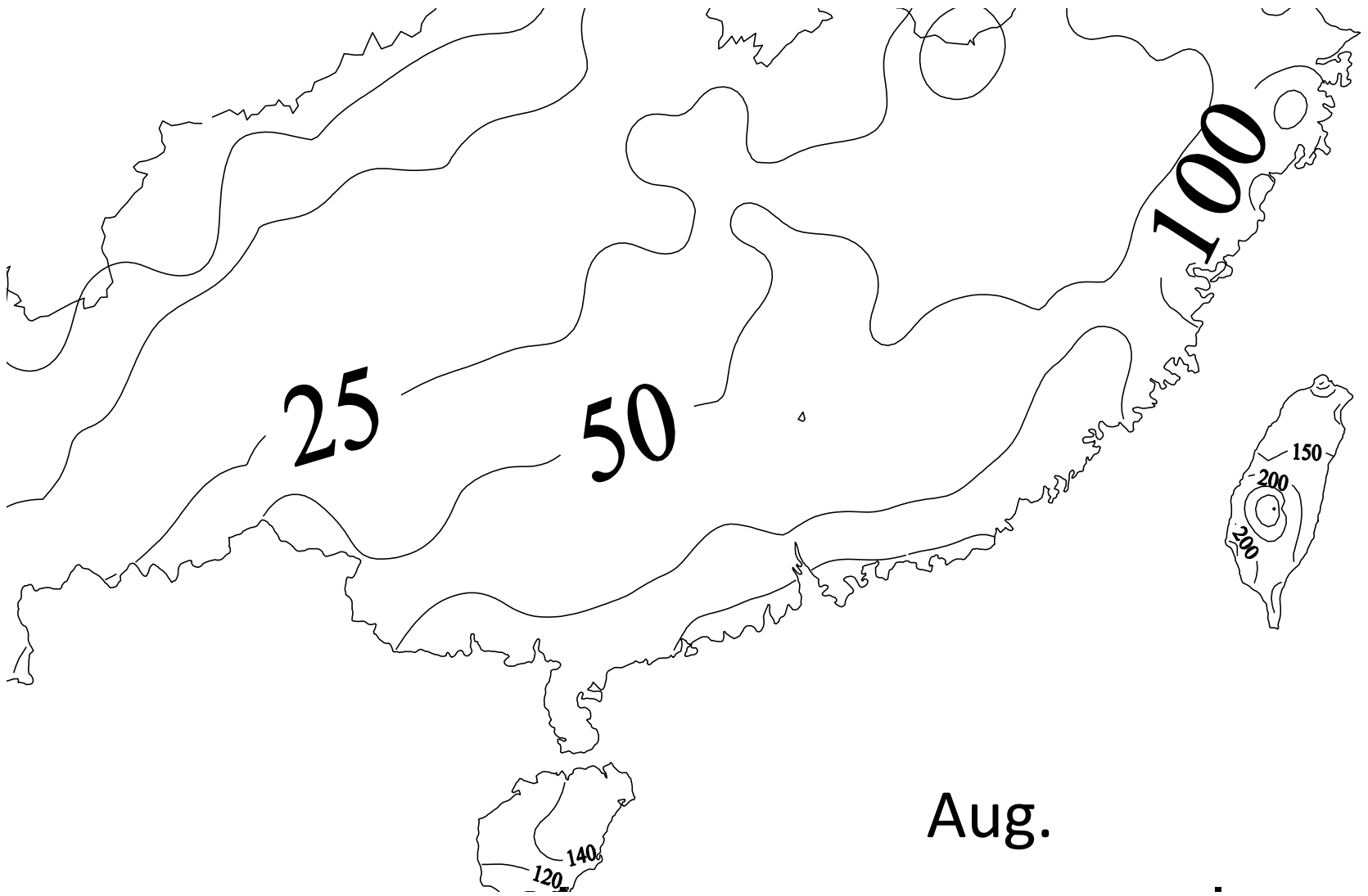


monthly mean TCP for Sep.



monthly mean TCP for Oct.





Aug.

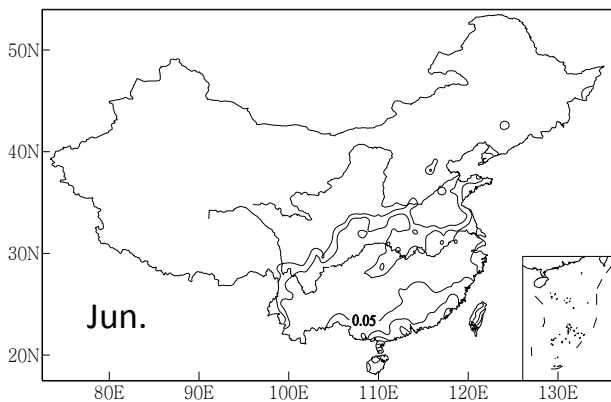
Climate Features of TCP over China

Climate Features of TCP over China

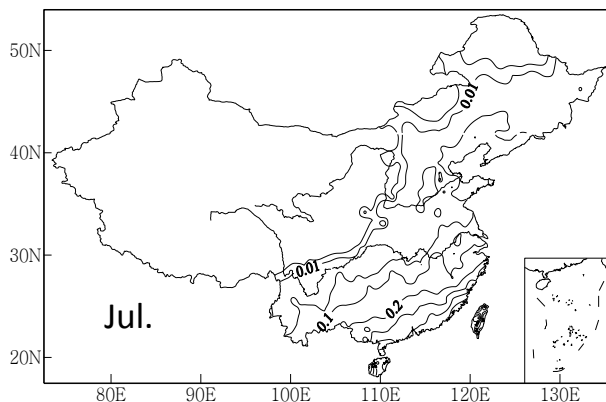
Seasonal variations(2)

Spatial distribution of ratio of average monthly typhoon precipitation to average total rainfall (unit: %)

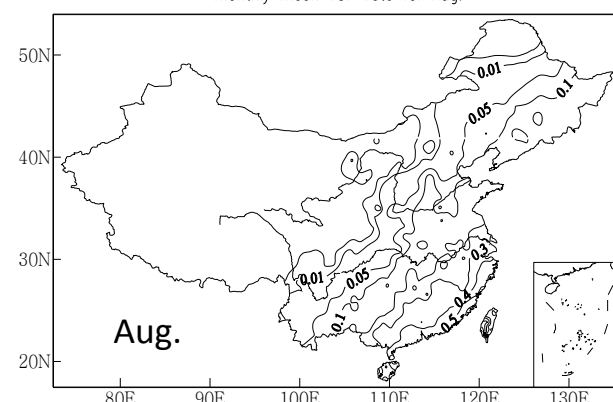
monthly mean TCP rate for Jun.



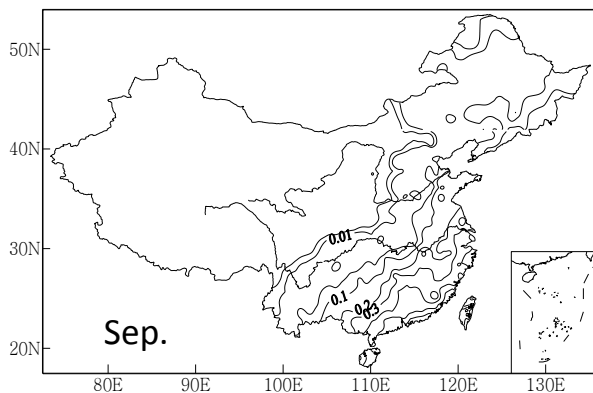
monthly mean TCP rate for Jul.



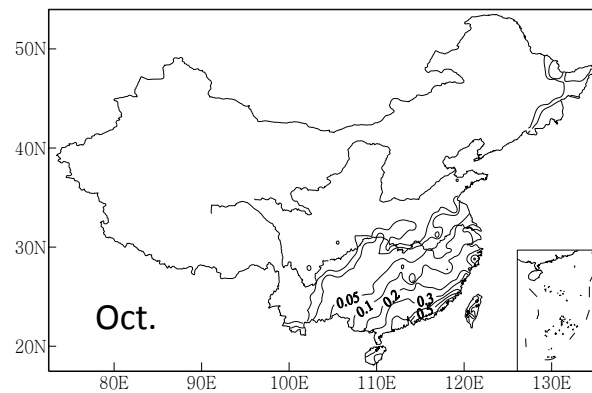
monthly mean TCP rate for Aug.

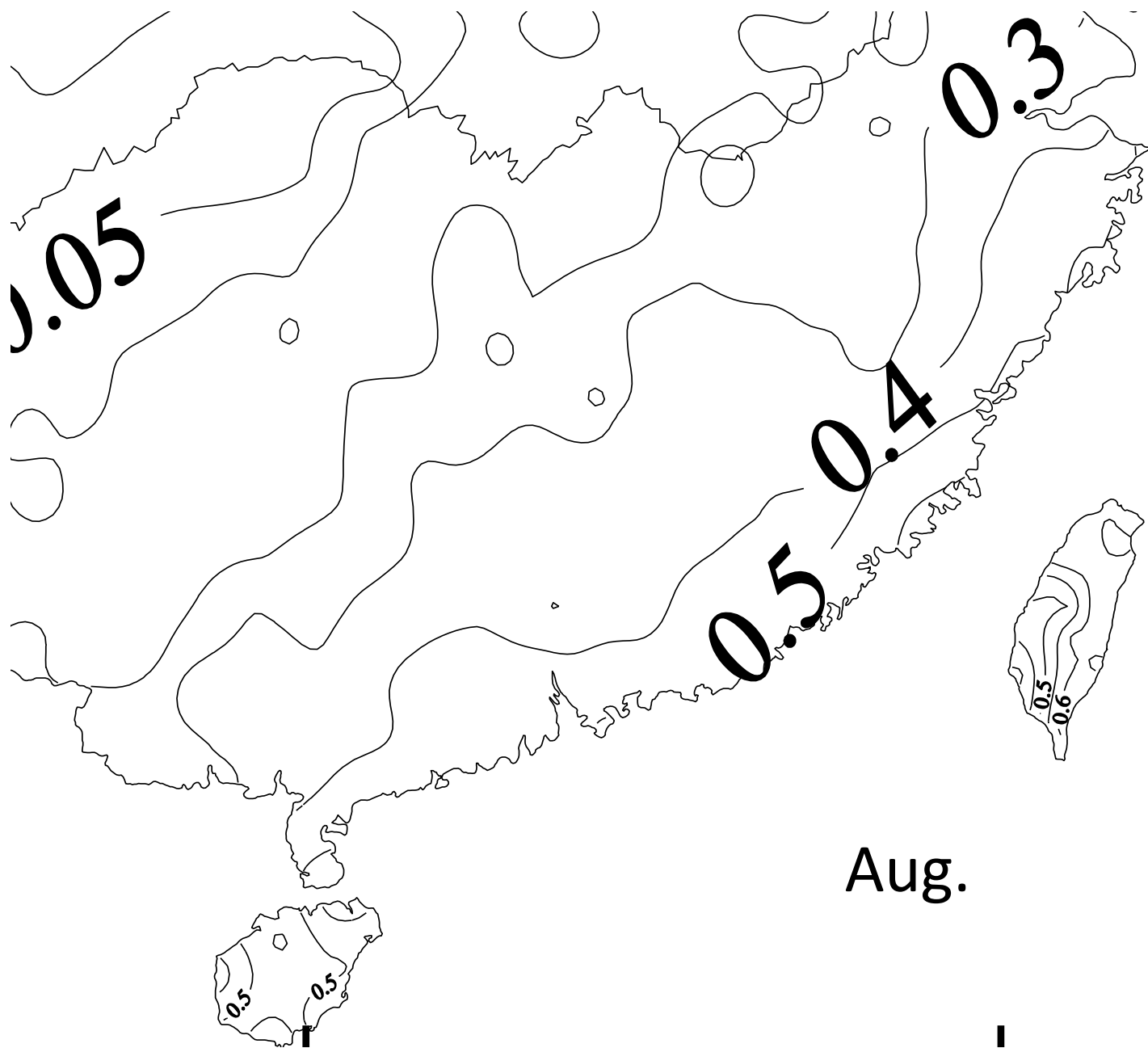


monthly mean TCP rate for Sep.



monthly mean TCP rate for Oct.





Aug.

I

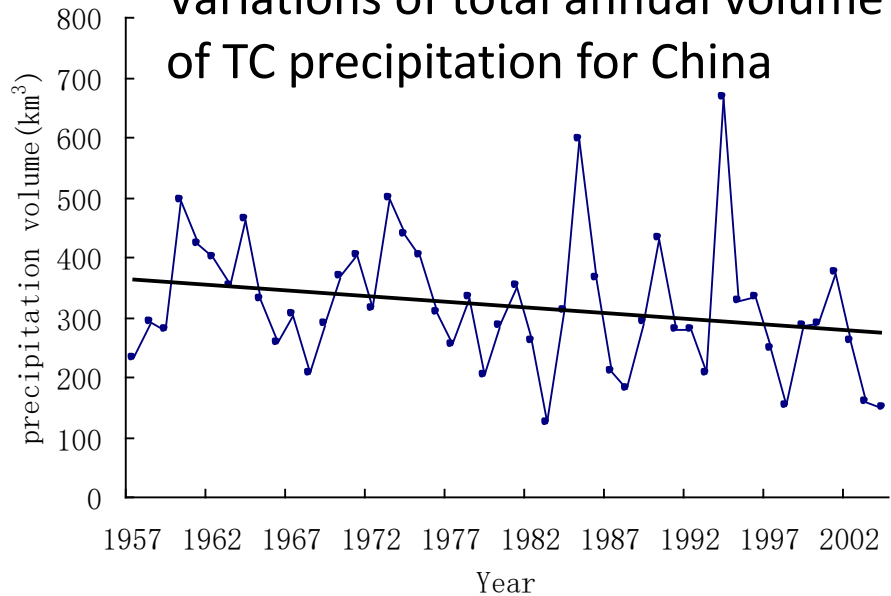
I

Climate Features of TCP over China

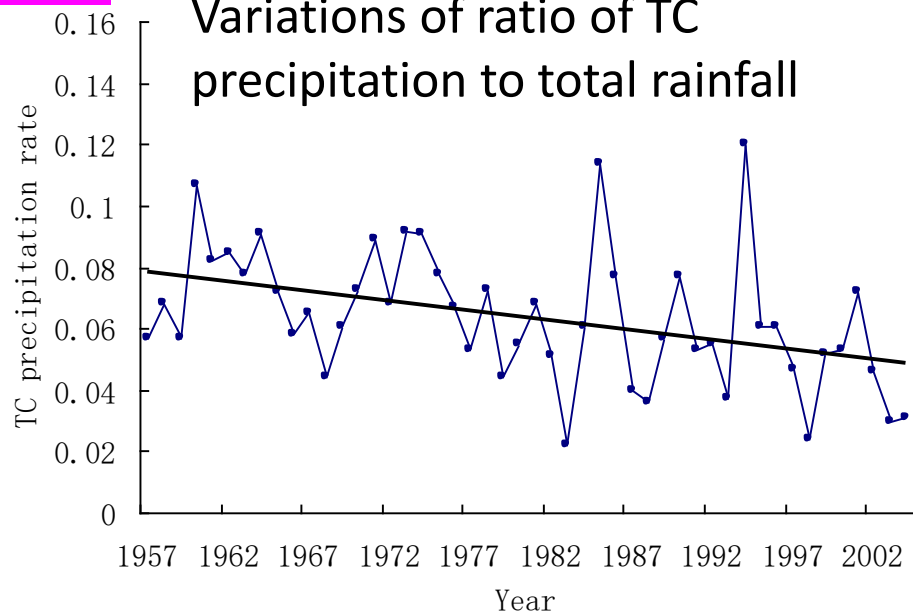
Climate Features of TCP over China

Climate changes(1)

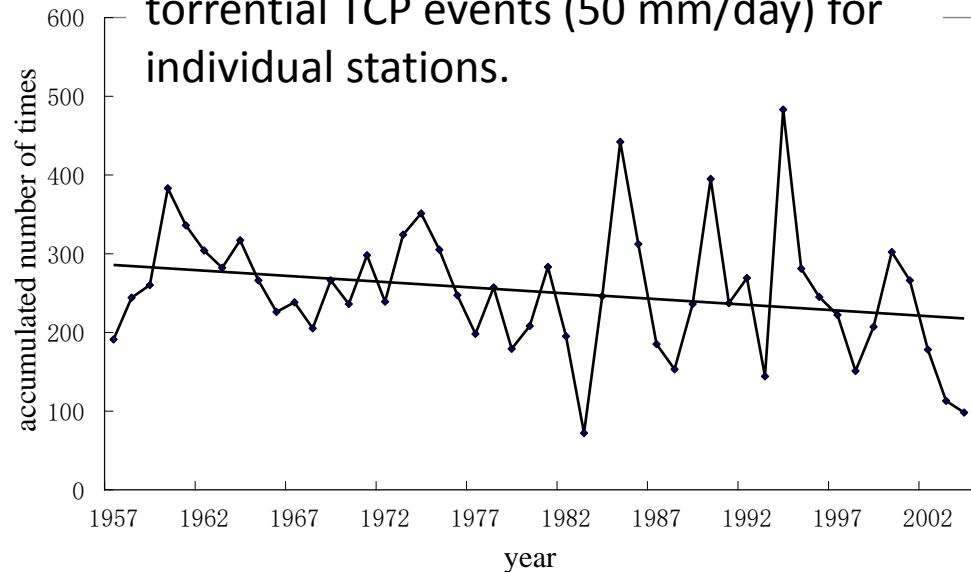
Variations of total annual volume of TC precipitation for China



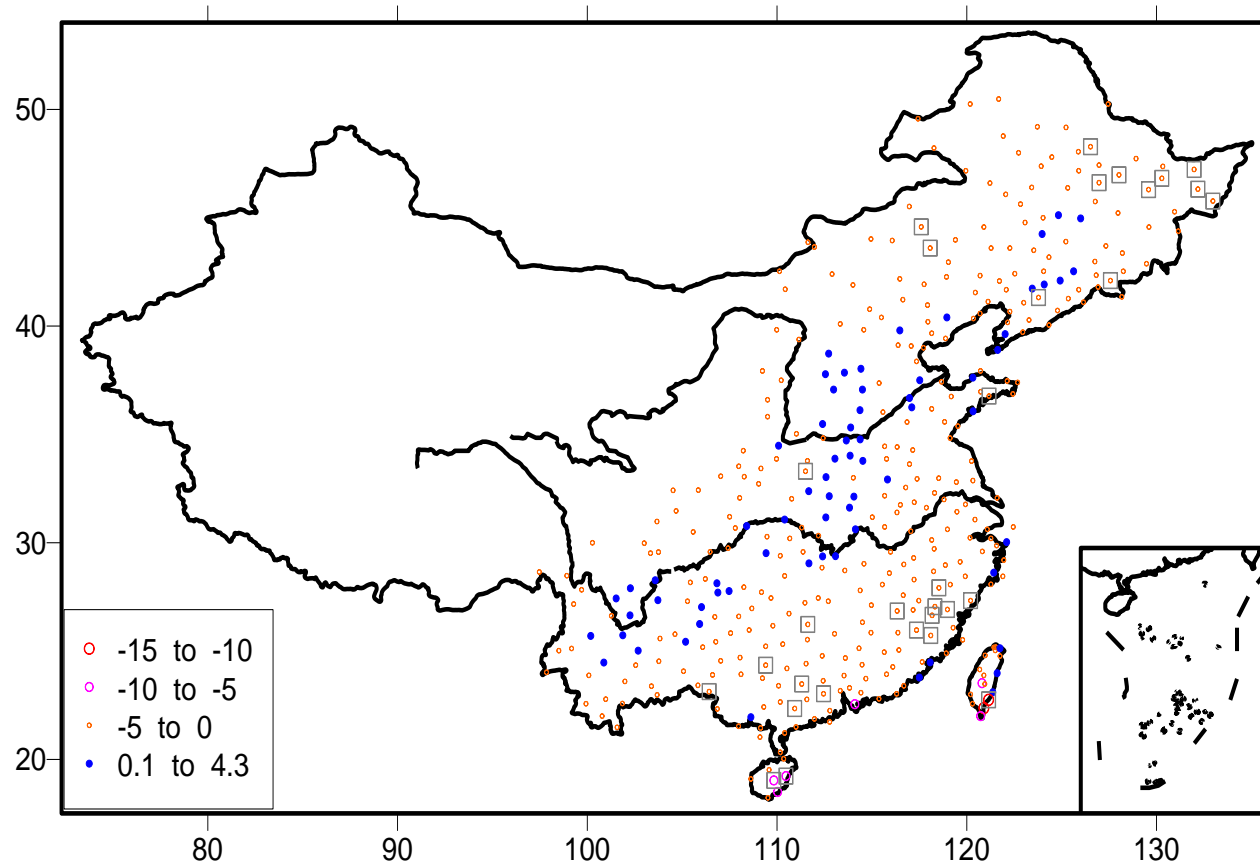
Variations of ratio of TC precipitation to total rainfall



Accumulated number of times with torrential TCP events (50 mm/day) for individual stations.



Climate changes(2)

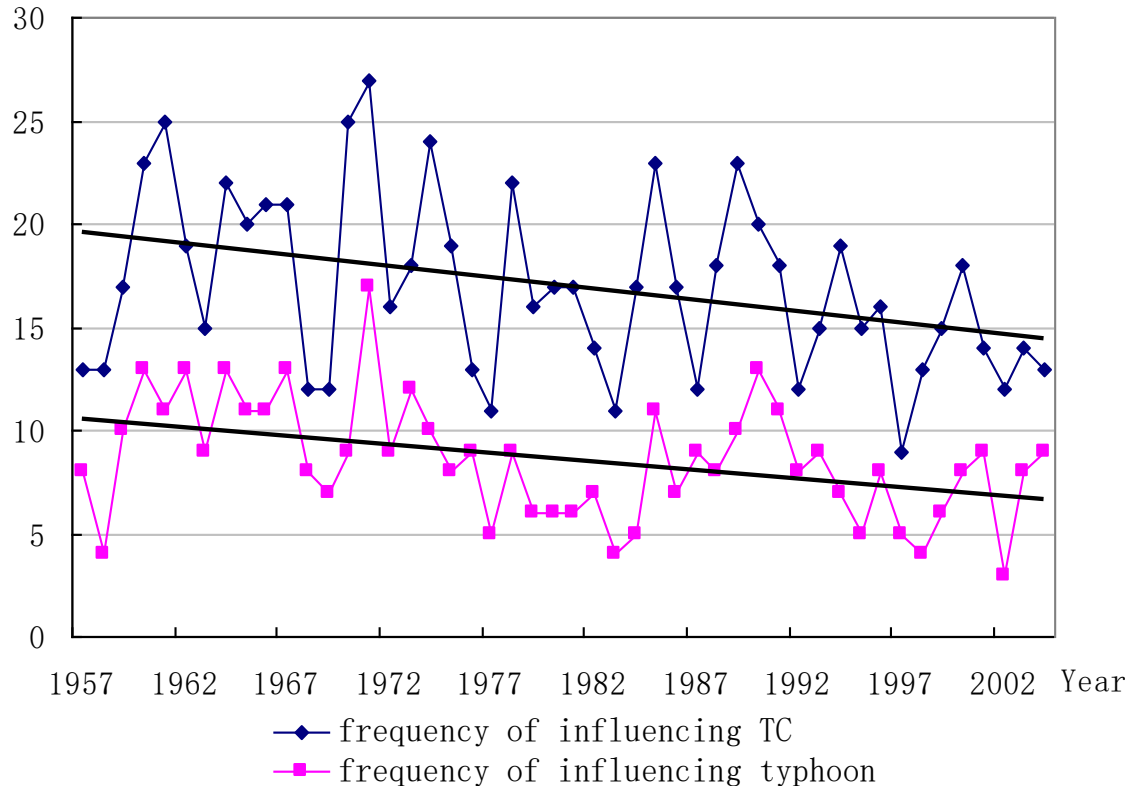


Spatial distribution of trends of annual TC precipitation 1957 to 2005

(square boxes indicating statistically significant at 0.05 level by Kendall test)

Despite interdecadal and interannual variations, a significant downward trend is found in the TCP volume, the total annual frequency of the torrential TCP events and the ratio of TC precipitation to total rainfall over the past about 50 years.

Climate changes(3)



Variations of frequency of influencing TC and influencing typhoon (MSWS $\geq 32.7\text{m/s}$) for China

coefficients with TC precipitation are 0.62 and 0.47, respectively

Tropical Cyclone– and Monsoon-Induced Rainfall Variability in Taiwan

Chen et. al 2010

- 1) Climatologically, what are the relative contributions of rainfall subcomponents associated with monsoon and TC activity to total rainfall for Taiwan?
- 2) On an interannual time scale, what are the major rainfall variability types induced by monsoon and TC activity for Taiwan? What are the corresponding large scale processes regulating rainfall variability?
- 3) Does the present approach of analyzing rainfall by two major subcomponents help us to better understand interannual rainfall variability as compared with the conventional approach of using total rainfall as an index?

Tropical Cyclone– and Monsoon-Induced Rainfall Variability in Taiwan

Chen et. al 2010 (July–September for the period 1950–2002)

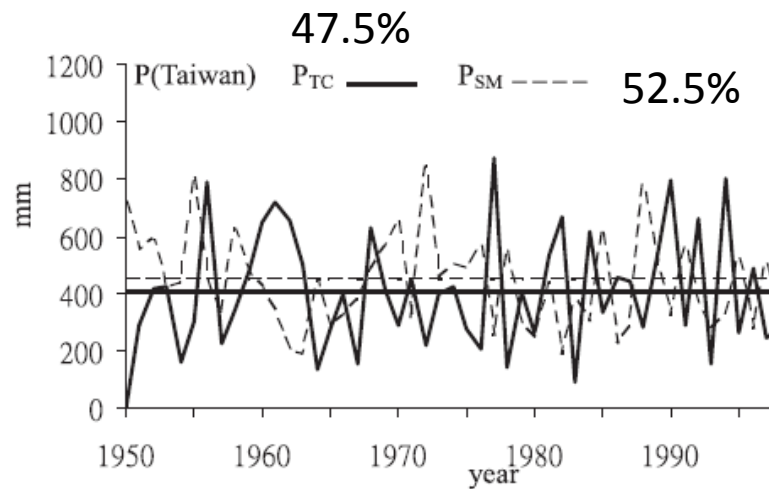


FIG. 4. The 1950–2002 time series of P_{TC} and P_{SM} averaged 10 major stations in Taiwan.

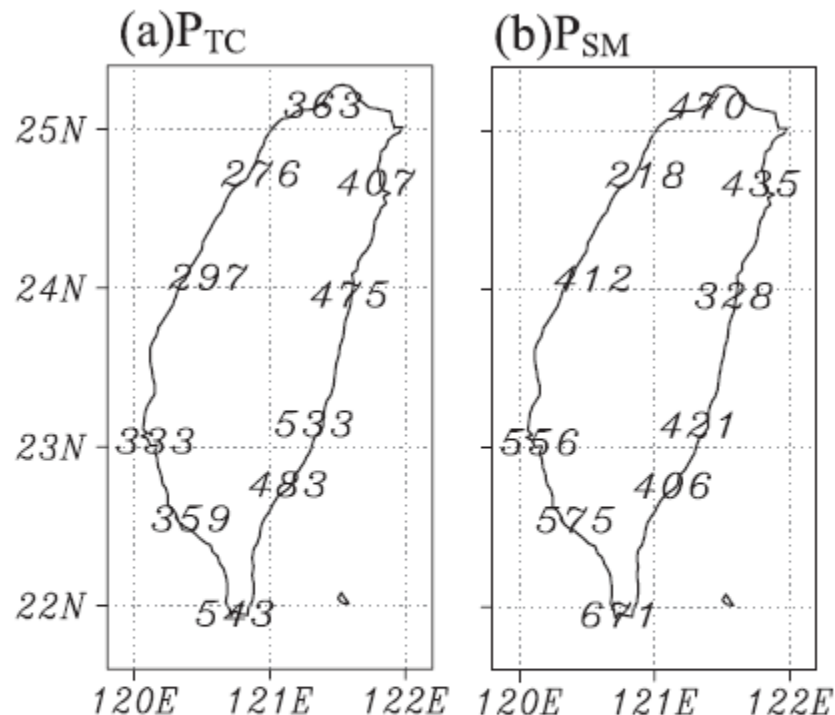


FIG. 3. The 1950–2002 climatology of rainfall subcomponents accumulated throughout July–September in the 10 major stations over Taiwan: (a) TC rainfall and (b) seasonal monsoon rainfall; unit: mm.

PSM and PTC tend to vary inversely, with a simultaneous negative correlation (-0.46) between their 1950–2002 time series.

Tropical Cyclone– and Monsoon-Induced Rainfall Variability in Taiwan

Chen et. al 2010

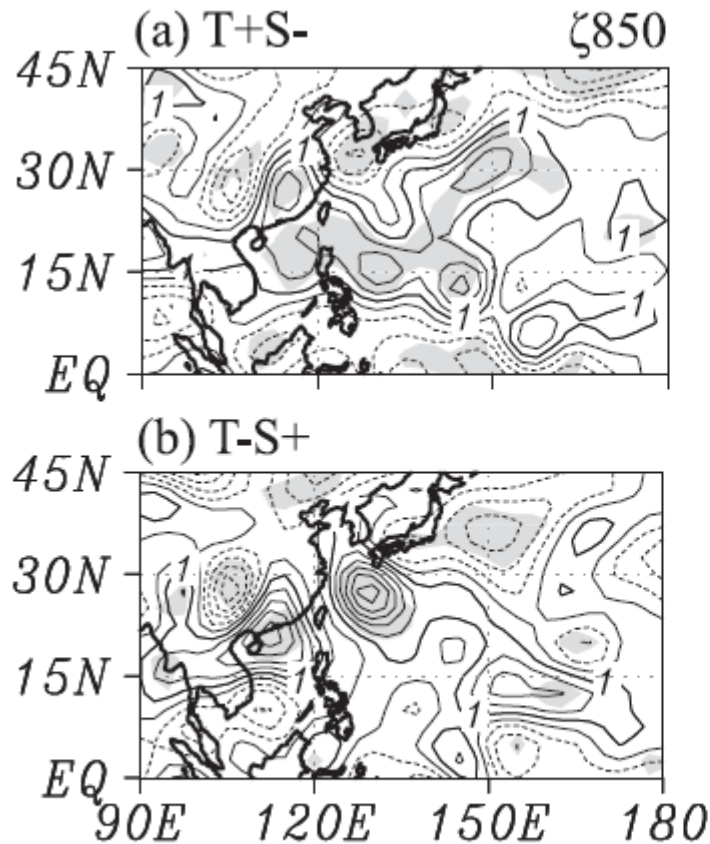


FIG. 9. As in Fig. 6, but for composite anomalies of 850-hPa relative vorticity. Contour intervals are $1 \times 10^{-5} \text{ s}^{-1}$. Composite anomalies significant at the 95% level are shaded.

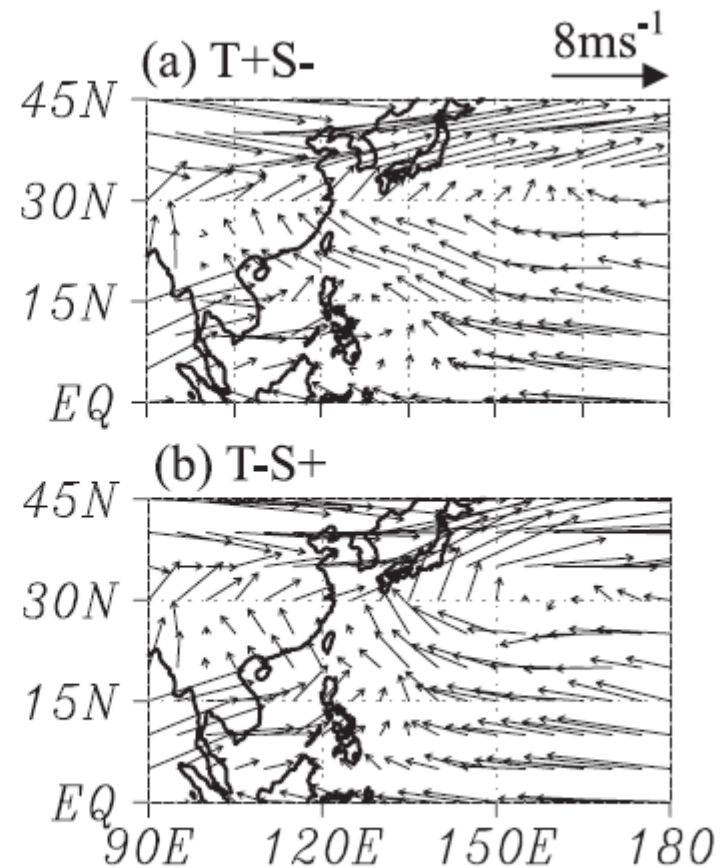


FIG. 10. Composite mean winds averaged from 850 to 400 hPa to represent steering flows for the two rainfall variability types.

Tropical Cyclone– and Monsoon-Induced Rainfall Variability in Taiwan

Chen et. al 2010

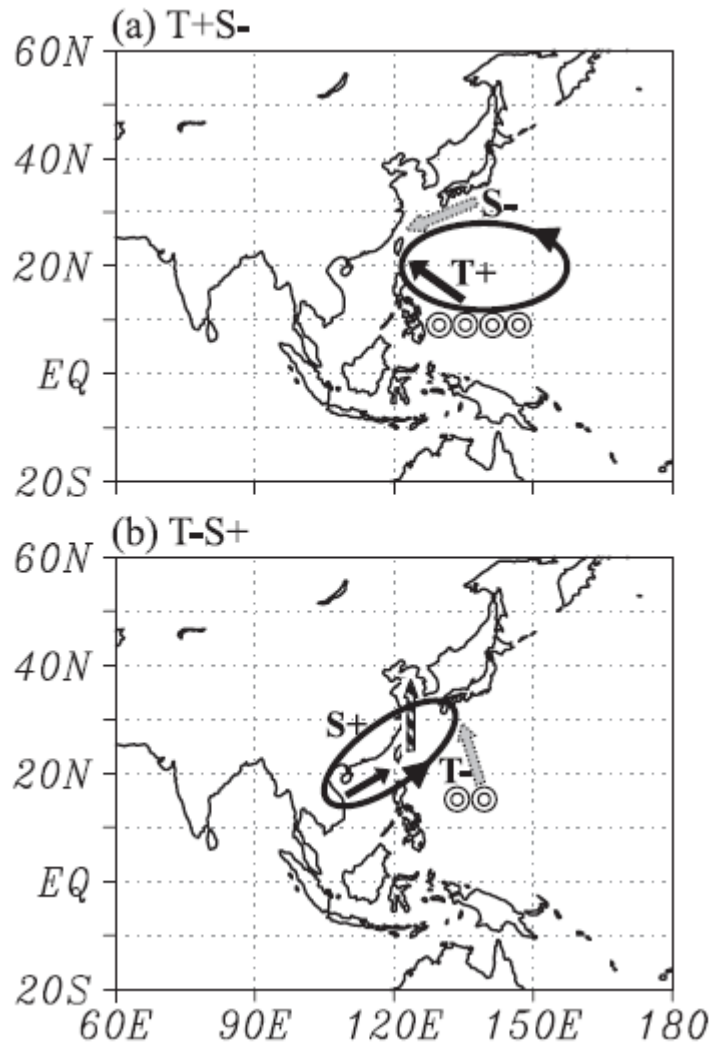


FIG. 12. Schematic diagrams for the major processes regulating rainfall variability in Taiwan: (a) the T+S- type and (b) the T-S+ type. In (a), decreased P_{SM} (S-) is caused by anomalous north-easterly water vapor fluxes (light arrow) and weak vertical motion over the western boundary of the anomalous cyclone. Increased P_{TC} (T+) concurs with more TC formation in the regions southeast of Taiwan (more \odot symbols) and mean southeasterly flows to steer TCs toward Taiwan (dark solid arrow). In (b), increased P_{SM} (S+) is induced by strong ascending motion (dark slashed arrow) and enhanced water vapor fluxes from the SCS into Taiwan (dark solid arrow) nearby the anomalous cyclone center. Decreased P_{TC} (T-) concurs with reduced TC formation (fewer \odot symbols) and mean southerly flows to guide TCs toward Japan and the North Pacific (light arrow).

These findings are potentially useful for improved regional climate prediction. Because the physical mechanisms that regulate the two rainfall subcomponents are different, it is necessary to predict TC and seasonal monsoon rainfall anomalies separately by building different statistical models.

Tropical cyclones and heavy rainfall in Fujian Province, China(66 station 1960-2007, Yin et. al 2010)

The number of heavy rain days is higher during El Niño years, although the number of TCs affecting Fujian in general is higher during La Niña years

On an average for the 30 coastal stations, 36 (El Niño years) and 28 (La Niña years) HRDs were measured 1960 to 2007. 56% of these were triggered by TCs during El Niño years and 47% of heavy rainfall days were triggered by TCs during La Niña years.

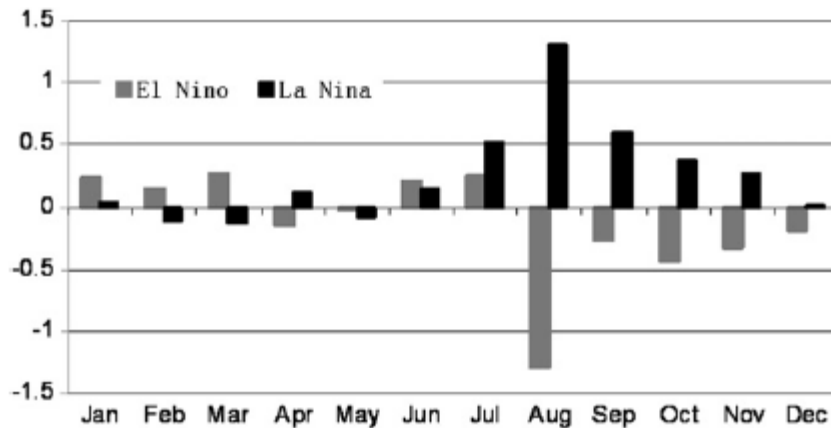


Fig. 3. Monthly deviation of tropical cyclones in the west North Pacific 1949–2007 during El Niño/La Niña years (0 depicts the monthly average).

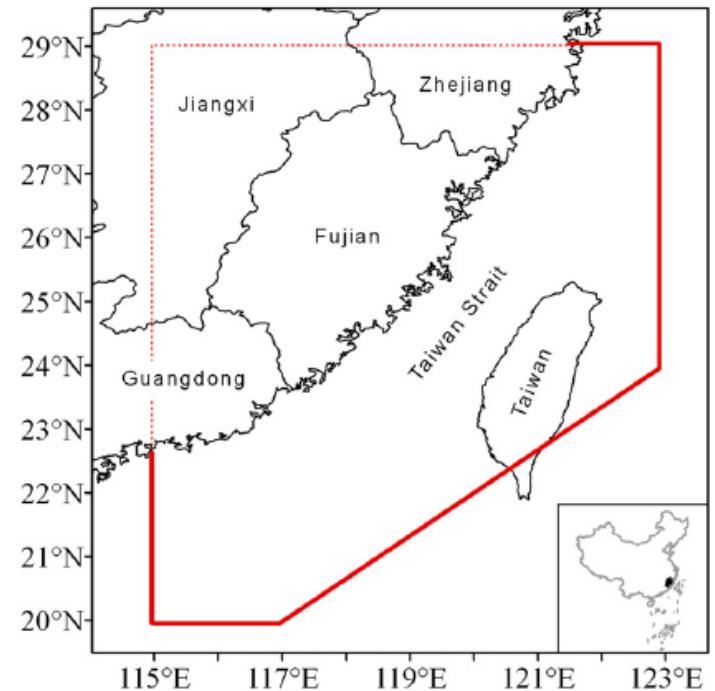


Fig. 1. Location of Fujian Province and zone marking impact of tropical cyclones.

◆ Overview of TC rainfall over Monsoon region in Western North Pacific

- Early development
- TC rainfall climatology

➤ **TC rainfall structure**

Rainfall structure in tropical cyclone (Rodgers et, al 1994 SSM/I)

- found that more intense systems had higher rain rates, more latent heat release, and a greater contribution from heavier rain to the total tropical cyclone rainfall.
- Heaviest rain rate were found near the center of the most intense tropical cyclones.
- Greatest rain rates in the inner-core regions were found in the right (forward) half of fast(slow)-moving tropical cyclone
- Found correlation of the changes inner core rainfall and subsequent intensity change

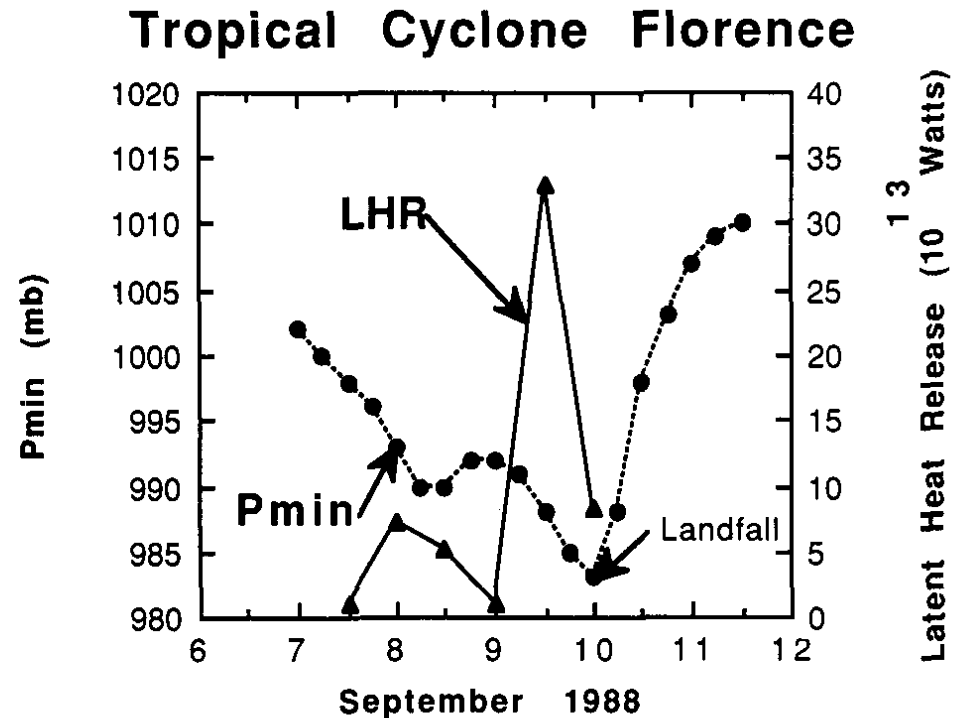


FIG. 7. The temporal change of the western North Atlantic Tropical Cyclone Florence (1988) minimum surface pressure (mb) and SSM/I-derived azimuthally averaged latent heat (10^{13} W) for rings 1 and 2 (111 km from the center).

Relation between rainfall and tropical cyclone over Atlantic and northern pacific region (CERVENY & NEWMAN 2000)

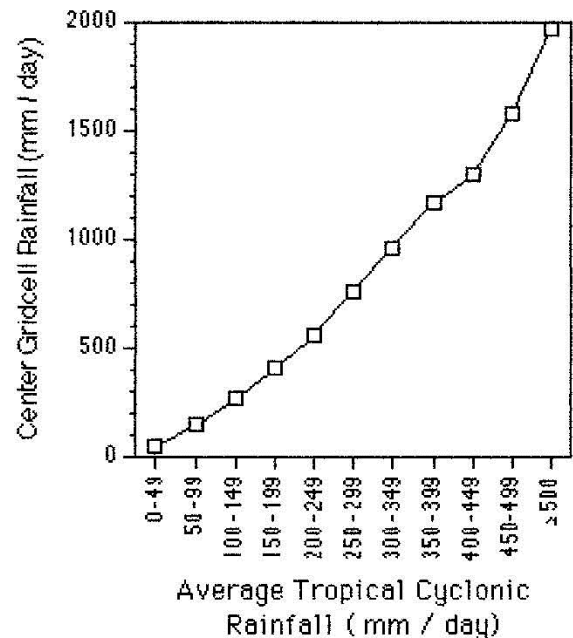
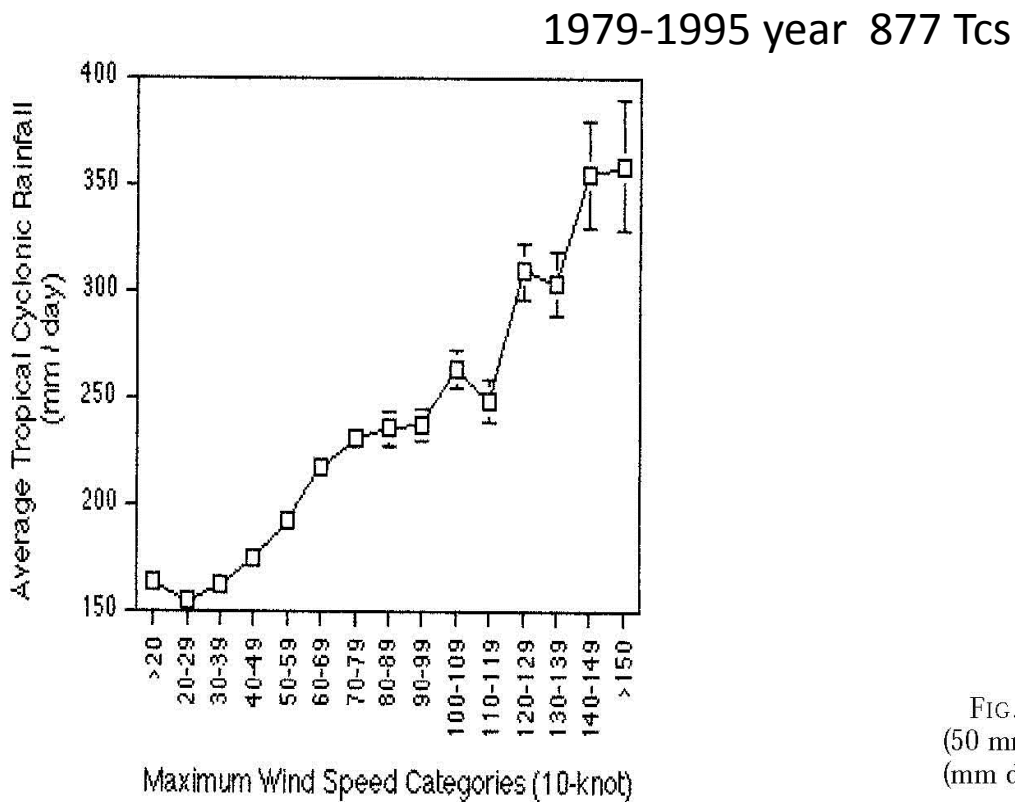


FIG. 4. Relationship between the average tropical cyclone rainfall (50 mm day⁻¹ categories) and the center grid cell (inner core) rainfall (mm day⁻¹).

Strong relationships were found to exist between daily rainfall accumulation and a TC's daily maximum surface wind speeds.

The precipitation associated with the inner core is generally representative of the cyclone's total rainfall.

Relation between rainfall and tropical cyclone over atlantic and northern pacific region (CERVENY & NEWMAN 2000)

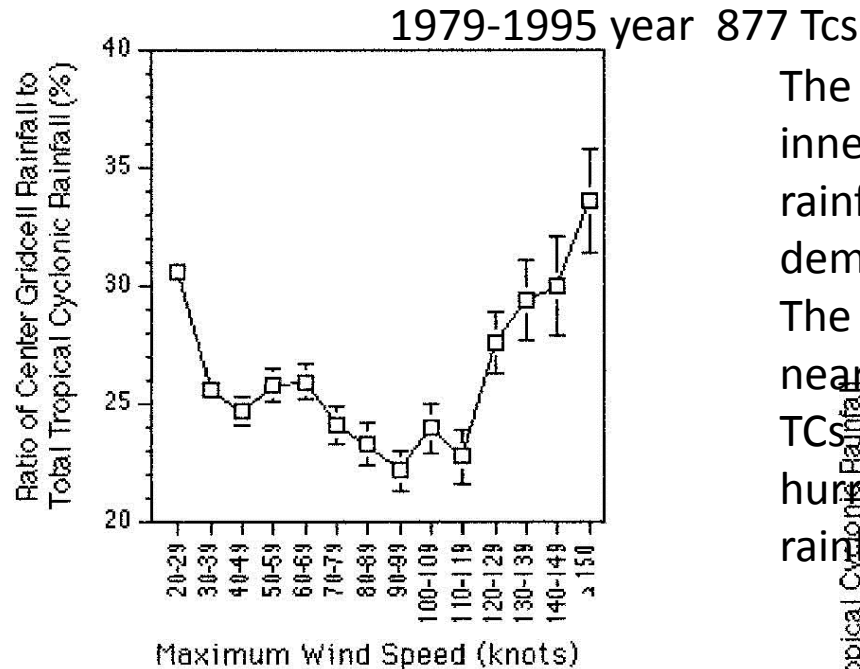


FIG. 5. Ratio of the center grid cell rainfall to the average tropic cyclonic rainfall (in percent) stratified by maximum surface wind speed (10-kt categories). Bars indicate one standard error deviation about the mean.

The relationship between the ratio of inner-core rainfall and the total storm rainfall with maximum surface winds demonstrates a U-shaped pattern. The inner-core precipitation accounts for nearly 35% of the total rain of the weakest TCs and also of the strongest hurricanes but less than 25% of the total rainfall for weak hurricanes.

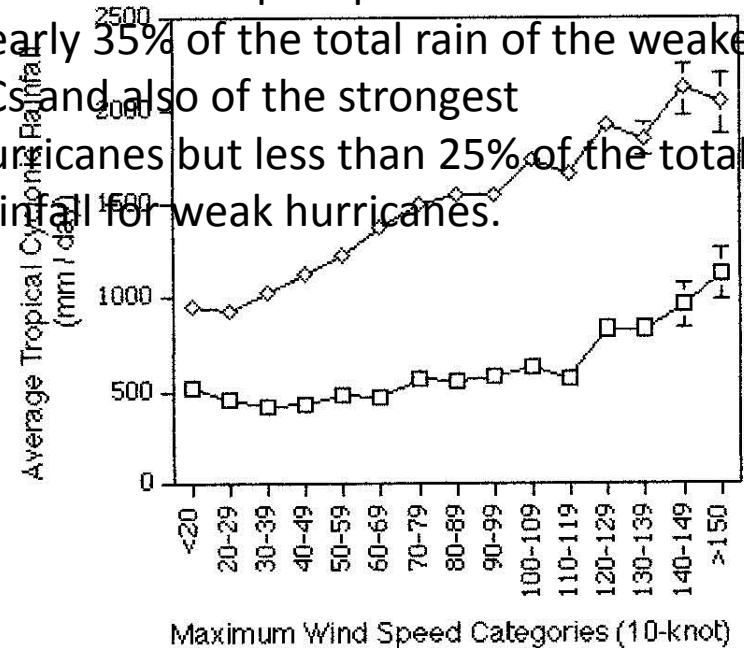


FIG. 6. Center grid cell (inner core) rainfall (squares) and outer grid cells (spiral band) rainfall (diamonds) stratified by maximum surface wind speed (10-kt categories). Bars indicate one standard error deviation about the mean.

TRMM TMI during the period from 1 Jan 1998 to 31 Dec 2000
2121 instantaneous TC precipitation observations
Lonfat et.al. 2004

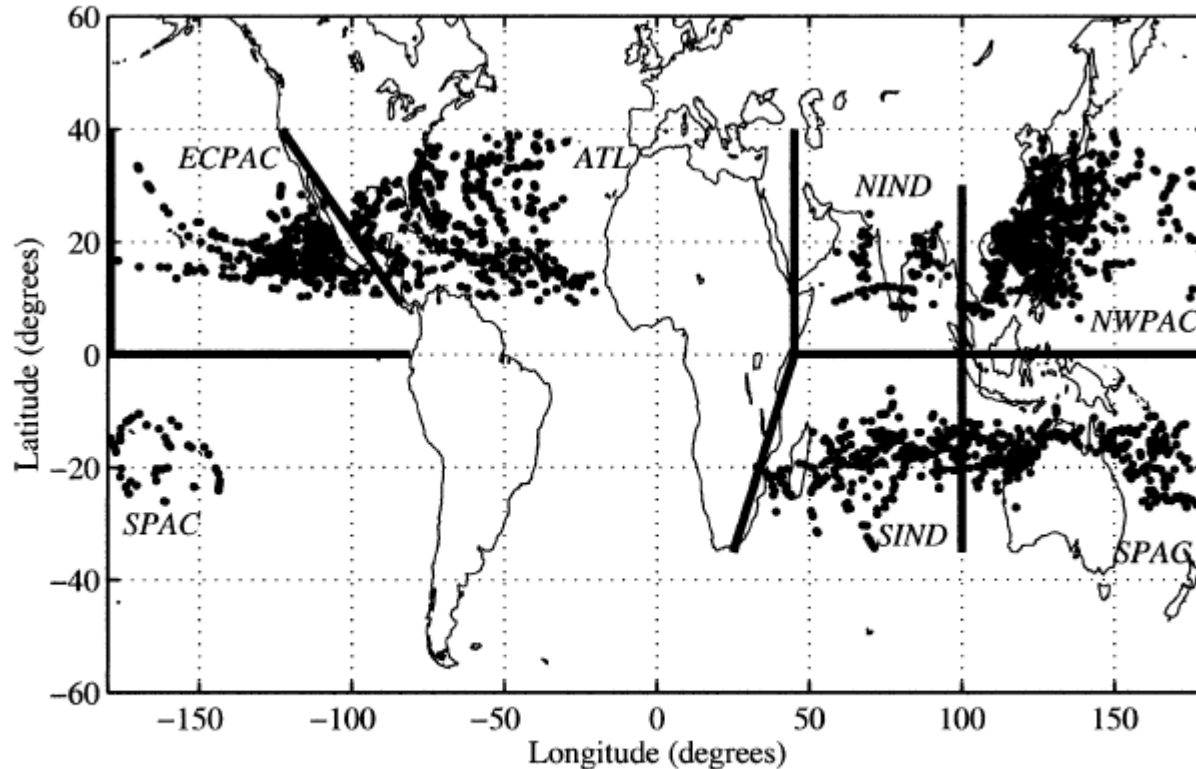
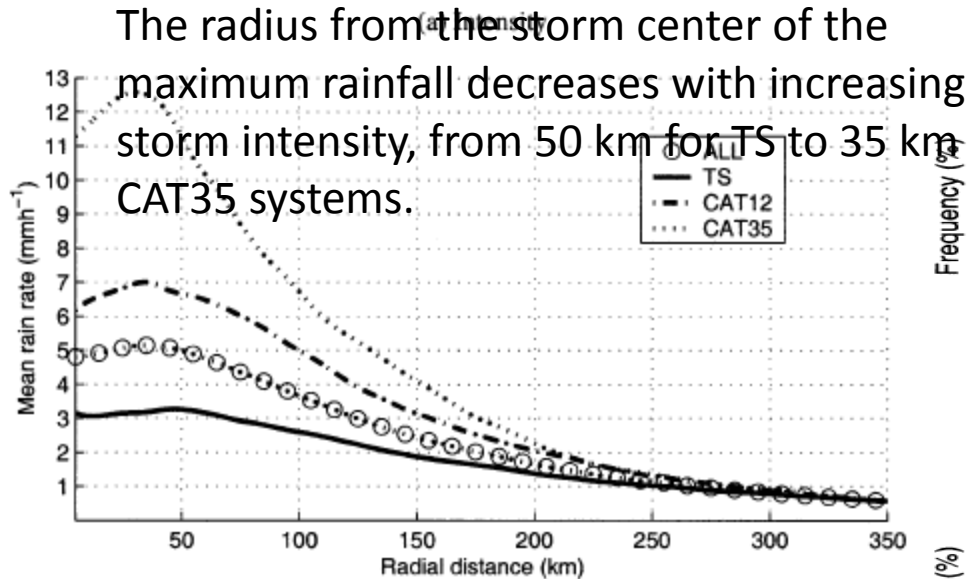


FIG. 1. Tropical cyclones observed by TMI during the period from 1 Jan 1998 to 31 Dec 2000. Each dot represents one TRMM observation. The solid lines indicate the boundaries of the six active oceanic basins.



(b) Geographic location

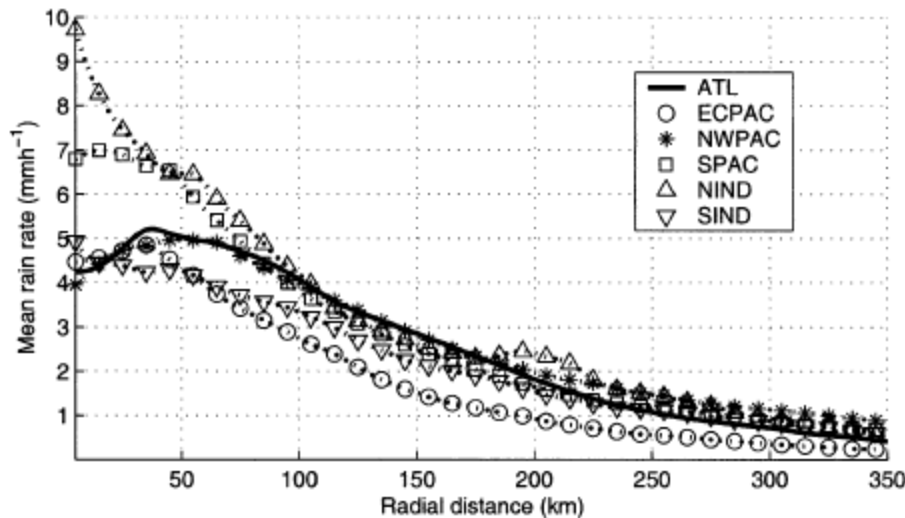


FIG. 11. Mean rain rates, all 2121 1998–2000 observations, (a) as a function of storm intensity, and (b) as a function of geographic locations.

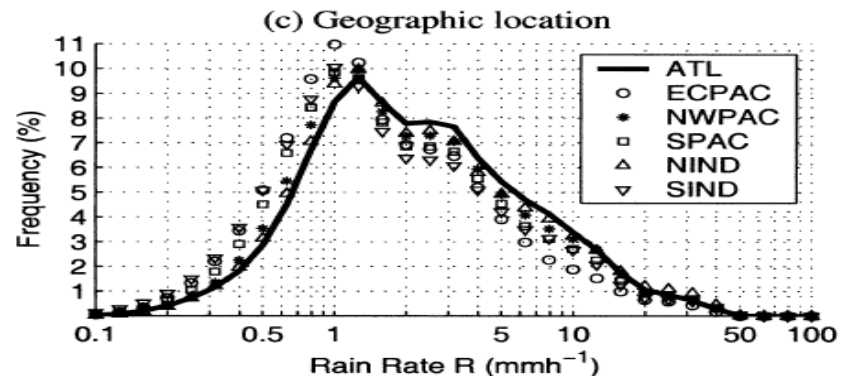
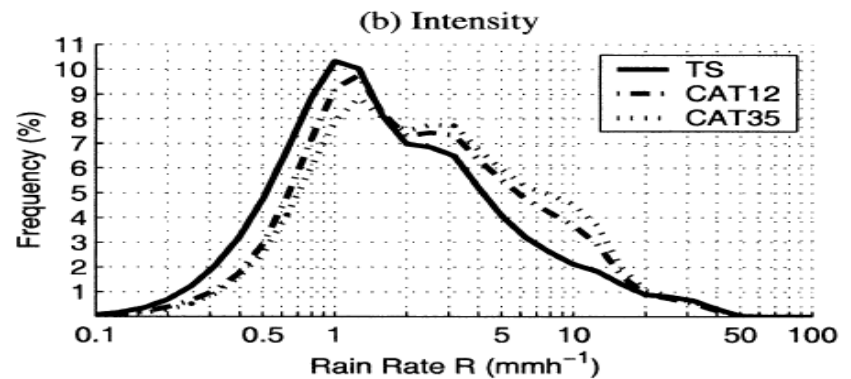
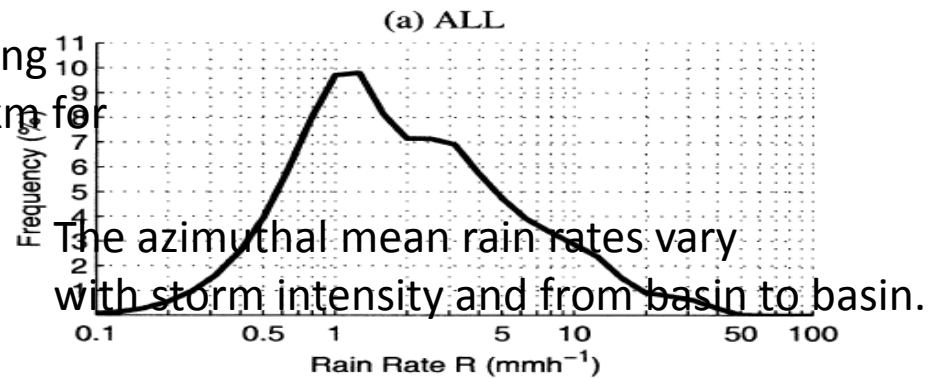


FIG. 10. Probability density functions calculated within 500-km radius of storm center (a) for all 2121 observations, (b) for TC intensity groups, and (c) for oceanic basin subgroups.

The location of the maximum rainfall shifts from the front-left quadrant for TS to the front-right for CAT35. The amplitude of the asymmetry varies with intensity as well; TS shows a larger asymmetry than CAT12 and CAT35.

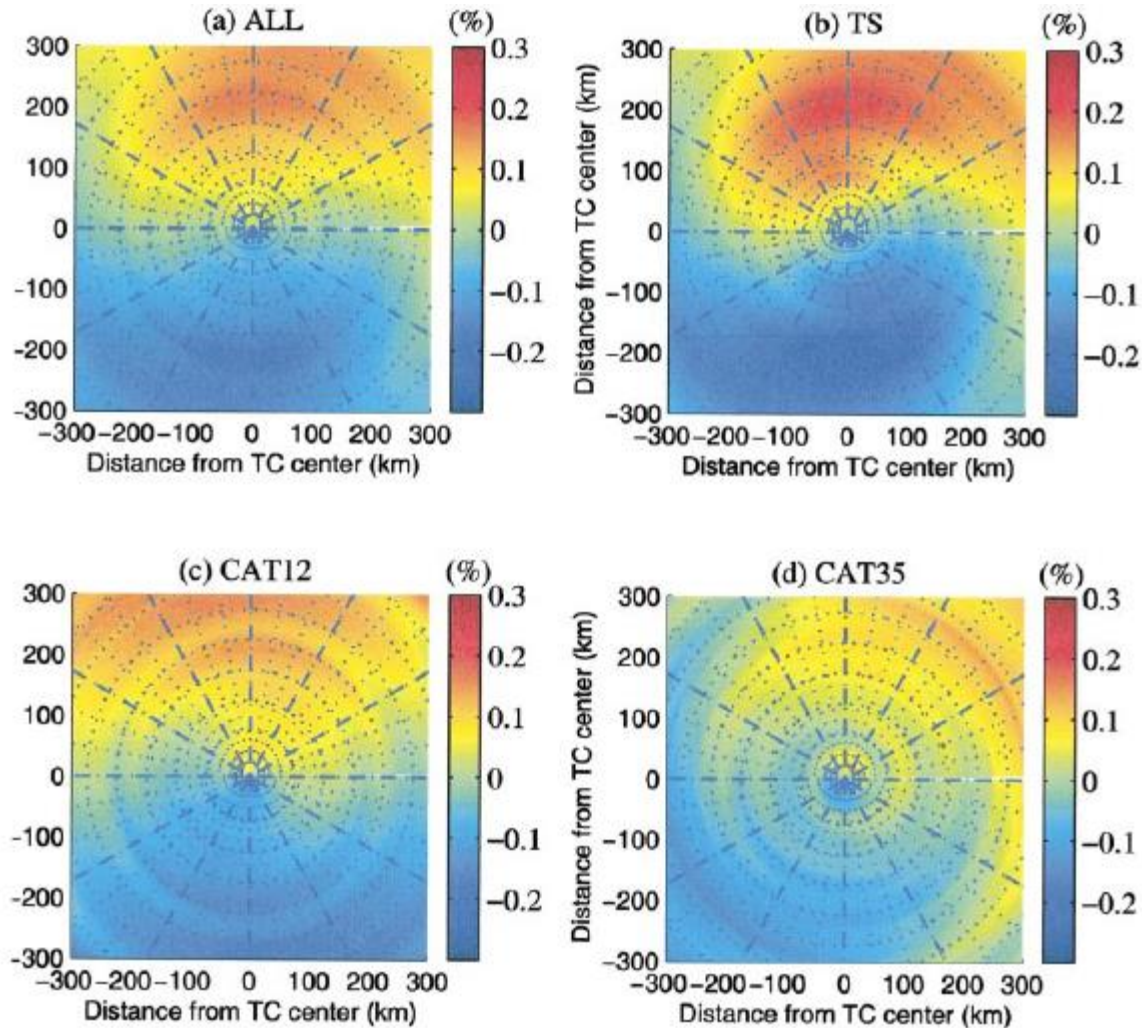


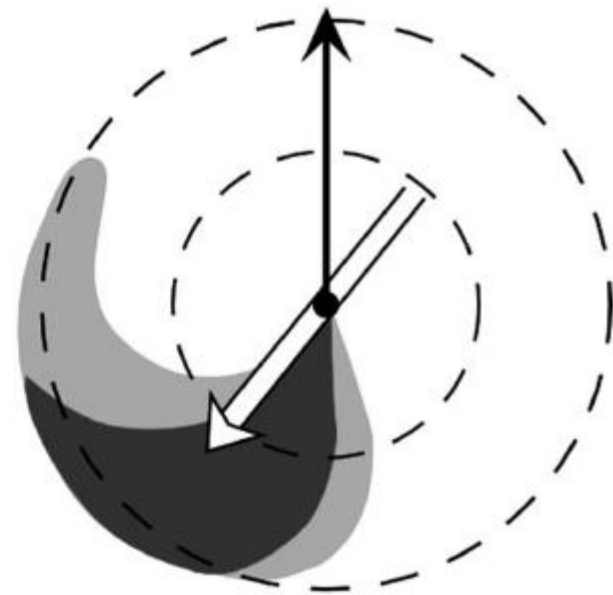
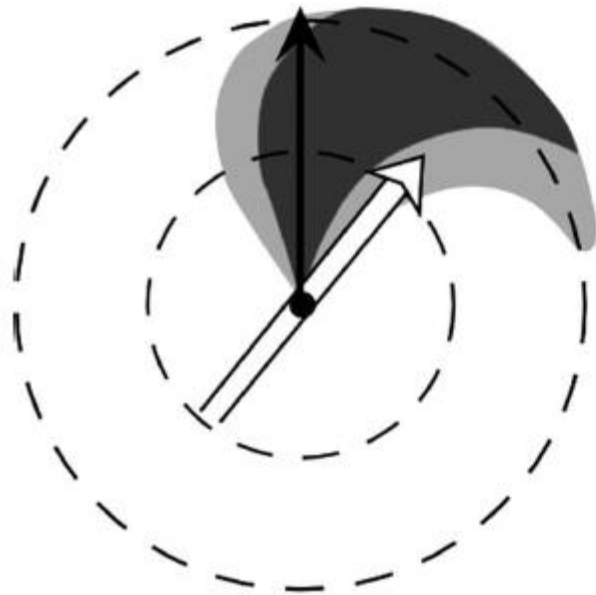
FIG. 17. Rainfall asymmetry calculated in 10-km rings around the storm center, as a function of storm intensity: (a) 2121 TC observations (total distribution), (b) TS, (c) CAT12, (d) CAT35. The storm motion vector is aligned with the positive y axis. The color scale indicates the amplitude of the normalized asymmetry. The red corresponds to the maximum positive anomaly and the blue the minimum rainfall within the storm.

Effects of Vertical Wind Shear and Storm Motion on Tropical Cyclone Rainfall Asymmetries Deduced from TRMM (chen et. Al. 2006) (global view data 1998-2000)

- The environmental vertical wind shear is defined as the difference between the mean wind vectors of the 200- and 850-hPa levels over an outer region extending from the radius of 200–800 km around the storm center.
- The wavenumber 1 maximum rainfall asymmetry is downshear left (right) in the Northern (Southern) Hemisphere. The rainfall asymmetry decreases (increases) with storm intensity (shear strength).
- The rainfall asymmetry maximum is predominantly downshear left for shear values 7.5 m/s

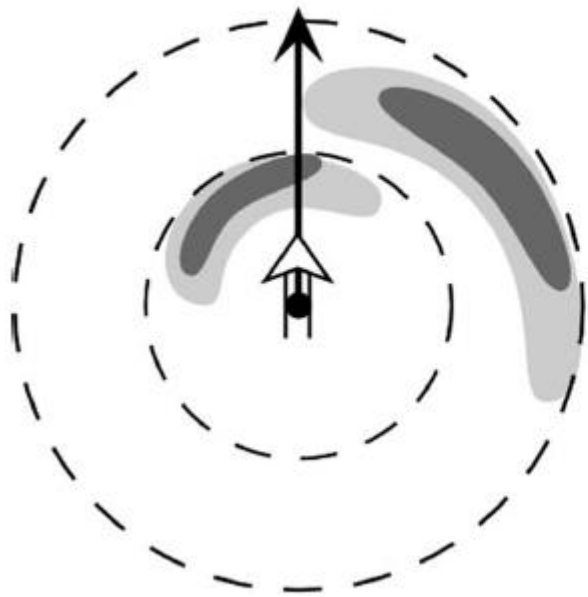
Effects of Vertical Wind Shear and Storm Motion on Tropical Cyclone Rainfall Asymmetries Deduced from TRMM (chen et. Al. 2006) (global view data 1998-2000)

- It is found that the vertical wind shear is a dominant factor for the rainfall asymmetry when shear is 5 m/s. The storm motion–relative rainfall asymmetry in the outer rainband region is comparable to that of shear relative when the shear is 5 m/s, suggesting that TC translation speed becomes an important factor in the low shear environment.

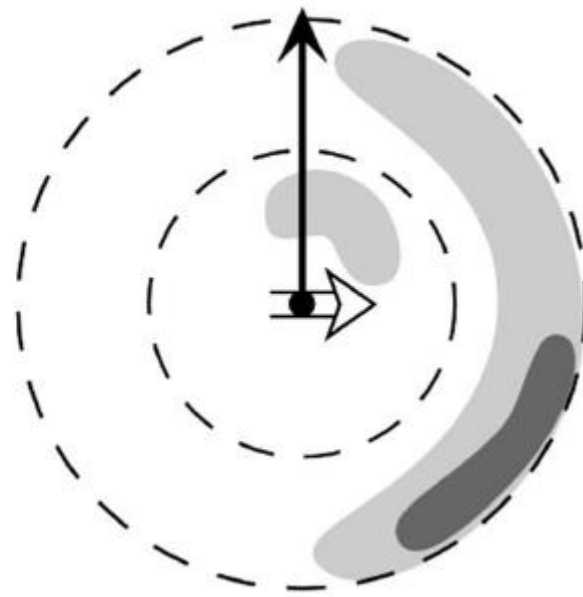


ypical

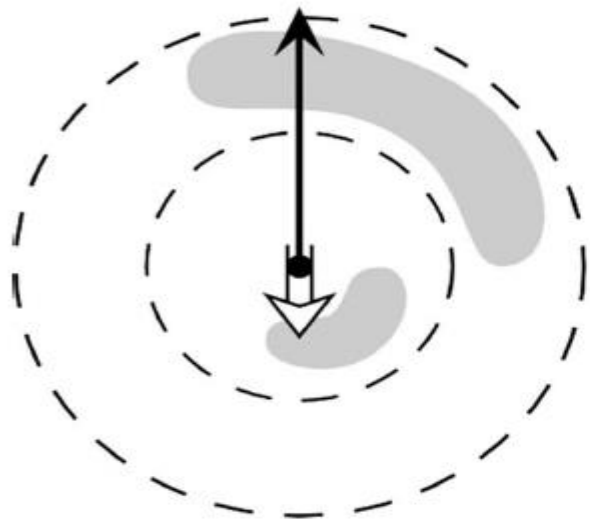
(c)



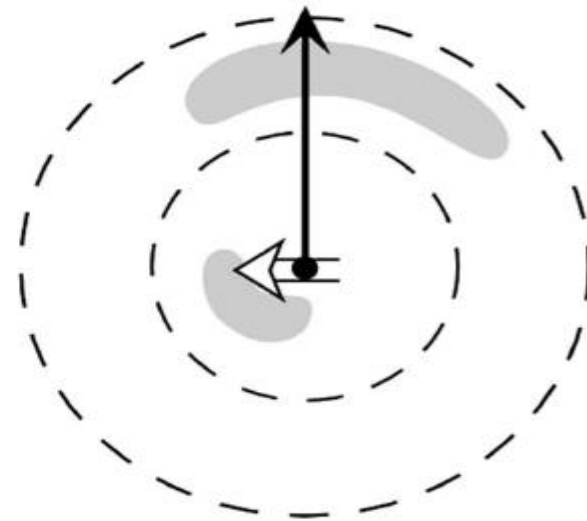
(d)



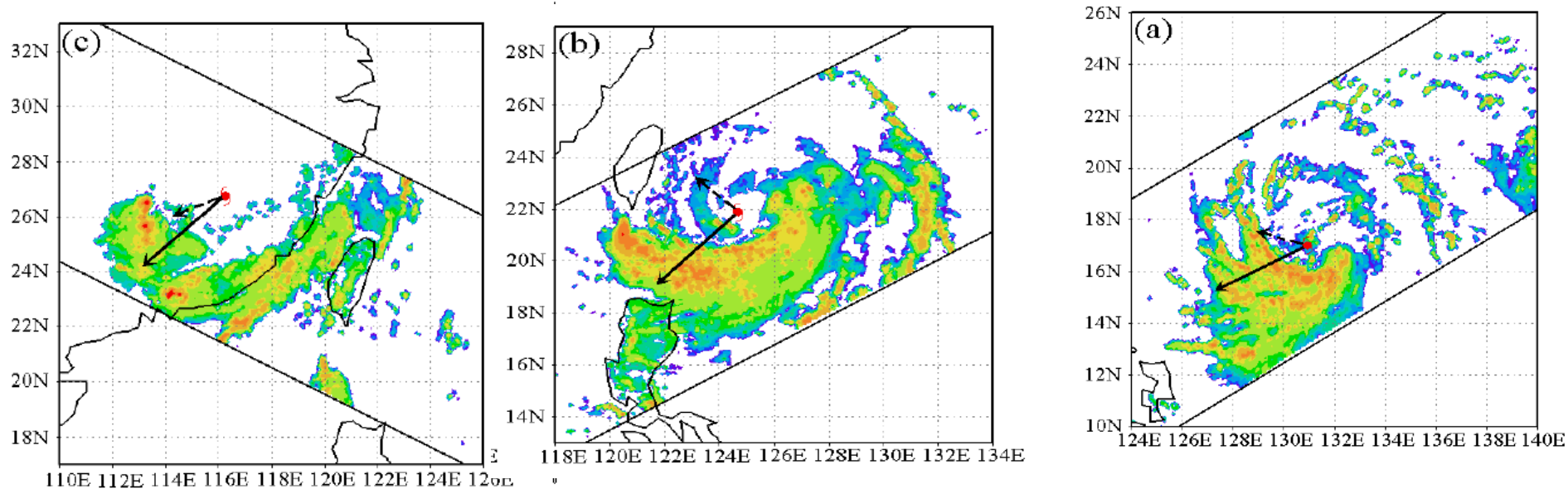
(e)



(f)



rainfall distribution in tropical storm Bilis 2006 (Yu et al 2009)



Consistent with previous modeling studies, heavy rainfall generally occurred downshear to downshear-left of the VWS vector both near and outside the eyewall

Further study on relationship on magnitude between vertical wind shear and rainfall asymmetry (UENO 2007)

$$\omega_{m,pM} = -\frac{p}{R} v_{m,pM} \times \left(f + \frac{2v_{m,pM}}{r_{m,pM}} \right) S / \left(\frac{\kappa T}{p} - \frac{\partial T}{\partial p} \right)_{m,pM}, \quad S \equiv 2U/(p_L - p_U),$$

Where the subscript m denotes that the quantity is evaluated at the radius of maximum wind R_m .

A similar expression for vertical p velocity on the up-tilt side.

It is time-independent solution, and gives an amplitude of vertical motion asymmetry.

Further study on relationship on magnitude between vertical wind shear and rainfall asymmetry

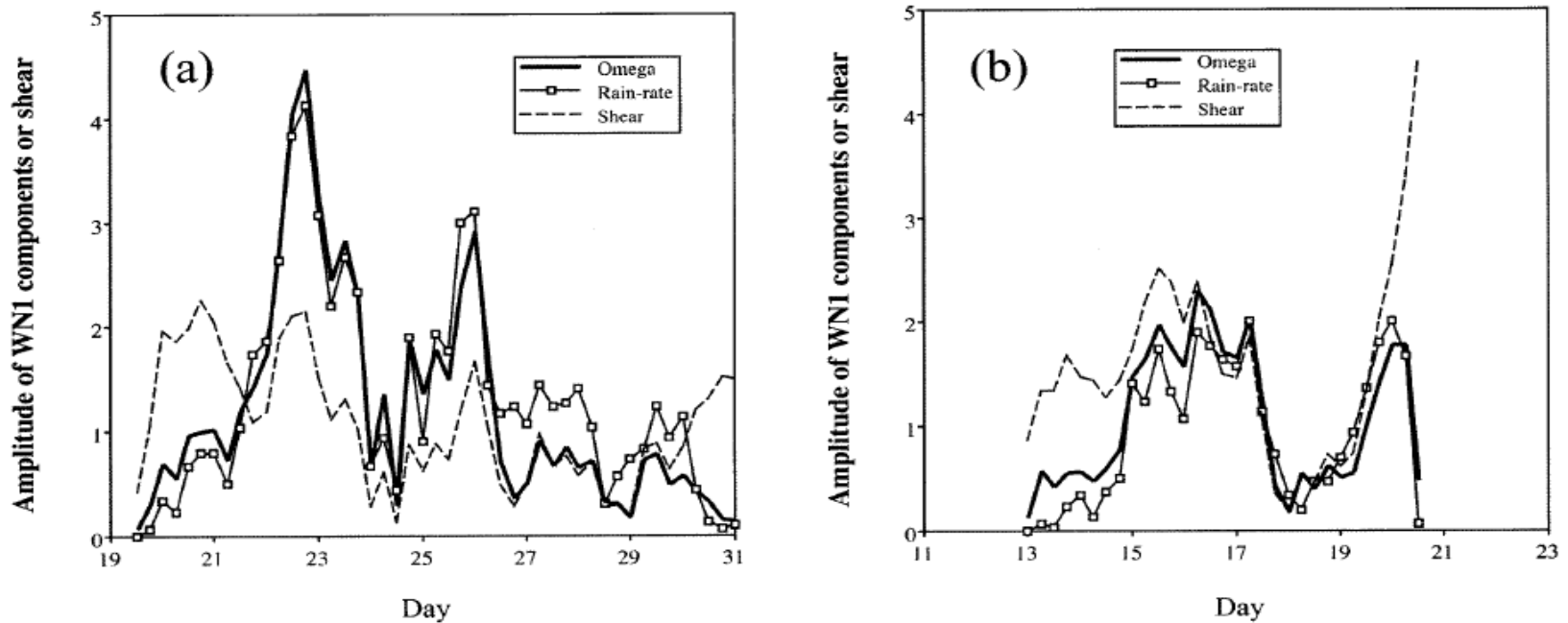


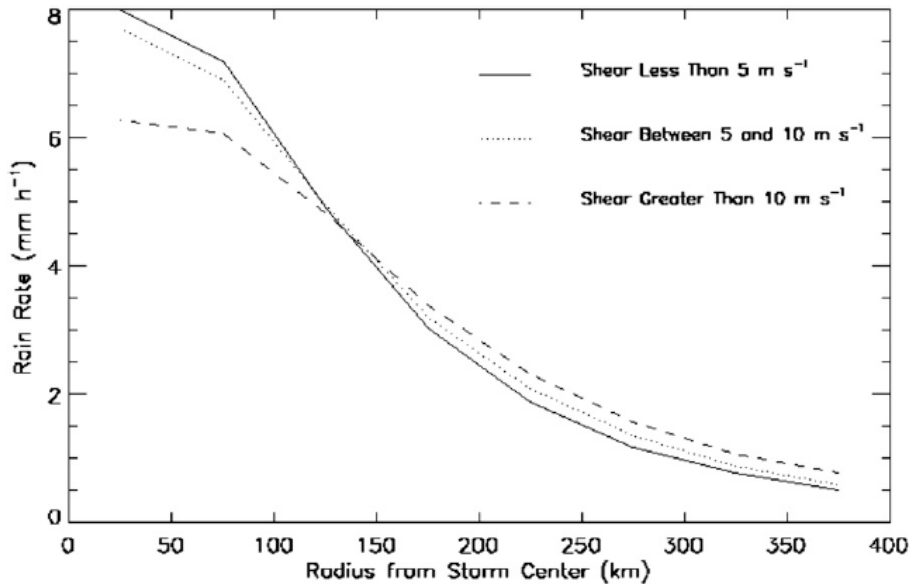
Fig. 11. Same as Fig. 7 but for comparison of “analytical” omega (thick solid line, in units of Pa s^{-1}) with magnitude of wavenumber-one rainfall asymmetry (thin solid line with open squares, mm h^{-1}), and vertical wind shear (dashed line, m s^{-1}). For plotting purposes, the magnitude of wavenumber-one rainfall asymmetry, and shear are divided by 3 and 7, respectively.

the magnitude of vertical motion asymmetry is well correlated with that simulated rainfall asymmetry in the inner-core region, suggesting a strong dependence of rainfall asymmetry on the vortex intensity, as well as the shear magnitude

Effects of Vertical Wind Shear on Tropical Cyclone Precipitation

Wingo* and Celic 2010

data 1988-2002 using 20 000 snapshots of passive-microwave satellite rain rates



- 1) Results indicated that precipitation is displaced downshear and to the left (right for Southern Hemisphere) of the shear vector.
- 2) The amplitude of this displacement increases with stronger shear.
- 3) The majority of the asymmetry found in the mean rain rates is accounted for by the asymmetry in the occurrence of heavy rain.
- 4) It is shown that the effect that shear has on the rain field is nearly instantaneous.

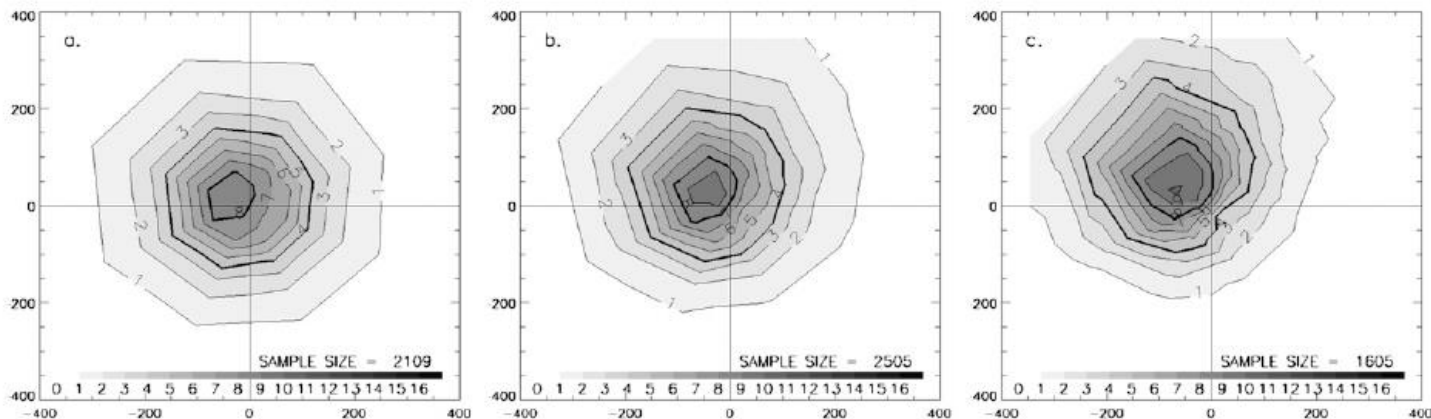


FIG. 4. Mean rain rates for hurricanes with shear (a) <5, (b) 5–10, and (c) >10 m s⁻¹. Contours of 4 and 8 mm h⁻¹ are in bold.

Effects of Vertical Wind Shear on Tropical Cyclone Precipitation

Wingo* and Celic 2010

data 1988-2002 using 20 000 snapshots of passive-microwave satellite rain rates

a decline in the asymmetry with increasing hurricane intensity. This seems to contradict Ueno's (2007) conclusion that the amplitudes of vertical motion and precipitation asymmetries increase with increasing shear magnitude and increasing vortex strength. More generally, major hurricanes do tend to appear more symmetric

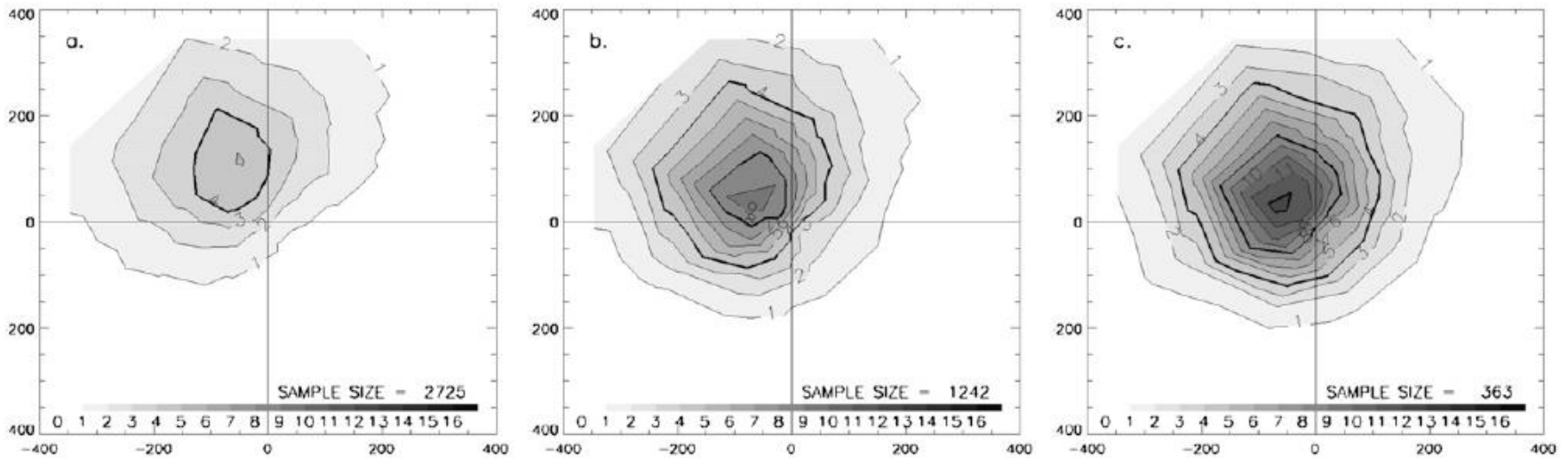


FIG. 11. Mean rain rates for (a) tropical storms, (b) CAT12 hurricanes, and (c) CAT35 hurricanes in a strong shear environment ($>10 \text{ m s}^{-1}$). Contours of 4, 8, and 12 mm h^{-1} are in bold.

Factors may affect TC precipitation (distribution, intensity and duration)

- **Climatology view**

- TC frequency
- TC track
- TC intensity
- TC size

- **Weather view**

- Environment flow
(Vertical wind shear)
- TC Size
- TC structure
- TC Track
- landuse

**Monsoon environment
(SST, MJO.....)**

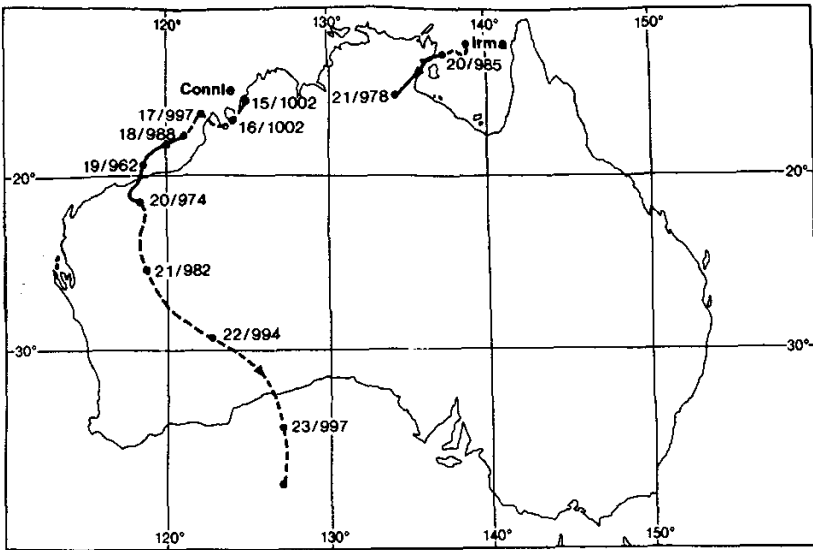
Index

- **Overview of TC rainfall over Monsoon region in Western North Pacific**
 - Early development
 - TC rainfall climatology
 - TC rainfall structure
- **Monsoon influence on TC precipitation**
 - SST
 - Meiyu front
 - subtropical high
 - Southwesterly monsoon
 - Northwesterly monsoon
- **Interaction between tropical cyclone and southwesterly monsoon**
 - Case study on Bilis 2006
 - Climatology
- **Study on the potential impact of landfalling TC in Mainland China (How to estimate economic loss by TC before their landfall in Mainland China)**
- *How to predict the development of tropical disturbance over SCS.*

SST

Increased evaporation and moisture cycling due to warm SST
 Enhanced convective activity due to destabilization and drying of the atmospheric boundary layer

2) Historical data indicate that SST is not the overriding factor in determining the maximum intensity attained by a storm, so other environmental changes will be critical to the ultimate intensity attained by a tropical cyclone.



SST variation (°C)

| Experiment name | SST variation (°C) | |
|-----------------|--------------------|-------------------|
| | Connie | Irma |
| OBS | 0. | Gulf as observed |
| IM2 | 0. | -2. (gulf = 27°C) |
| Control | 0. | 0. (gulf = 29°C) |
| IP2 | 0. | +2. (gulf = 31°C) |
| IP4 | 0. | +4. (gulf = 33°C) |
| CM2 | -2. | 0. |
| CP2 | +2. | 0. |
| CP5 | +5. | 0. |
| ALL2 | +2. | +2 |

| Experiment 24-h results | Connie | | Irma | |
|-------------------------|-------------|--------------|-------------|---------------|
| | Rain | Pressure | Rain | Pressure |
| OBS | 33.5 | 993.0 | 29.0 | 1008.0 |
| IM2 | 34.8 | 993.1 | 26.3 | 1008.7 |
| Control | 33.4 | 993.1 | 28.5 | 1008.5 |
| IP2 | 33.7 | 992.9 | 32.1 | 1007.7 |
| IP4 | 33.6 | 993.0 | 39.7 | 1006.6 |
| CM2 | 30.4 | 993.9 | 29.4 | 1008.7 |
| CP2 | 37.5 | 992.2 | 28.7 | 1008.6 |
| CP5 | 54.0 | 984.3 | 28.5 | 1008.1 |
| ALL2 | 37.4 | 992.2 | 33.3 | 1007.6 |

Sensitivity of Tropical Cyclone Rainfall Intensity to Sea Surface Temperature (Evans 1994)

Intensity change

GANDIKOTA V. RAO AND P. DOUGLAS MACARTHUR

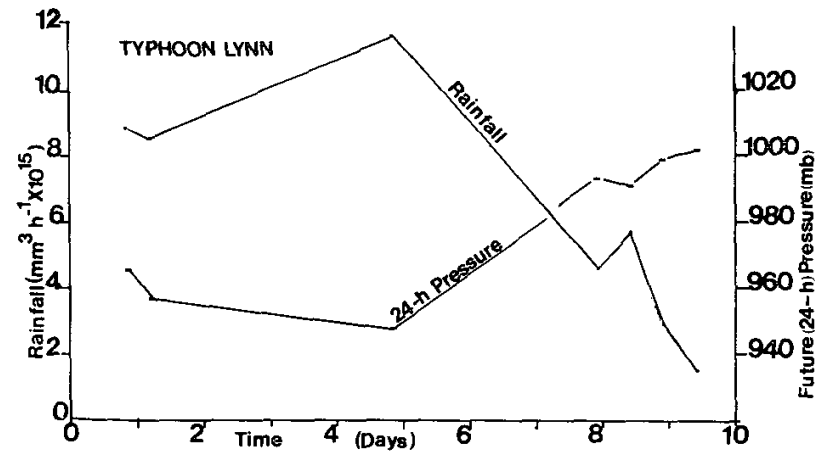


FIG. 6. Rain volume rates within 55.5-km boxes of Typhoon Lynn (1987) and 24-h central pressure. Time is counted from 0000 UTC 17 October 1987. Linear fit data: for 55.5 km boxes, $P = -5.9R + 1016.3$; R is in units cubic millimeters per hour. Note the negative correlation between rain volume rates and 24-h pressure of Typhoon Lynn.

SSM/I rainfall rates from 27 maps times 12 typhoon of 1987

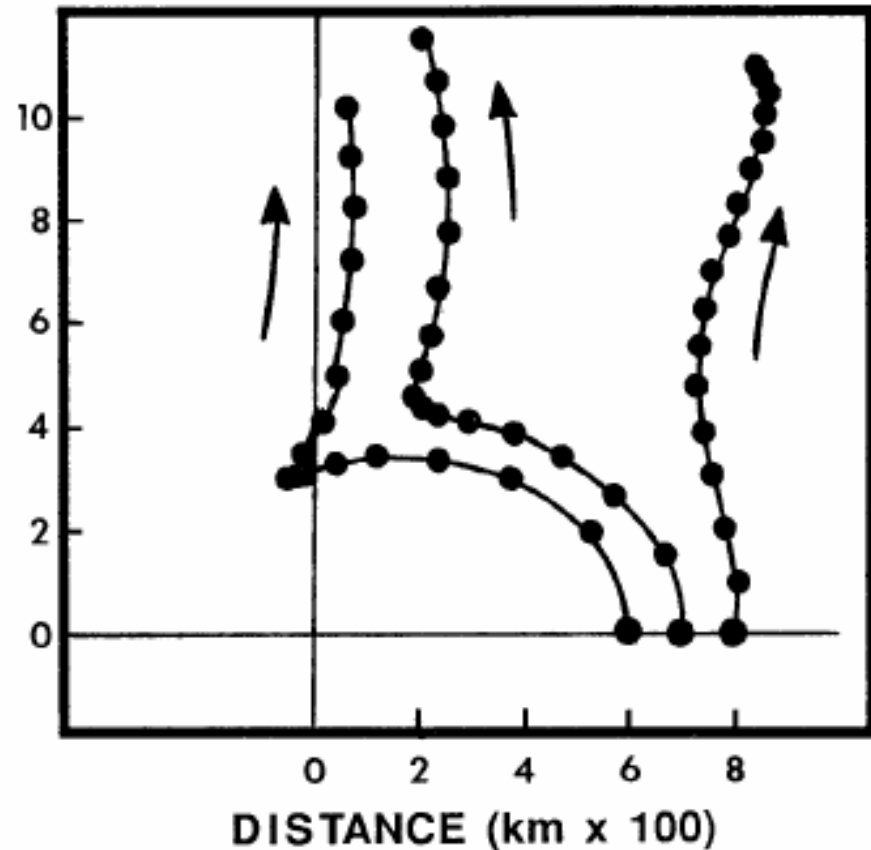
Rain volume rates within a 444-km box correlate with the future 24-h pressure was -0.68

A northwestward-moving storm was likely to deepen if lighter ($\leq 3\text{mm/h}$) rainfall rates dominated a 222-km box

Monsoon Environment and Tropical Cyclone Motion

Typical track changes associated with the interaction between a tropical cyclone and a monsoon gyre. Dots indicate 6-h positions for 96 h of simulated tracks of three tropical cyclones placed at 600, 700, and 800 km east of the center of a monsoon gyre. (Adapted from Carr and Elsberry 1995).

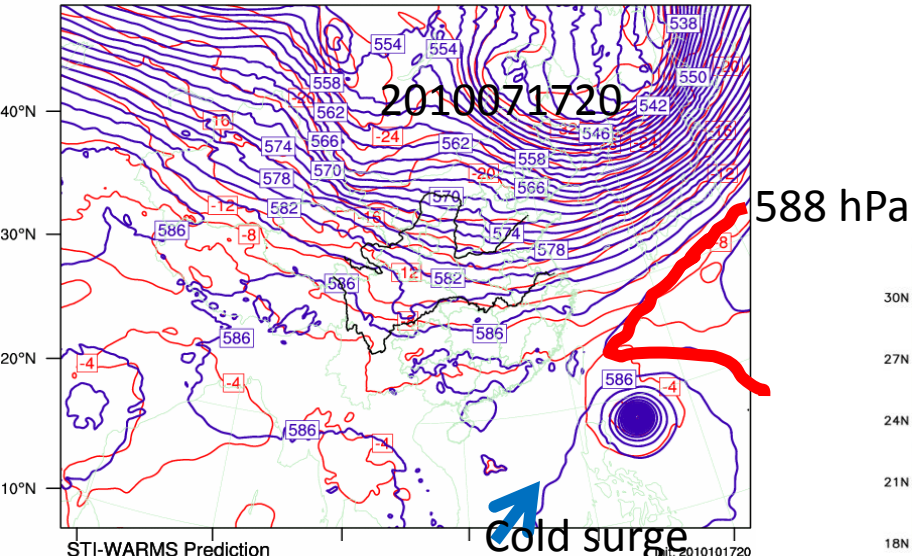
Carr and Elsberry (1995)



2010 Megi

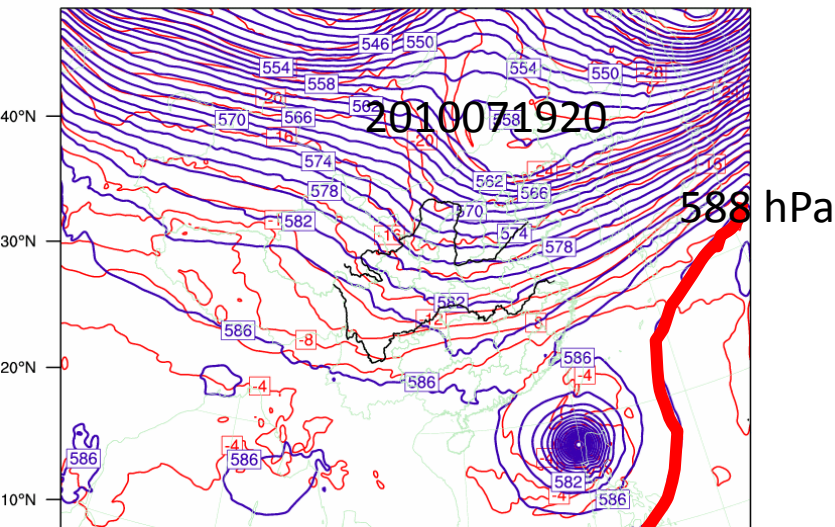
STI-WARMS Prediction
 Temperature (C) at 500 hPa
 Height (10m) at 500 hPa

Init: 2010101720
 Valid: 2010101720

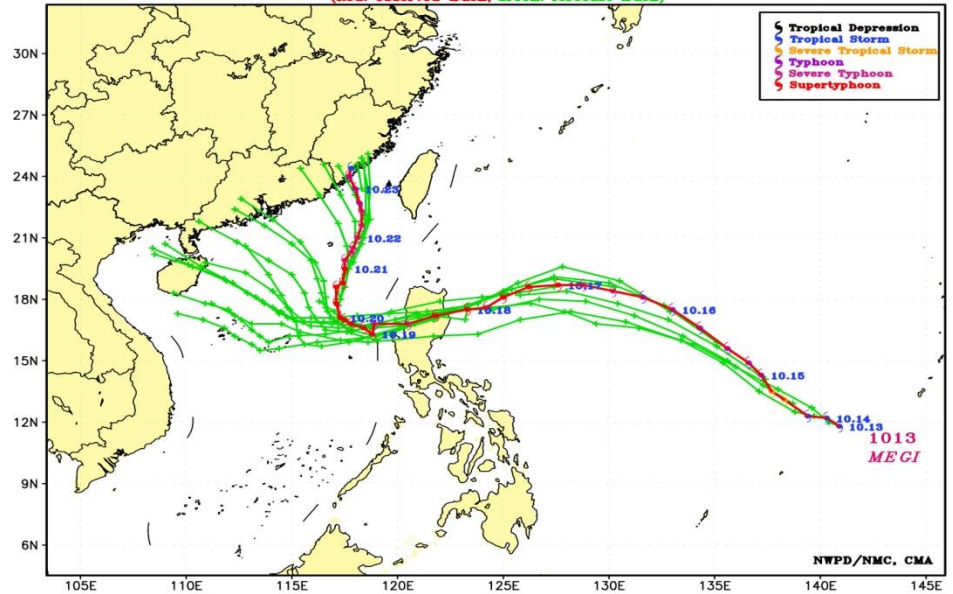


STI-WARMS Prediction
 Temperature (C) at 500 hPa
 Height (10m) at 500 hPa

Init: 2010101720
 Valid: 2010101920



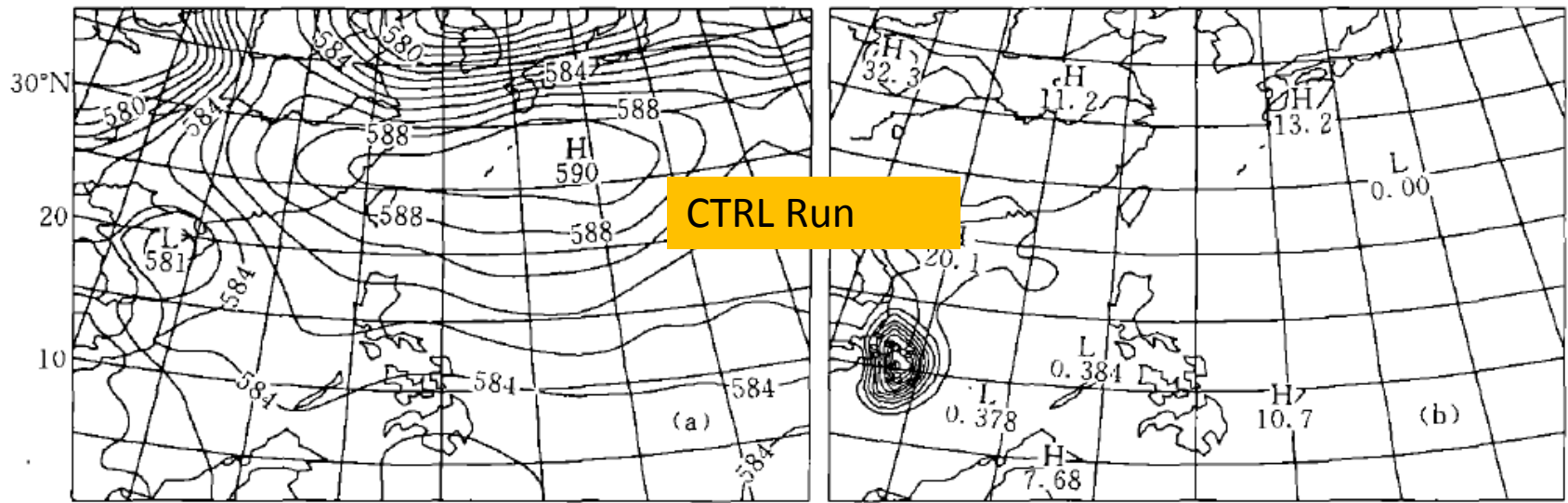
TC Track Forecast by GlobalModel at ECMWF
 (Red: observed track, Green: forecast track)



TC influence to Meiyu front

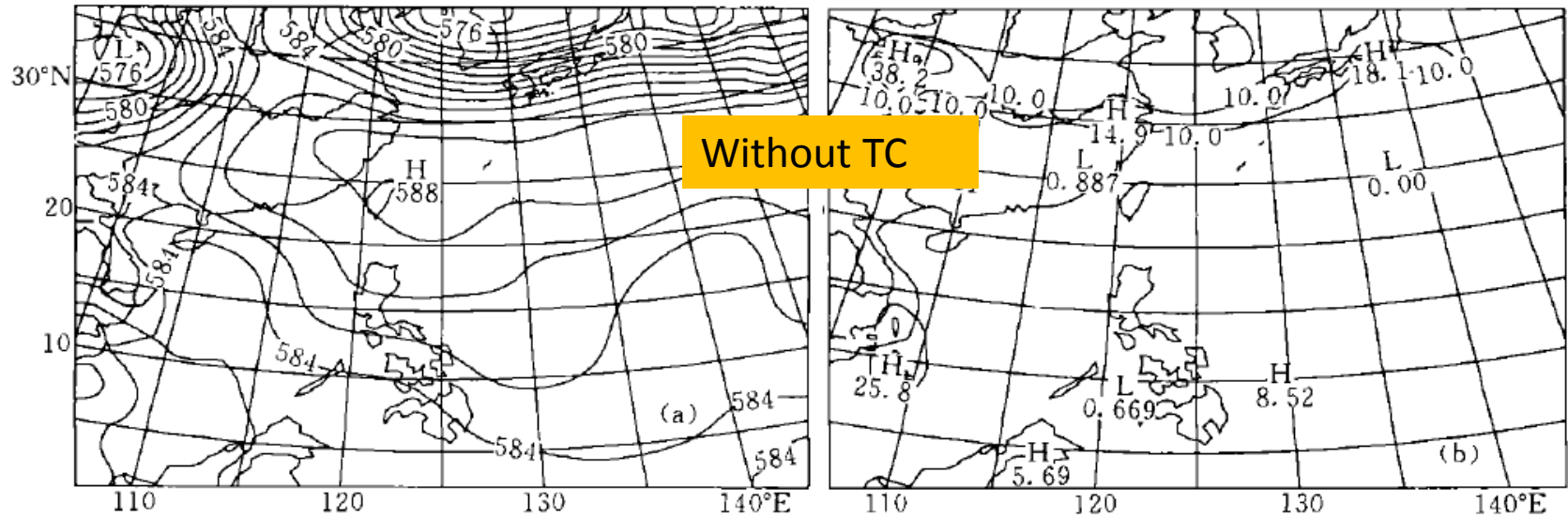
Chen et. al. 1999

- Statistics (Cheng et al. 1999) show that 85% of Mei-yu rainfall can be reduced, suspended or ended when a typhoon appears in southern coastal waters or makes landfall in South China.
- compared results with and without Typhoon Zeke showed that, during landfall, it could affect the moisture transportation channel from the Bay of Bengal and South China Sea to the Yangtze River Basin.
- Additionally, the western ridge of the subtropical high was shifted significantly northward by the typhoon. Meanwhile, mei-yu Front circulation and its energy cycle structure were destroyed by the approach of Typhoon Zeke.



CTRL Run

compared results with and without Typhoon Zeke showed that, during landfall, it could affect the moisture transportation channel from the Bay of Bengal and South China Sea to the Yangtze River Basin. Additionally, the western ridge of the subtropical high was shifted significantly northward by the typhoon. Meanwhile, mei-yu Front circulation and its energy cycle structure were destroyed by the approach of Typhoon Zeke.



Without TC

Zhu et al. (2000)

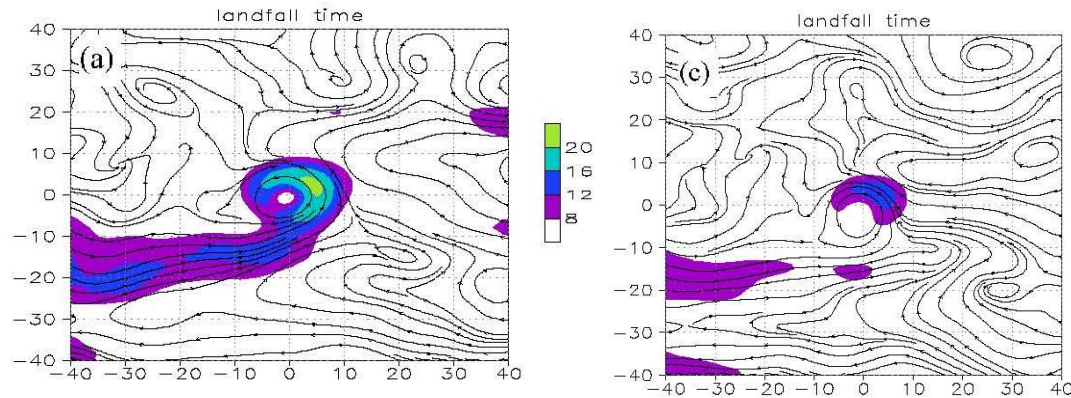
- the rainfall in the mid latitudes in front of the westerly trough was closely related to moisture transport by the strong southeasterly flow in the eastern periphery of the typhoon, which stretched the moisture channel to the area in front of the trough.



Interaction with southwesterly monsoon (moisture supply)

Chen et. al 2008

Li et. al 2005)



Cheng (2008) studied the relationship between the moisture channel and rainfall in two groups of LTC. One group was composed of five strong rainfall cases and the others of five weak rainfall cases. Additionally, the vapor flux fields of the groups were studied with data compositing analysis.

The results showed that LTC heavy rainfall occurs when a strong vapor transport channel is present with weak rainfall occurring in the absence of such a channel. In another study by Li et al. (2005) numerical simulations of Typhoon Bilis (0010) showed that rainfall would be significantly reduced from the control simulation if the moisture transport was cut.

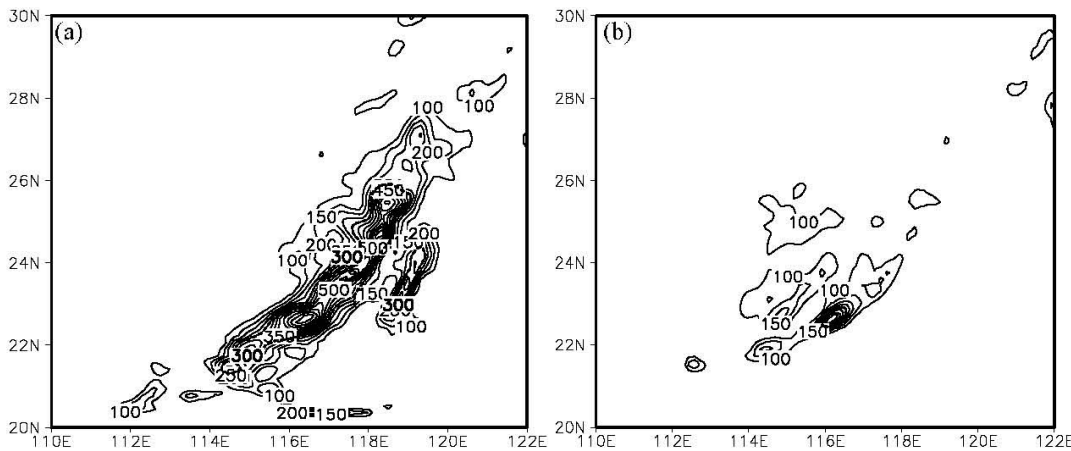


Fig. 3. The accumulated rainfall distribution (≥ 100 mm) associated with Typhoon Bilis (0010) during 60 hrs of simulation (from Li and Chen, 2005): (a) control simulation with moisture transport; (b) without moisture transport.

Interaction of Typhoon Babs (1998) and the Northeasterly Monsoon (Wu 2010)

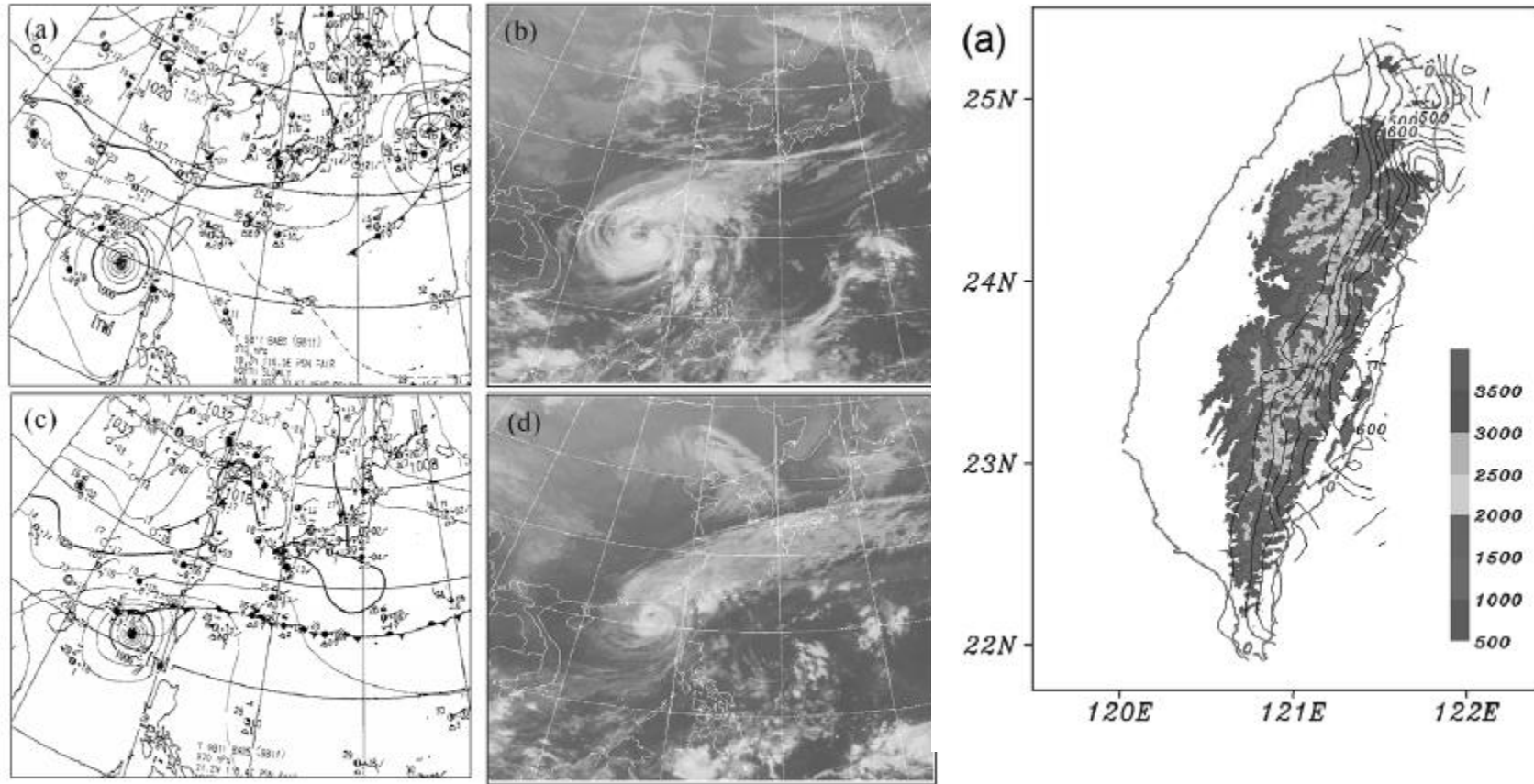
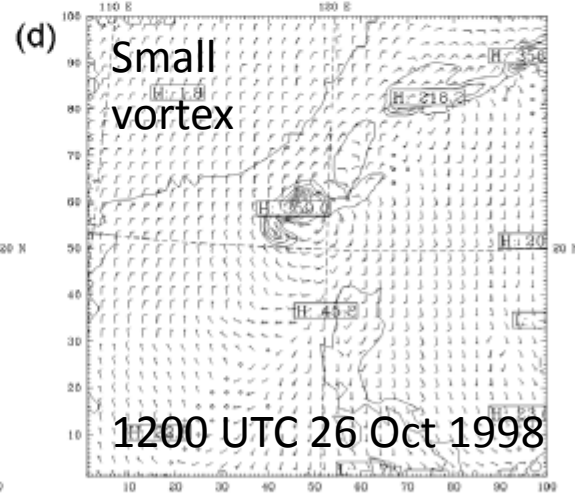
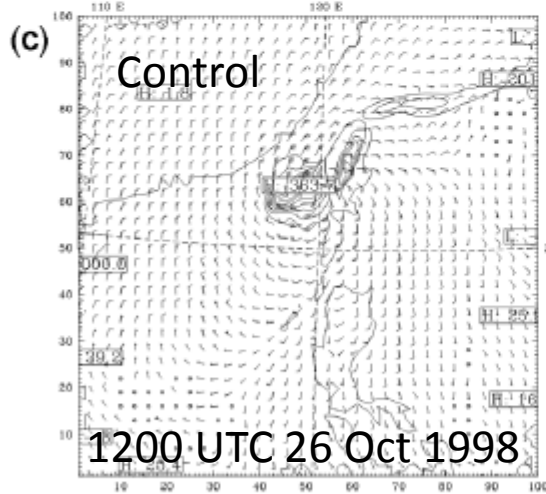
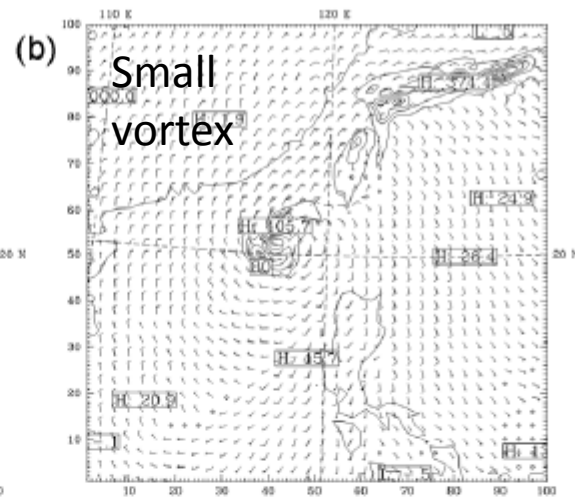
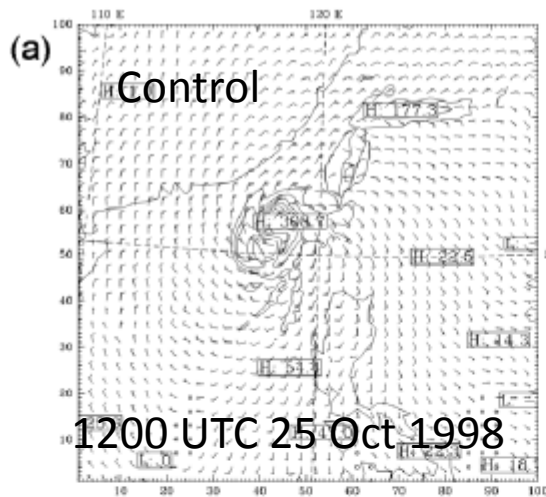


Fig. 1 (a) Surface weather map (JMA) and (b) GMS-5 infrared satellite imagery at 0000 UTC 25 Oct 1998. (c) and (d) As in (a) and (b) except at 0000 UTC 26 Oct 1998.

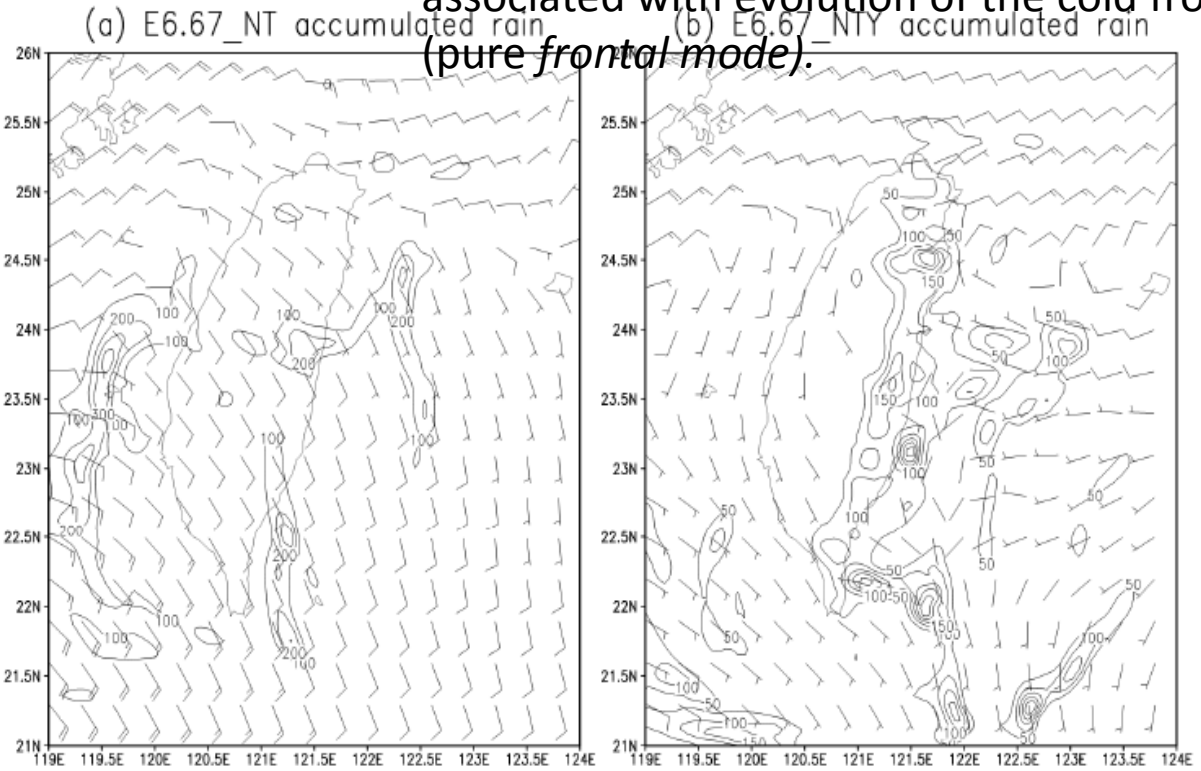
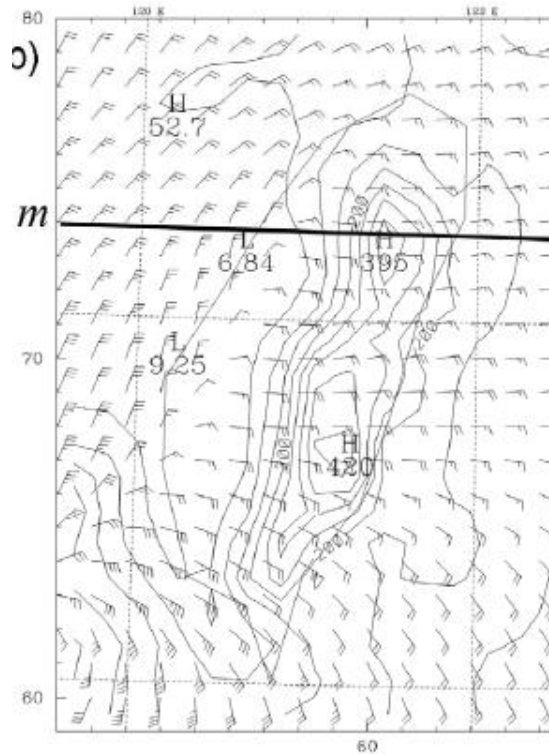


When the radius of the bogus vortex is reduced, the cold front to the north migrates southward in a faster pace than in the control simulation, and rain rate at the front also increases such that total accumulated rainfall at northern Taiwan is comparable with that in the control simulation but with shifted maximum position.

9 Simulated 1000-hPa wind field (one full wind barb = 10 m s^{-1}) and 12-h accumulated fall (contour interval of 50 mm) in experiment (a) E20_KF and (b) E20_small valid at 1200 C 25 Oct 1998. (c) and (d) As in (a) and (b) except valid at 0000 UTC 26 Oct 1998.

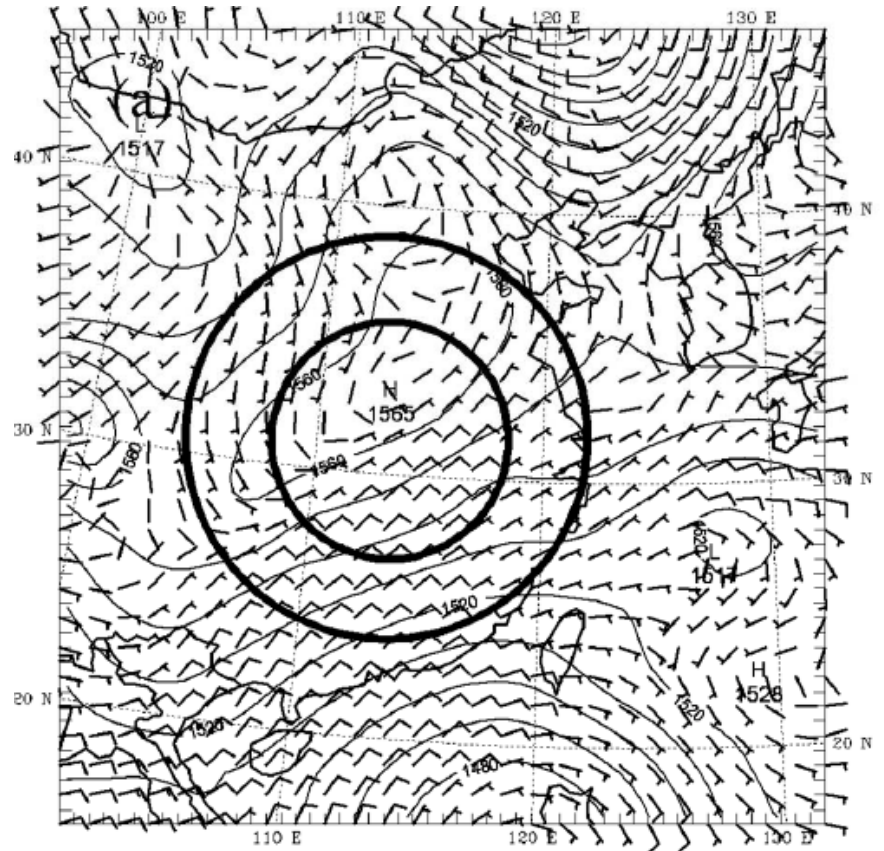
Comparison of rainfall in No-terrain, no-Typhoon and control experiment

In the extreme case in which no bogus vortex is implanted at all, rainfall is mainly associated with evolution of the cold front (pure frontal mode).



Removal of the Taiwan terrain in one of the sensitivity experiments results in completely different rainfall distribution due to the lack of the convection by orographic lifting,

reduce the relative vorticity at each individual level between 1000-700-hPa (1000-300-hPa) for experiment E20_M1 (E20_M2) in the model initial condition at 0000 UTC 23 Oct to half of the original value inside a circular domain with a radius of 600 km



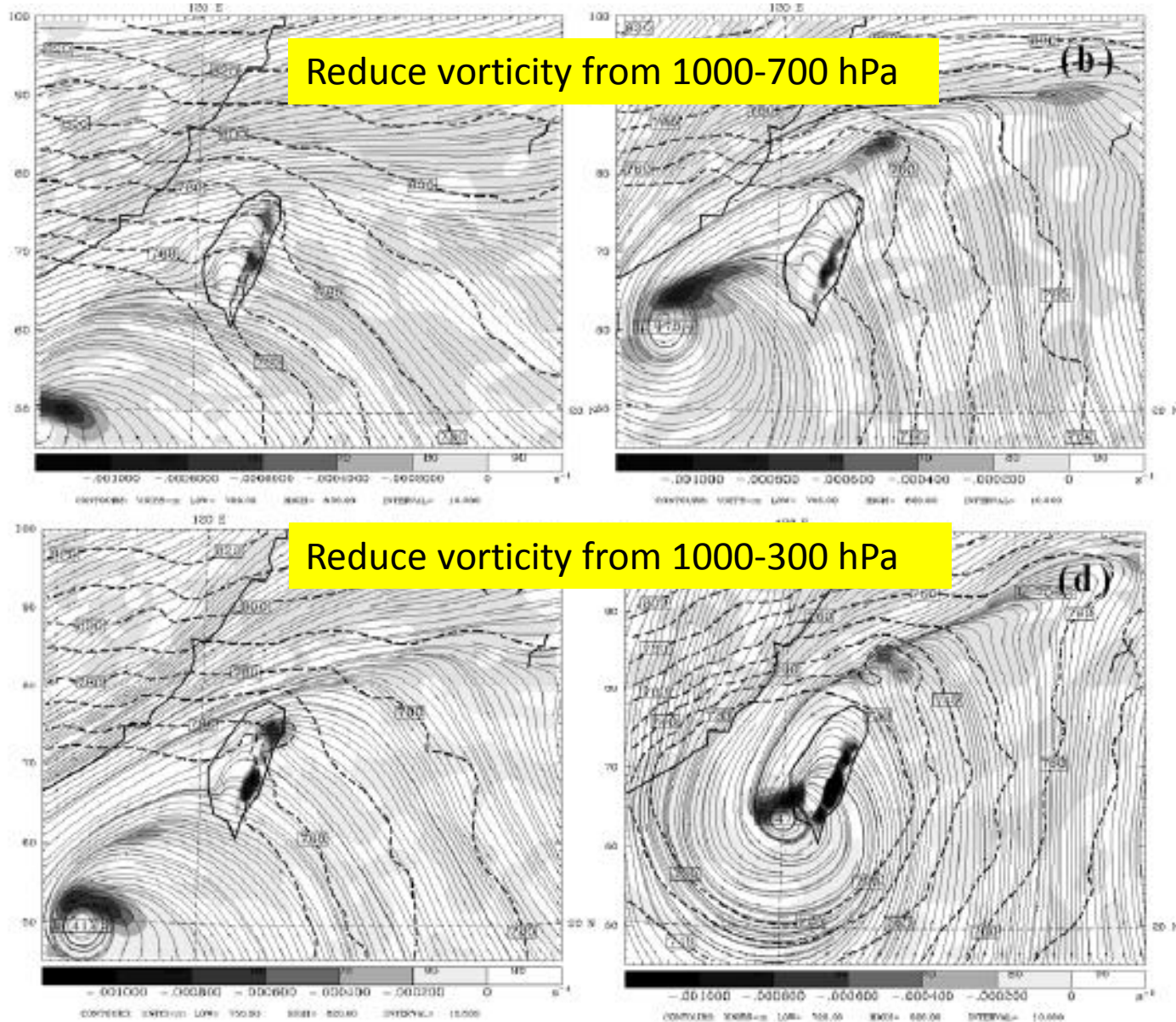


Fig. 12 Simulated 925-hPa streamline, geopotential height (dashed line, m) and divergence (shaded, contour interval is $2 \times 10^{-4} \text{ s}^{-1}$) in experiment E20_M1 at (a) 1800 UTC 24 Oct and (b) 0000 UTC 26 Oct. (c) and (d) As in (a) and (b) except for experiment E20_M2

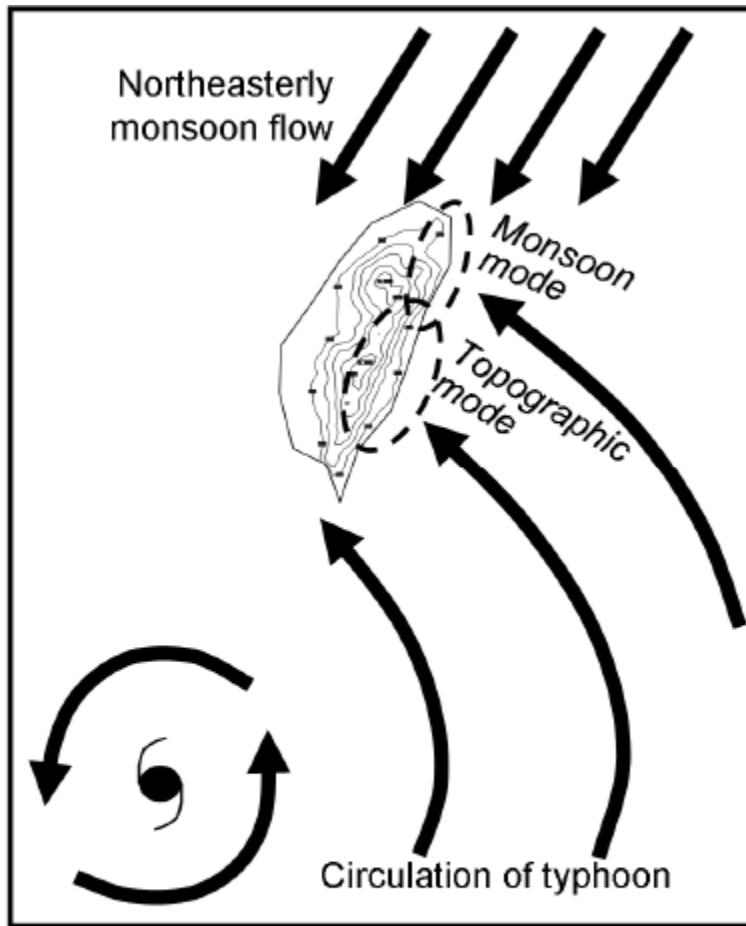


Fig. 13 Schematic diagram of the rainfall mechanisms associated with the monsoon mode and the topographic mode, as a response to the interaction among the typhoon circulation, northeasterly monsoon flow, and terrain of Taiwan (contour interval of 500 m).

Radar Observations of Intense Orographic Precipitation Associated with Typhoon Xangsane (2000)

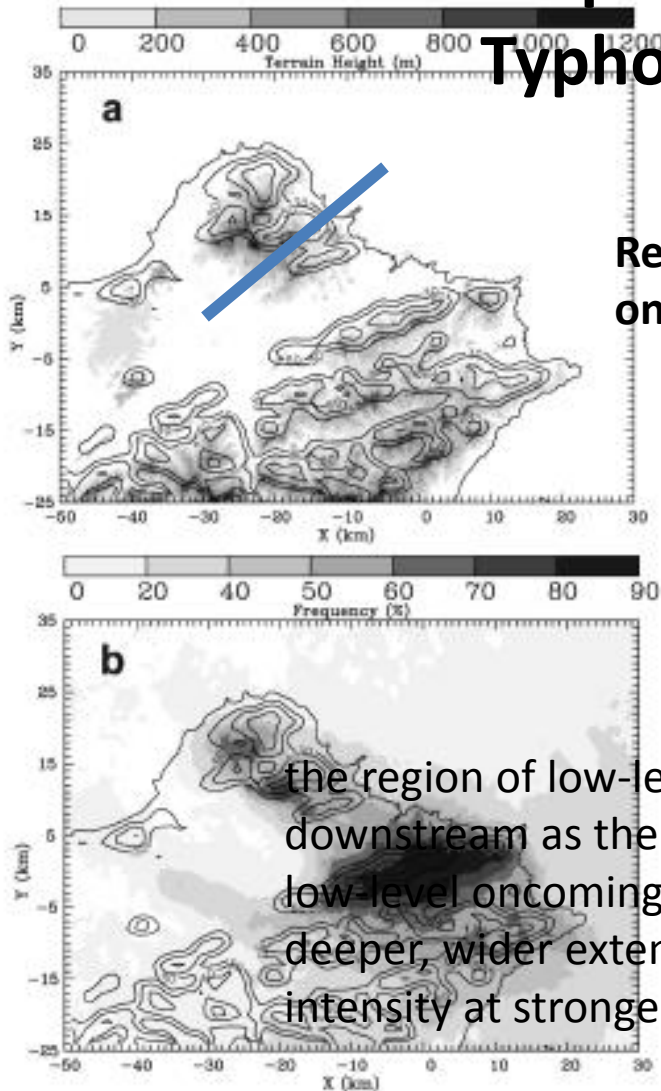


FIG. 10. (a) Frequency distribution of topographically forced vertical velocities ($>1 \text{ m s}^{-1}$) during the 30-h period from 2000 UTC 31 Oct to 0600 UTC 1 Nov 2000, with a contour interval of 30%. Shading indicates terrain height (m MSL). (b) As in (a), except that shading indicates the frequency distribution of heavy precipitation ($>40 \text{ dBZ}$).

Relation of precipitation to low-level upstream oncoming flow

the region of low-level heavy precipitation tended to shift downstream as the low-level oncoming flow intensified, and the precipitation exhibited a deeper, wider extent and stronger intensity at stronger oncoming flow regimes.

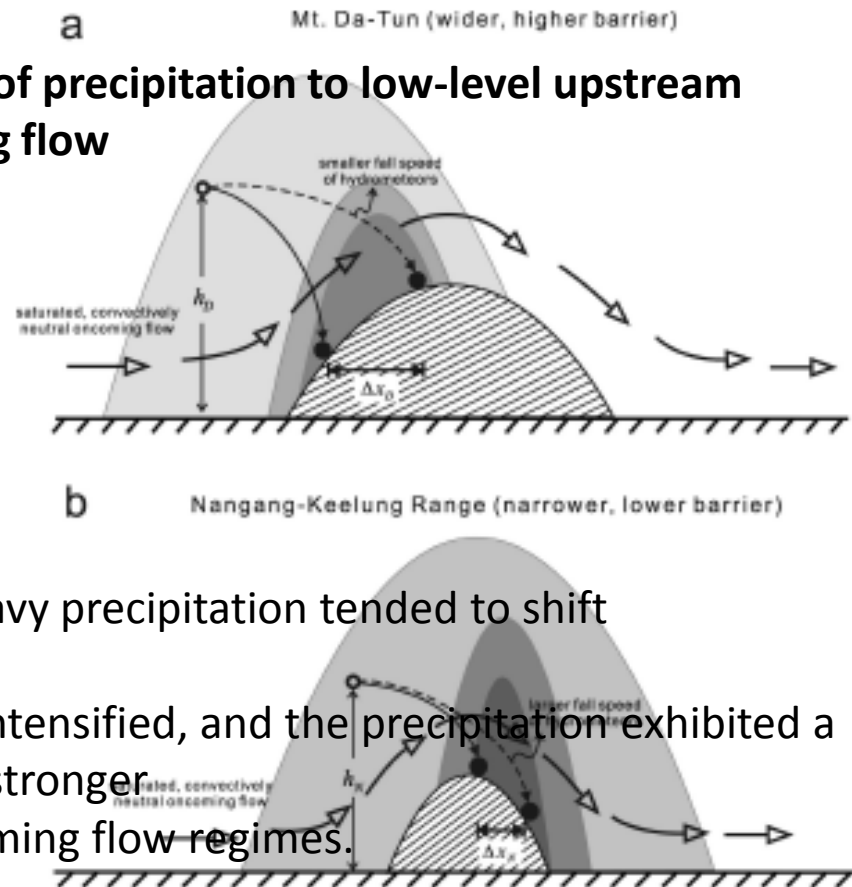
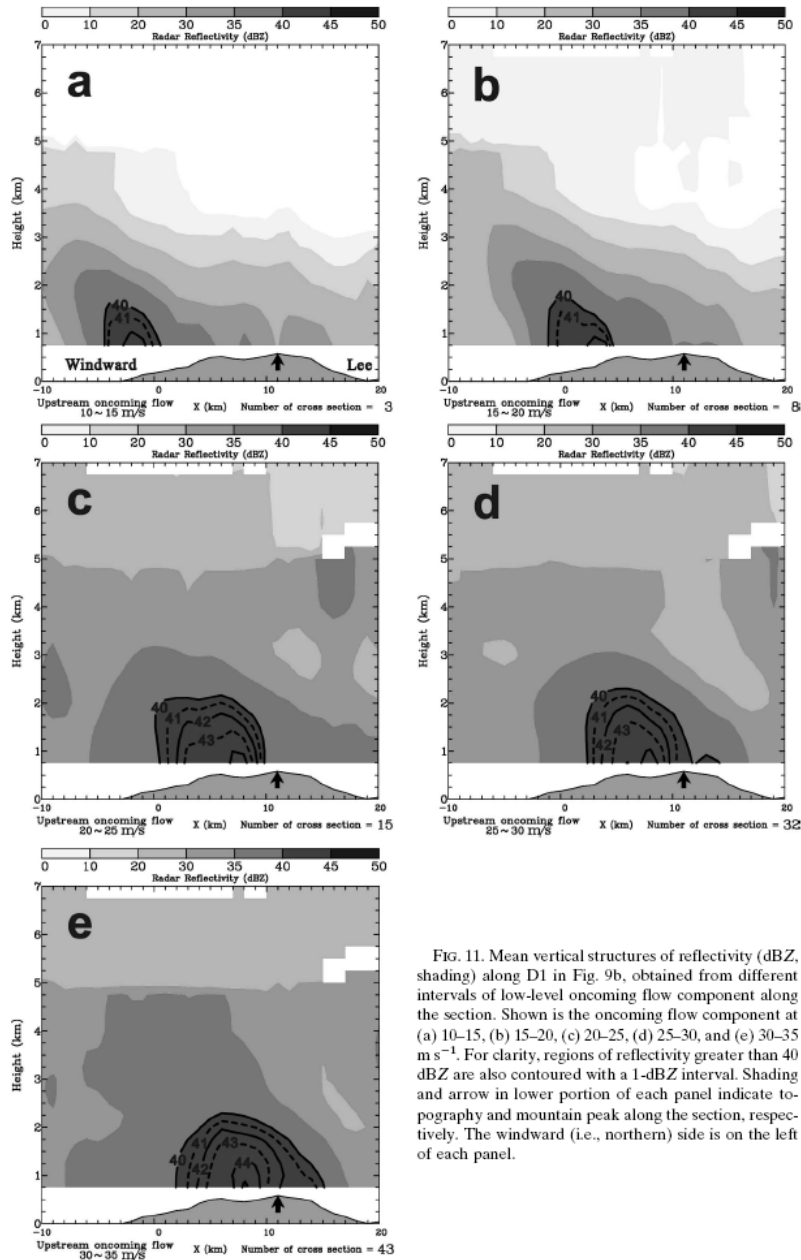


FIG. 16. Schematic diagram illustrating the downstream shift of hydrometeors over (a) DT and (b) NKR due to changes in upstream oncoming flow. Shading denotes the main region of heavy precipitation with darker shading representing stronger precipitation intensity. Solid (dashed) arrows indicate the trajectory of hydrometeors in the weak (strong) oncoming flow condition. Open arrows denote airflow patterns over mountains. The h_0 and h_0' represent the altitude for hydrometeors starting their descent to the ground over DT and NKR, respectively. The " Δx_0 " and " $\Delta x_0'$ " represent the distance of downstream shift of hydrometeors over DT and NKR, respectively.



low-level oncoming flow intensified, and the precipitation exhibited a deeper, wider extent and stronger intensity at stronger oncoming flow regimes

FIG. 11. Mean vertical structures of reflectivity (dBZ, shading) along D1 in Fig. 9b, obtained from different intervals of low-level oncoming flow component along the section. Shown is the oncoming flow component at (a) 10–15, (b) 15–20, (c) 20–25, (d) 25–30, and (e) 30–35 m s^{-1} . For clarity, regions of reflectivity greater than 40 dBZ are also contoured with a 1-dBZ interval. Shading and arrow in lower portion of each panel indicate topography and mountain peak along the section, respectively. The windward (i.e., northern) side is on the left of each panel.

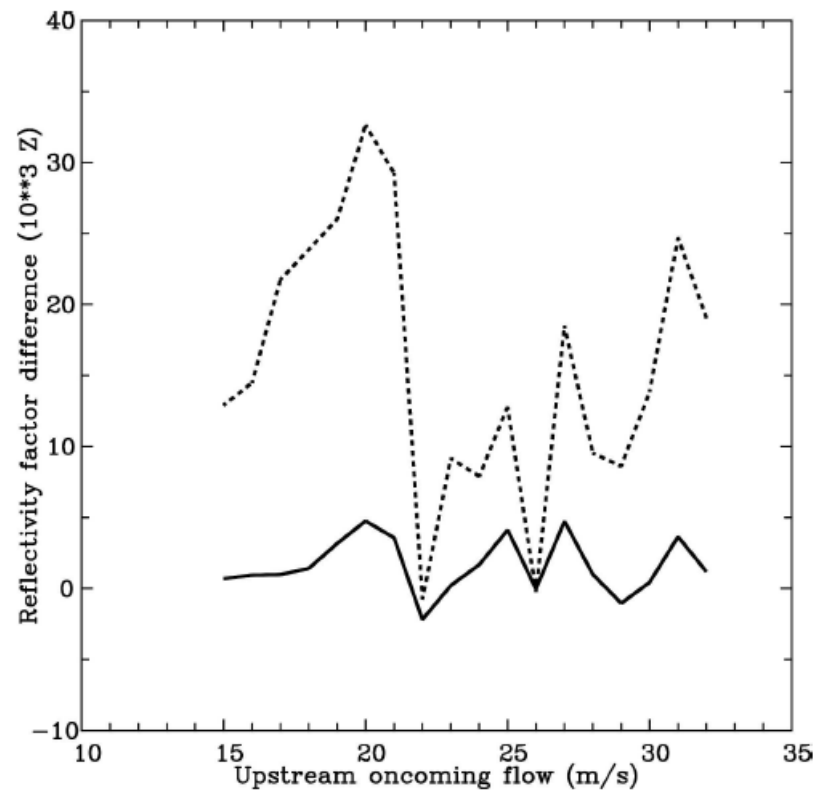
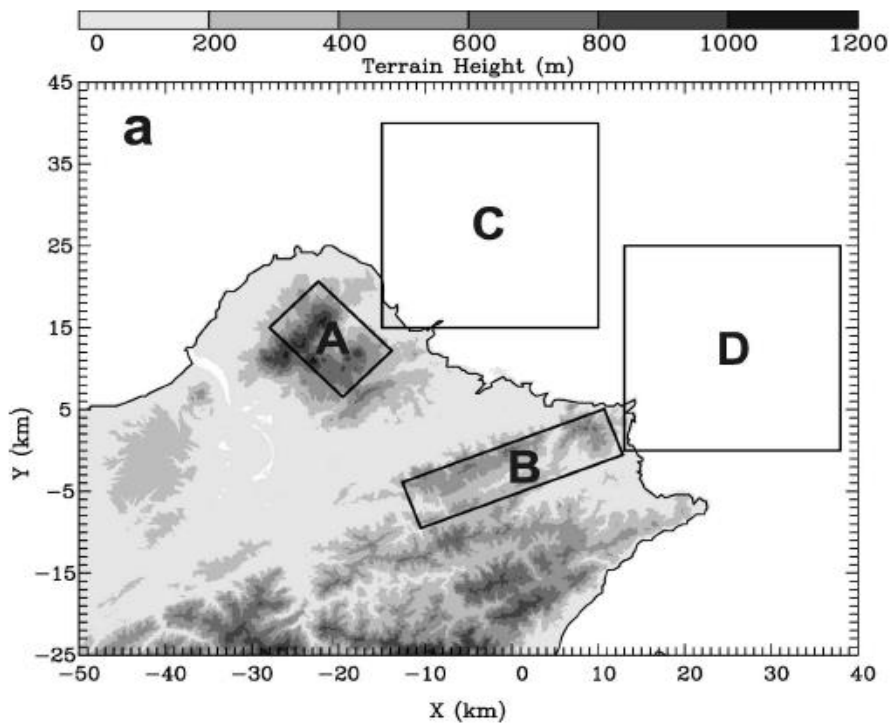


FIG. 19. Differential reflectivity factors ($Z \times 10^3 \text{ mm}^6 \text{ m}^{-3}$) averaged in the lowest 1 km (MSL) as a function of low-level oncoming flow. Dashed (solid) curve denotes results calculated over A and B (C and D) shown in Fig. 17a.

Rainfall Reinforcement Associated with Landfalling Tropical Cyclones in Mainland China

(Dong et. al. 2010)

the rainfall reinforcement of a landfalling tropical cyclone (RRLTC) is realized whenever the rainfall increment between two time levels equals or exceeds a threshold rainfall amount.

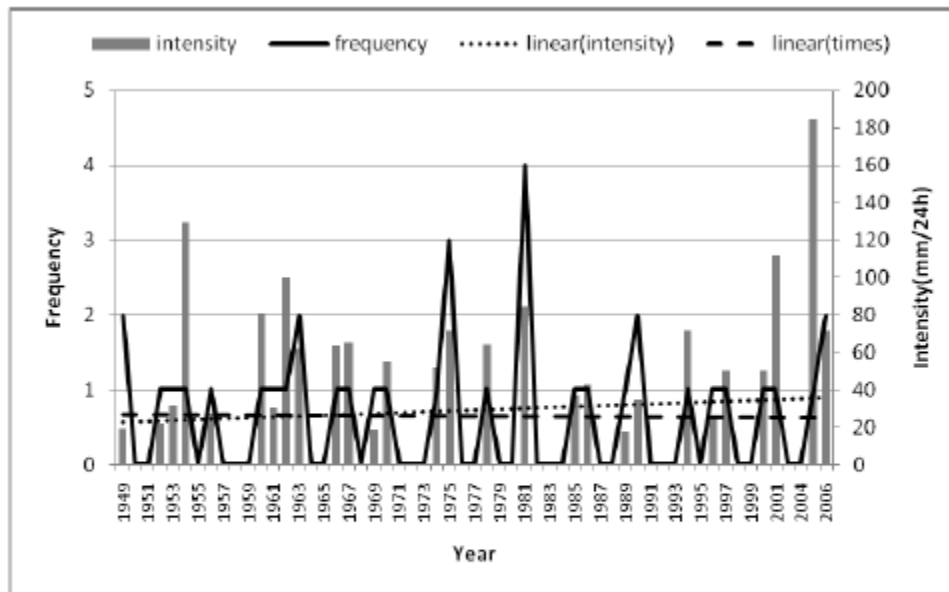


FIG. 1: Interannual variability of RRLTC occurrence frequency and intensity from 1949 to 2006.

The TCs triggering rainfall reinforcement account for 9.7% of the total number of TCs that make landfall on mainland China

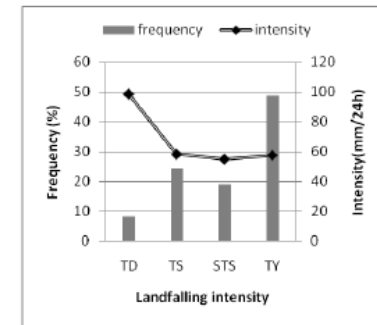


FIG. 5: Relationship between RRLTC occurrence frequency/intensity and TC category at landfall. The standard deviations of intensity for TD, TS, STS, and TY are 39.0, 47.4, 36.0 and 41.6mm/24h, respectively.

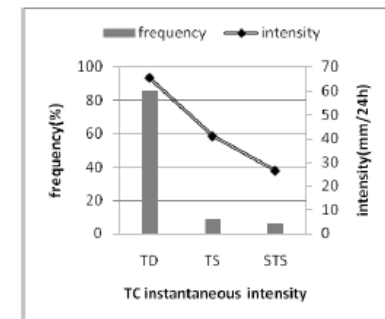
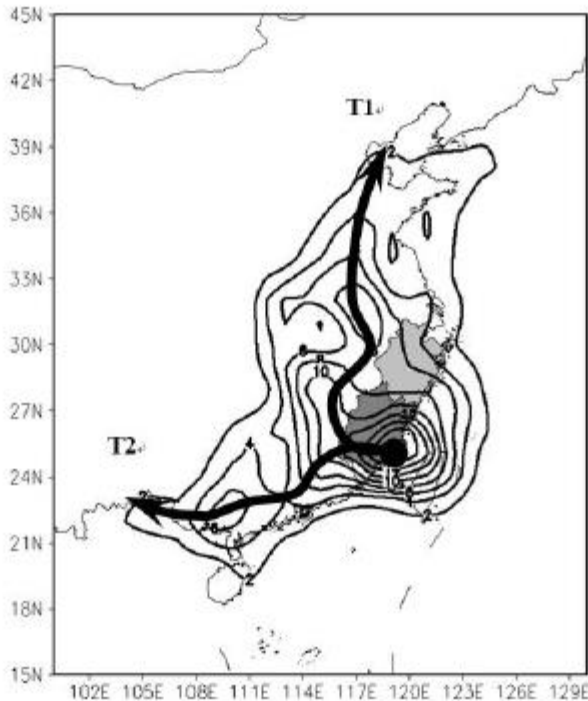


FIG. 6: Relationship between RRLTC occurrence frequency/intensity and TC category at the time of RRLTC occurrence. The standard deviations of intensity for TD, TS, and STS are 42.4, 12.4 and 14.4mm/24h, respectively.

Rainfall Reinforcement Associated with Landfalling Tropical Cyclones in Mainland China (Dong et. al. 2010)



attributed to the interaction between westerly troughs and tropical cyclone. This is the way for remnant to gain the baroclinic energy from the mid-latitude trough

Rainfall reinforcement for the TCs with a westward track is mainly due to the interaction between monsoon surge cloud clusters and tropical cyclone. to TCs gain moisture and latent heat.

FIG. 4: Distribution of frequency of all TCs with rainfall reinforcement over land (unit: ‰, the thick solid lines with arrows display the two categories of northward and westward tracks represented by T1 and T2, respectively. The dark and light gray shading respectively denotes Fujian and Zhejiang province)

Rainfall Reinforcement Associated with Landfalling Tropical Cyclones in Mainland China (Dong et. al. 2010)

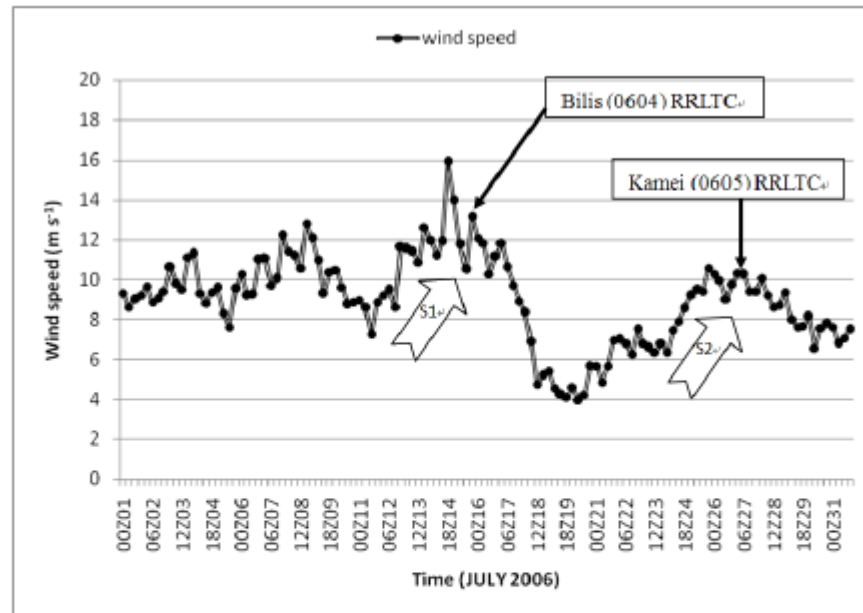


FIG. 17: Monsoon (unit: m s^{-1}) variation during July 2006. The wind speed is an area mean of total wind over the northern South China Sea (105-120E, 10-20N) at 850hPa. Open arrows with label S1 and S2 respectively denote monsoon surges during Bilis (0604) and Kamei (0605) affecting China.

Index

- **Overview of TC rainfall over Monsoon region in Western North Pacific**
 - Early development
 - TC rainfall climatology
 - TC rainfall structure
- **Monsoon influence on TC precipitation**
 - SST
 - Meiyu front
 - subtropical high
 - Southwesterly monsoon
 - Northwesterly monsoon
- **Interaction between tropical cyclone and southwesterly monsoon**
 - Case study on Bilis 2006
 - Climatology
- **Study on the potential impact of landfalling TC in Mainland China (How to estimate economic loss by TC before their landfall in Mainland China)**
- *How to predict the development of tropical disturbance over SCS.*

reference

- See attachment file